APPENDIX III

The Adaptive Control Model of a Pilot in V/STOL Aircraft Control Loops

This is a version of the Thesis for a Master of Science Degree

by Senol Kucuk

AN ADAPTIVE HUMAN RESPONSE MECHANISM CONTROLLING THE V/STOL AIRCRAFT

Department of Electrical Engineering
University of Pittsburgh, 1988.

LEWIS
GRANT

IN-09-CR

279346

P-182-183

Final Report for NASA Grant NAG 3-729

Computer Simulation of a Pilot in V/STOL Aircraft Control Loops

PRINCIPAL INVESTIGATORS:

William G. Vogt
Professor of Electrical Engineering
University of Pittsburgh
Pittsburgh, PA 15261
(412) 624-9686

Marlin H. Mickle
Professor of Electrical Engineering
University of Pittsburgh
Pittsburgh, PA 15261
(412) 624-9682

PARTICIPANTS:

Mark E. Zipf, Research Assistant
Department of Electrical Engineering
University of Pittsburgh
Pittsburgh, PA 15261

Senol Kucuk, Research Assistant
Department of Electrical Engineering
University of Pittsburgh
Pittsburgh, PA 15261

AN ADAPTIVE HUMAN RESPONSE MECHANISM CONTROLLING THE V/STOL AIRCRAFT

by

Senol KUCUK

B.S. in E.E., Middle East Technical University, TURKEY, 1985

Submitted to the Graduate Faculty

of the School of Engineering

in partial fulfillment of

the requirements for the degree of

Master of Science

in

Electrical Engineering

University of Pittsburgh

1988

The author grants permission

to reproduce single copies

Signed_____

ACKNOWLEDGMENTS

I would like to thank my major advisors Dr. W. G. Vogt and Dr. M. H. Mickle for their support and guidance in the course of this project. I would also like to thank to the member of my thesis committee Dr. E. W. Kamen for his efforts on the behalf of my thesis.

I wish to dedicate this thesis to my family for their unfailing concern, understanding and support throughout my graduate career in the U.S.A.

ABSTRACT

SIGNATURE _____

AN ADAPTIVE HUMAN RESPONSE MECHANISM CONTROLLING THE V/STOL AIRCRAFT

Senol KUCUK, M.S.

University of Pittsburgh

Importance of the role of human operator in control systems has lead to the particular area of manual control theory. Human describing functions have been developed to model human behavior for manual control studies to take advantage of the successful and safe human operations. Although adaptivity of the complex human mechanism is known to occur, no complete human response model can simulate this while actively participating in a manual control task. Single or multi-variable models, as well as optimal control models are available but require the knowledge of the controlled element dynamics. Here, we present a single variable approach that can be extended for multi-variable tasks where a low order human response model is used together with its rules, to adapt the model on-line, being capable of responding to the changes in the controlled element dynamics.

Basic control theory concepts are used to combine the model, constrained with the physical observations, particularly, for the case of aircraft control. Pilot experience is represented as the initial model parameters. An adaptive root-locus method is presented as the adaptation law of the model where the closed loop bandwidth of the system is to be preserved in a stable manner with the adjustments of the pilot model parameters. Pilot operating regions are taken from case studies of pilot handling qualities which relate the latter to the closed loop bandwidth and damping of the closed loop pilot-aircraft combination. Pilot limitations are characterized by the amount of force to be exerted on the controls by the pilot model. A Kalman filter parameter estimator is presented as the controlled element identifier of the adaptive model where any discrepancies of the open loop dynamics from the predicted one, are sensed to be compensated. The model is simulated in a non-linear aircraft simulation environment under different scenarios where it is subjected to perform simple maneuvers over a thrust vectored V/STOL aircraft.

DESCRIPTORS

Adaptive human model	Human describing function
Human pilot	Human response
Kalman filter	Man-machine systems
Manual control	Parameter estimation
Root locus	V/STOL

1.0 INTRODUCTION

Man-machine systems have been an important research area in recent years. Among these is the modelling of non-linear human behavior under different circumstances, especially in closing the loop of a control system. The latter is of great significance to control engineers and designers because it enables the possibility of digital or analog computer simulations of the complex human mechanism to perform certain tasks. Although it may not be possible or even not desirable to eliminate the human component in most control systems, it certainly is worth while to obtain mathematical models describing the relationship between man and machine where his presence can make a system self-optimizing. His ability to learn and adjust so as to adapt to the environment suggests that human study himself. In other words, it is "human modelling of human behavior". We will discuss the human pilot-aircraft combination, in that respect.

1.1 The Human Pilot

The mathematical analysis of two different aircraft may differ in general. For the pilot, however, aircraft and their control systems are deliberately designed so that there are only minor differences. After a short training period which involves trial-and-error, the human pilot can fly either of the aircraft. Both aircraft obey the same equations of motion, and since the pilot is the same, one analysis can be applicable to the other. Indeed, pilot opinion is an important issue in the design and testing of a new aircraft. This is because of the close relationship between what the pilot considers a "flyable" aircraft and the small perturbation analysis of the dynamics of the aircraft.

The pilot flies the airplane by the feedback method. He senses by sight or feels by "the seat of the pants" the motion of the aircraft, and moves the controls so as to minimize the error difference between the actual and some desired motion. In other words, the pilot responds to the motion of the aircraft, perceived by the sense organs, both directly and indirectly through the flight instruments such as the altimeter, speedometer, etc. He has other cues, the more the better, but they should all be in perfect harmony, and not contradictory.

The efficiency of the controls depends on the relation between the dynamic characteristics of the airframe and those of the control system, particularly on the length of any time lags. A certain interval of time elapses between the instant a disturbance appears and the instant the corresponding control movement or force becomes active as a result of the control applied. During this short interval, another signal can not take effect. This appears to be the basic non-continuity of the sensation response activity. This time delay plays an important role in the stability of the closed loop system since any stable system can be made unstable by introducing sufficient time delay into the loop. The pilot is then required to adjust his gain to produce the optimum response consistent with the stability within his human limitations. We can summarize the processes occurring in this interval in the following sequence: (see Figure (1))

1. Sensing of the disturbance or the controlled element by the pilot,
2. Response of the pilot which includes the computing element, selecting the variables that will be acted upon, choosing the controls considered to be the most efficient as well as the manner in which they will be acted upon, (the computing element consists in comparing the signal at the input with the known potentialities of the controls of the machine and the experience of the pilot)
3. The muscular movement of the pilot,
4. Further transmission of the controls through the respective control system

linkage to the output (aerodynamical control surfaces, engine throttle, etc.) and the transition process until a steady state is reached; at this stage mode switching of the pilot from dynamic operator to static takes place.
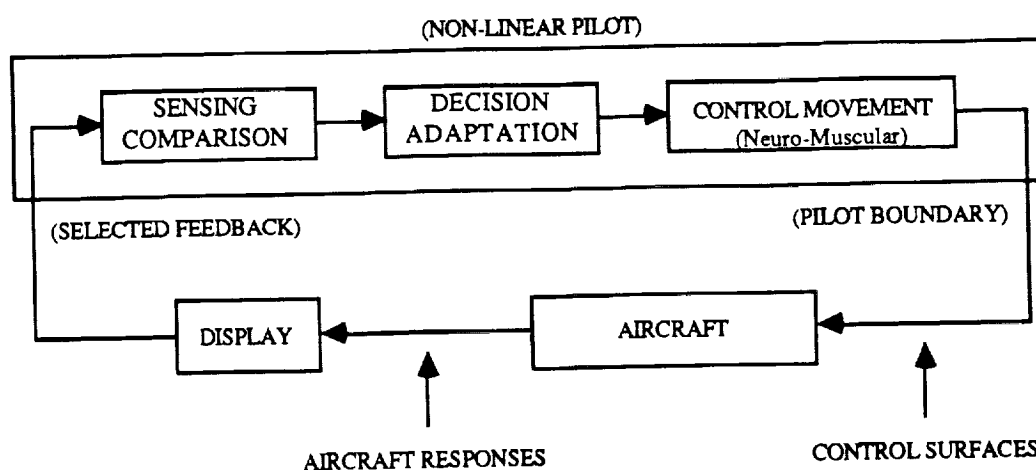

Figure 1. Processes occurring in the manual pilot control

This is a negative feedback control, where the controller (pilot), must close the loop according to some desired, overall behavior. Therefore, we will use the term, pilot "closes the loop", for this process. Furthermore, this behavior can be related to the bandwidth and damping ratio of the closed loop system. Kolk (1961) has studied the handling qualities and described a typical pilot in terms of the undamped natural frequency and the damping ratio, while rating them as "best", "good", "fair" and "poor" (see Figure (2)). Ashley (1972), reproduces Kolk's results in his small perturbation stability and response analysis. The ξ in the range, 0.5-0.8, and ω_n in the range, 3-4 rad/sec, retain considerable validity today as a basis for preliminary determination of what constitutes a good pilot or equivalently good-flying airplane. Etkin (1972), also has

a similar analysis. Thus, Kolk's chart will be our main design consideration. Judgements on simulating pilot model effectiveness will be done by comparison with the desired ranges.
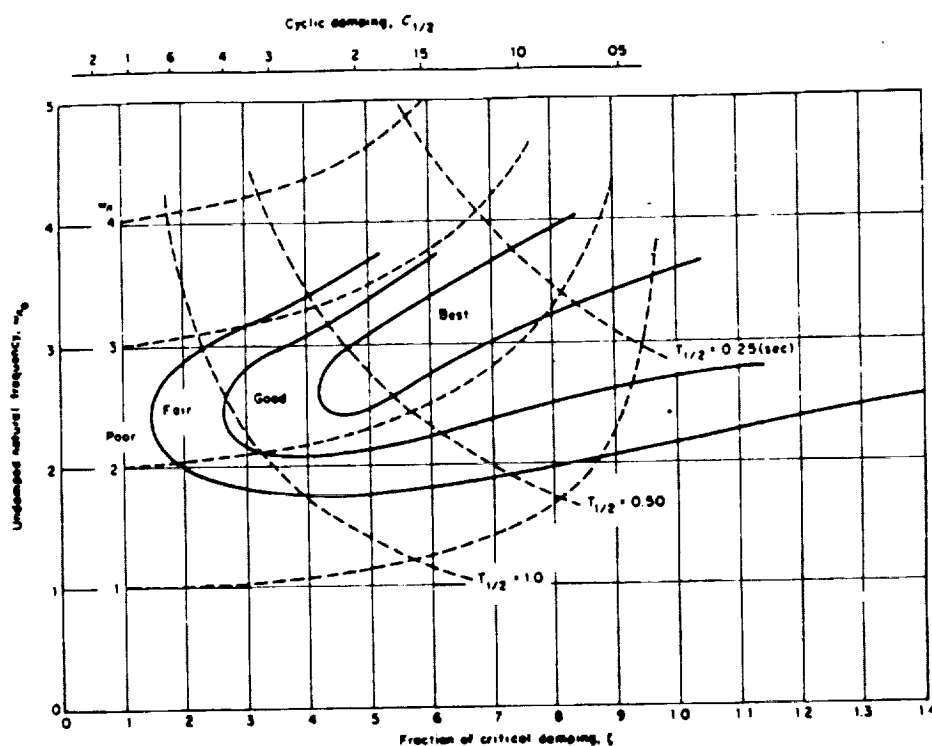

Figure 2. Kolk's chart on closed loop pilot characteristics

There is also an element of the control system, whose response characteristics vary not only from person to person, but also in the same individual according to his degree of fatigue, psychological and physiological condition which will later be referred to as the remnant. Unlike the automatic pilot, where the equations of motion for the control system are known with sufficient accuracy, it is not possible to permit the description of the control system by means of dynamic equations.

A human pilot reasons on the basis of the total information received but not necessarily simultaneously, about the controlled variable, relying on his flying experience. The processing of the information may not be instantaneous, moreover some information may not be used at all. In this respect, the possibilities of the computing element of the automatic pilot are inevitably more limited. In the case of the automatic pilot, by its detecting instruments (sensors, on-line computers, estimators, etc.) certain input signals, representing the well-defined components of the motion, should cause the autopilot to react. Under all circumstances, an automatic pilot watches only certain selected components of motion.

Many of the pilot's impression's of an airplane's flying qualities are related to the forces he must exert on the controls to hold them in the positions required to trim the airplane. If they are too large, he will be called upon to supply unreasonable exertion. If they are too small, the airplane may seem too sensitive or "touchy" or insufficient margin of stability may be indicated. In general, a pilot's flying qualities can be divided into two parts: static and dynamic responses. Static characteristics involve mainly the relationships between control deflection and force to trim the aircraft in steady equilibrium flight conditions of various sorts. This is the case of unaccelareted flight where a pilot responds mostly to disturbances. If these relations are regular and familiar, the control lever position and force provide the pilot with an immediate sense of the aircraft state, (angle of attack, sideslip, or speed). Proper static characteristics are prerequisite to good dynamic response.

Dynamic response, refers to the character of aircraft motions following disturbances from equilibrium. They may be atmospheric gusts, control movements to re-adjust the angular positioning, speed or the altitude of the vehicle, or any other events

producing unbalanced force or moments in general resulting in linear and angular acceleration. The airplane responds to these in characteristic ways, which define its dynamics, and which greatly affect a pilot's ability to fly easily and with precision.

The pilot is more or less concerned with the behavior of some of the many responses of the aircraft (pitch, roll, yaw, rates, speed, altitude, etc.), seeking to maintain them within certain limits or to cancel them by adequate control movements, which will be referred to as the controlled or the constrained variables. Hacker (1970) characterizes this relation by a system of partially controlled motion and discusses the stability in the case of a human pilot in parallel with constrained stability.

The remaining will be uncontrolled or free variables. However, the solution of the dynamic equations with some of the variables being constrained will also affect the free variables. Furthermore, the aircraft is to be controlled as a whole. Therefore, it is more appropriate to refer to the free variables as indirectly controlled variables.

The pilot's reflexes are selective with respect to the components of the motion. The control in this case is exerted over the sufficiently low modes of the motion induced by the disturbance, and in the rest of the flight, the stability is to be secured through the inherent properties of the machine.

Under standard flying conditions, like cruising along a straight path, (except when crossing a zone of intense atmospheric turbulence), the pilot usually achieves a correction through the controls that is even more efficient. In practice, he succeeds by achieving a satisfactory approximation of the controlled variables, induced by the disturbances and the deviations of those variables.

In order to secure the highest efficiency of control so as to determine in a given case, the optimum action to the deviation of a certain variable induced by the disturbance, the pilot generally resorts to several controls simultaneously. But one control also affects the quasi-totality of the equations of motion. The number of controls available, in general, is not equal to the number of the constrained variables, yet an experienced pilot is able to control all of the aircraft responses. Therefore limitation of the controllable variables, with the number of inputs seems artificial in the human pilot-aircraft combination case, due to the nature of partially and simultaneous control.

In summary,

- The pilot closes the loop in a stable manner,
- Closed loop bandwidth and damping are the measure of his flying qualities,
- There is a time delay between the sensed feedback element and the action,
- The pilot resorts to controls simultaneously,
- The pilot's decision process includes the estimation of the aircraft states and motion, and his opinion based on his flying experience,
- The pilot responses can be divided into static and dynamic; static response is the case of equilibrium flight where the pilot trims the aircraft to cancel the moments and balance the forces acting on the aircraft while dynamic response includes the control movements for maneuvering or changing the aircraft state,
- In general, the response of a human pilot will be different than the auto-pilot: it is not possible to relate human behavior to the equations of motion directly,
- There are stability considerations in the sense of delayed closed loop motion due to visual pilot feedback and partially controlled motion due to simultaneous control,
- There are bandwidth considerations since there is a limit of how rapidly and how strongly the pilot can move the controls.

Combining the above aspects, we come up with the general model shown in Figure
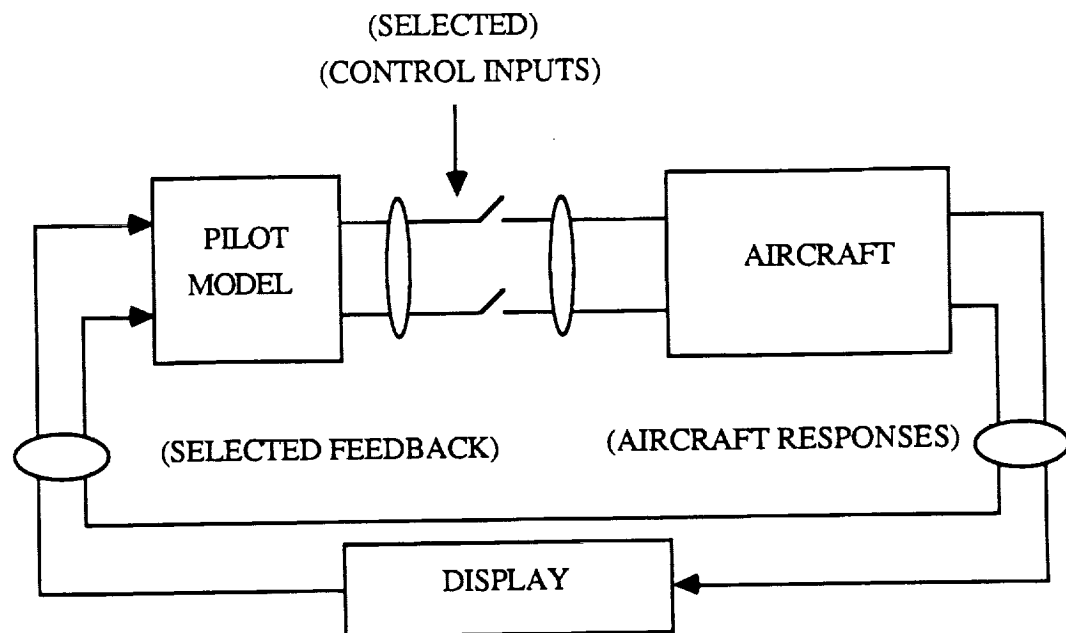
(SELECTED)
(CONTROL INPUTS)

```
                        (SELECTED)
                    (CONTROL INPUTS)
                           |
                           v
   +--------+           /      +----------+
   | PILOT  | --( )-- /  --( )--| AIRCRAFT |
   | MODEL  | --( )-- /  --( )--|          |
   +--------+                   +----------+

        (SELECTED FEEDBACK)    (AIRCRAFT RESPONSES)

              +-------------------+
              |     DISPLAY       |
              +-------------------+
```

Figure 3. General Pilot Model

(3). Which set of controls are to be selected, or which set of aircraft responses are to be used for feedback, are the decisions of the pilot. In most of the cases, one of those inputs, the primary control input, is for the control of a specific response of the aircraft, while the other controls act as a regulating or a secondary control set, trying to stabilize the modes of the aircraft motion disturbed by the primary input. The primary control set will be characterized by a single variable compensatory loop as in Figure (4). The system is compensatory since the pilot acts depending on the error information only. The rate of error signal which is estimated by the pilot by differentiating the error signal is also available. This information is the measure of pilot's estimation and detection process of the adaptation to the changes in the aircraft dynamics.

For example, the lateral control is activated by the ailerons through the lateral stick,

REFERENCE

COMPARISON → PILOT DESCRIBING FUNCTION → CONTROLLED ELEMENT DYNAMICS

(SELECTED FEEDBACK ELEMENT)
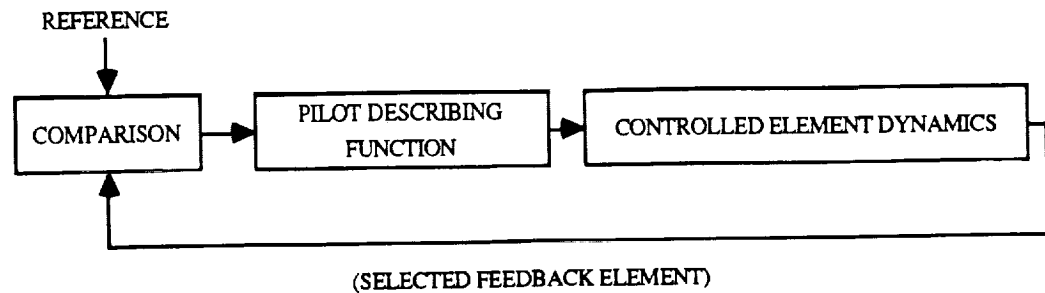
Figure 4. Single variable pilot model

but this causes a non-zero sideslip angle which is regulated by the rudder pedals. Also the pitch angle of the aircraft changes slightly, and that is regulated by the longitudinal stick changing the elevator angle. This is called a "coordinated-turn".

Further discussion of the human pilot for engineering analysis can be found in Kolk (1961), Seckel (1964), Hacker (1970) and Etkin (1972). These books discuss the aircraft dynamics and equations of motion while relating the theory to the human pilot. Seckel has more than five hundred references on handling qualities, human pilots, aircraft dynamics and theory.

1.2 The Aircraft

The aircraft is a rigid body consisting of a fuselage which carries the pilot and the wings to lift the aircraft. From the pilot's point of view, there is the cockpit with the provided instrumentations and the control units. Since we are discussing what the pilot observes in the aircraft, we will only mention the basic parts of the aircraft control mechanism.

Ailerons, elevators, rudders and tabs are typical parts of an aircraft that can move relative to the airframe. These are activated by the pilot for different purposes. The forces that would be required for the pilot to hold or displace them directly over some region of the flight envelope, far exceed the human capability. They are, therefore, provided by power boost in the form of hydraulic actuators. The pilot feels the artificial force of these actuators which define his boundary. These power boosted and manual controls, together with automatic gadgetry, assist the pilot, e.g., autopilots are employed to help maintain the direction, speed, and altitude of flight, while Stability Augmentation Systems (SAS) modify the apparent behavior so as to improve controllability of the aircraft and make the handling qualities more acceptable to the pilot.

Thrust is the reactive force applied to the vehicle, which may simply counterbalance drag (the aerodynamic force opposing the direction of the motion in the atmosphere), or may produce longitudinal acceleration or increased altitude. The thrust or engine throttle setting is the most common input for controlling the rate of climb or descent.

The propulsion system is often housed in a distinct element of vehicle such as a nacelle or jet-engine pod. Alternatively, it may be internal with only an air inlet or exhaust nozzle visible from the outside.

Weight is another force that dominates the performance of the vehicle. In level cruising flight, weight is counterbalanced by an aerodynamic force (lift) normal to the flight direction. Some lift is usually contributed by the fuselage, but a more efficient device for its production is the wing. A wing is a flattened, often cambered or twisted surface which intersects the fuselage, but usually has its longest dimension (span) normal to the airspeed vector. A well designed wing is an effective device for lift generation.

The most common arrangement, for lifting surfaces, known as a tail or empennage, has its location at the rear of the fuselage and consists of one portion (horizontal stabilizer) roughly parallel to the wing plane and a second (vertical stabilizer or fin) which is perpendicular to the wing plane, lying in the vehicle's central plane of symmetry.

The horizontal stabilizer applies pitching moments, which work to fix the inclination of the relative wind to the wing plane (angle of attack). It also assists in the trimming process of cancelling pitching moments about the center of mass due to the wing lift, fuselage, etc.

The wing lift depends on both angle of attack and airspeed so that this angle must be readily adjustable to ensure that the weight can be supported in various flight conditions. The most efficient way to make the required pitching moment adjustments has usually proved to be by controlling the tail lift with a trailing edge elevator.

Yawing control is supplied by the rudder, a flap acting at the trailing edge of the vertical stabilizer. The rudder has a trimming function in such situations as a steady turn or multi-engine flight when one engine is inoperable.

Rolling is accomplished by the ailerons and/or spoilers, placed near each wing tip and deflected in an anti-symmetrical manner. At high speeds, rolling moment may be exerted simply by the differential rotation of two all movable horizontal stabilizers.

The wing flaps resemble control surfaces but they are actuated slowly and only at low speeds where they augment wing lift to facilitate landing or take-off.

As mentioned earlier, trimming is one of the activities of the pilot. There are trimming devices, usually tabs, that help the pilot maintain the equilibrium so that controlled free flight can be set up at any speed by the appropriate settings.

For a conventional aircraft, the longitudinal control system consists of the engine throttle setting and the elevator angle through the longitudinal stick (forward and backward movements). The lateral control system is the ailerons (rightward and leftward movements of the lateral stick) and the rudder pedals operated by the feet. Although in mixed modes both of the control units affect each other, it is sometimes useful to separate the control mechanisms into longitudinal and lateral. The tabs are manually adjusted by the pilot for control free flight.

We will use a V/STOL (Vertical and Short Take-Off and Landing) aircraft in our simulations which is capable of adjusting the direction of the engine gross thrust vector as opposed to the conventional aircraft. Thrust vectoring is used to lift the aircraft for VTOL and STOL mode or to adjust the thrust vector to the optimum angle for a given flight condition.

1.3 The Simulation Program

The Harrier AV-8B model is a single seat transonic light attack V/STOL aircraft. Conventional aerodynamic controls are utilized for wingborne flight and engine bleed air reaction controls are used in jetborne flight with both systems operative during transition modes.

The Harrier AV-8B flight control system consists of conventional ailerons, rudder,

and stabilizer with a reaction control system (RCS) acting about all three axes during hover and transition. The stabilizer and ailerons are power operated while the rudder is connected directly to the rudder pedals. A single channel, limited authority Stability Augmentation System (SAS) is provided to facilitate control in hover and transition.

The engine provides lift thrust for take-off and landing, cruise thrust for conventional wingborne flight, deflected thrust for inflight maneuvering and compensator bleed air for the aircraft RCS. This is achieved by a nozzle system that can direct the engine thrust from zero degrees through vertical and even a reverse thrust position relative to the engine center line. The nozzle lever is the only additional cockpit instrument required for the V/STOL operation, and the only additional cockpit instrument is the gauge which displays the angular position of the nozzles. Engine operation in the conventional flight is similar to that of other engines.

The non-linear simulation program for Harrier AV-8B[1]*, provided by NASA-Lewis, computes six degree of freedom aircraft motion[2] and some of the aircraft performance parameters. The program is based on wind tunnel measurements and parameter identification methods[3], and it will be our basic simulation environment for model testing and insertion of the pilot models. The simulation program provides all the cockpit controls (longitudinal stabilizer, ailerons, rudder, thrust and nozzle angle setting) and the switches (SAS, RCS, Gear, etc.) that are used by a human pilot[4][5].

---

*Parenthetical references placed superior to the line of text refer to the bibliography.

1.4 Equations of Motion

Although we will not discuss the equations of motion for the aircraft in detail, we suggest the book by Etkin (1959) and his revised (1972) texts. Like Ashley (1972), most of the recent text books refer to Etkin's work. There are other books by Moses (1945), Babister (1961) and Miele (1962), that are worthy of note.

As Ashley discusses in chapter two of his book, the six-degree of freedom aircraft motion can be characterized by nine states, (U,V,W), (P,Q,R), (Φ,Θ,h) (see Appendix A for the definition of aircraft parameters). One can also add Ψ, but since it has no influence on gravitational terms or the airloads, it can be dropped. Linearized analysis on the equations suggest that the longitudinal and lateral components of the motion can be de-coupled into two four state equations, even for the case when bank, turn and sideslip angles are small but non-zero. Although longitudinal components appear in lateral motion equations, and vice versa, in most of the practical cases coupling can be ignored.

If the aircraft is symmetrical, it is legitimate to consider pure longitudinal motions when the initial lateral rates are zero. These changes are basically in forward velocity, angle of attack and pitch attitude. The affected states are (U,W,Q,Θ). This results in a fourth order characteristic equation whose roots are the modes of the longitudinal motion. In general, the longitudinal characteristic equation has two complex conjugate roots: one defining the short-period mode, and the other having very small damping defining the phugoid (see Ashley (1974), Etkin (1972), Kolk (1961), Hacker(1970)) mode. If the change in the rate of altitude, h, is not negligible with respect to the other variables, then it should be added to the state equation, but for small perturbation analysis we can always neglect its effect.

Of the two modes, the short period is the most important one to the pilot, because these poles define how the aircraft will react shortly after he applies control movement to the longitudinal stick. It contains most of the angle of attack response to control deflection and the variation of the normal acceleration necessary for maneuvering. When the mode is of high frequency and well-damped, the airplane responds almost instantly, without overshoot to elevator movements. If the reaction of the aircraft is poor or there is a delay, it will be difficult for the pilot to handle efficiently for which he uses the term "sluggish". On the other hand, the phugoid mode does not have a significant effect on pilot's flying qualities. The phugoid poles are very close to the origin, even unstable in some of the cases. However, the mode is usually so long in period that it has very little influence on the pilot and is easily guided or altered. Consider a human guiding an automobile for example. Continuous adjustments must be made to correct the heading of the car depending on the road conditions, but these corrections are so small in magnitude that, they do not affect the quality of driving. The same situation applies for the aircraft case. In conditions, where continuous, active control is required anyway, the phugoid properties are probably not even perceptible to the pilot.

The corresponding lateral-directional modes can be characterized by the spiral mode, roll mode, and the oscillatory Dutch-Roll mode, which primarily affect the states (V,W,P,Φ). The spiral mode is like the phugoid (except that rather than a complex conjugate pole pair, the spiral mode is characterized by a very large negative pole), the pilot counteracts any evidence of these motions long before they have time to build up or become unstable. The other modes are, however, primary determinants of the pilot's perception of aircraft handling qualities. While there is no simple way of analyzing these important lateral-directional modes, Seckel (1961) has an interesting discussion of a human pilot trying to control the bank attitude by positioning the ailerons in the right

direction and in proportion to the error between the actual and desired bank angle. By linearized equations of motion and root locus techniques (see Figure (5)), Seckel shows that the closed loop system can be unstable for specific values of the pilot gain.This is what is known as the Dutch-Roll excitation. The sideslip swings back and forth, accompanied by oscillations in pitch angle. The solution is, of course, introducing the rudders, for coordinating the roll. This becomes highly difficult especially at high speeds due to the limited abilities of the human pilot.
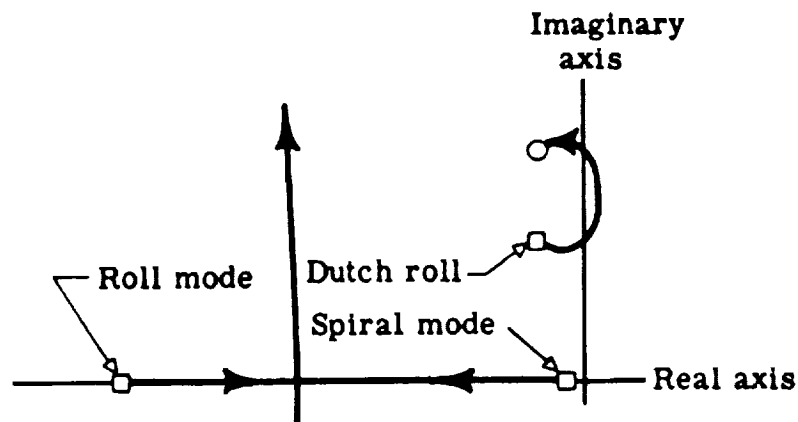
Figure 5. Root Locus of lateral control modes, from Seckel

1.5 Statement of the Problem

We wish to investigate the properties of models that can describe the human behavior in feedback type of systems by simulating these models in linear or non-linear environments. In other words, we want models that resemble human behavior or at least behavior a human can be capable of performing. In the presence of such models, the

analysis of the complex control tasks performed easily by humans, such as driving a car or flying an airplane, become available. It is the adaptive behavior of the human mechanism, without knowing the exact dynamic equations, capable of re-adjusting to different environments, that forces the search for mathematical describing functions. Unfortunately, the theory of adaptive control is not directly applicable for such an analysis. Such a model has been investigated at Wright Air Development Center in the late 1950's. Extensive amounts of experimental data have been studied and a fairly simple, yet effective model has been developed[6]. The details of the model can be found in the final version of the paper written by D.T.McRuer and E.S.Krendel[7]. One such application of the model is its performance while actively participating in the control of an aircraft, and being capable of responding to the changes in the aircraft model as well as to certain maneuvers.

One of the difficulties in utilizing the McRuer-Krendel human response model for different flight configurations is that parameters of the human model must be re-adjusted as parameters of the plant change. Consider an inexperienced human pilot being trained to control the aircraft for the first time. He will be provided with the control units and their purposes, but this alone is not sufficient enough to fly the aircraft without the actual training. As soon as he is given the full control of the aircraft, he will be in an action-reaction state, observing the responses corresponding to his commands while collecting and using this information for his next control attempt. As he begins to get used to the controls, he will be able to guess how the aircraft will respond depending on his command and if there are any discrepancies, he will correct them as in the case of guiding the automobile. The experience of the pilot reflects how well this estimation procedure is performed. In other words, the experience of a pilot is his knowledge of the open loop dynamic behavior of the aircraft. However, this knowledge can not be

expressed by a numerical dynamic set of equations. The pilot has an internal representation of the plant dynamics. Now consider the experienced pilot. It is clear that, even if the pilot is experienced, his action will differ depending on the aircraft configuration. This is partly due to the randomness of the human nature and partly to the changes of the dynamic relationship of the aircraft, especially to the speed and the angular rates. Therefore the adaptation process of the pilot continues even if he is an experienced pilot. In order to model this experience, we must have some knowledge of the open loop dynamics as the human pilot gets through training. As the human pilot selects the parameters best suited for the aircraft's configuration, we must obtain a set of human model parameters to be used at specific flight configurations. However, before a new pilot model is developed, a new set of transfer function estimates relating the behavior of the aircraft at the specified flight condition has to be obtained from the trimmed (unaccelerated) aircraft. These flight tests involve low order approximations of the primary responses through impulse, pulse or step inputs from the control mechanisms. This is exactly how the human pilot proceeds in controlling the aircraft, approximating the modes of the open loop dynamics that are perceptible to him and altering his parameters accordingly.

Once the estimate of the open loop transfer function is available, the loop is then closed using root locus techniques for the selection of the closed loop poles. The selection of the human pilot involves the proper assignment for a stable closed loop system with the desired bandwidth. So we will select our human model parameters that will satisfy the latter constraint used by the human pilot. As we will discuss in Chapter 2, the McRuer-Krendel human response model has a non-linear delay term, $e^{-T_D s}$ for the pure transmission delay of the visual lag. However, to be able to apply the root locus method, the non-linear delay element $e^{-T_D s}$ has to be handled before any analysis. One

way of proceeding is to approximate $e^{-T_b s}$ by a finite number of poles at a large distance from the origin, on the negative real axis[8]. Unfortunately, numerical problems are inevitable.

The most important drawback is that, all the following analysis must be done off-line: (1) trim the aircraft at the desired initial flight configuration; (2) record the impulse responses; (3) approximate low order transfer functions using time and frequency domain data; (4) choose primary response variables and control set; (5) calculate the human response parameters via root locus techniques; (6) insert the pilot model and (7) repeat this process until satisfactory responses are observed.

Our aim will be to simplify this process and close the loop on-line and adaptively, as the actual pilot does. We therefore need an on-line estimator scheme to monitor the changes in the open loop transfer function which the pilot is closing and use these estimates to adapt the pilot model. While the actual pilot just "does" the estimation, we need a parameter estimator for the simulation.

In Chapter 2, we develop a discrete time McRuer-Krendel human response model using the step invariant transformation. Although the transformation is trivial, the resulting model eliminates the non-linear delay element yielding a finite number of poles at the origin in the z-domain. Therefore we can use ordinary root locus analysis.

In order to close the loop with the desired bandwidth and damping, no way other than the root locus method is known and implementable. In Chapter 2, we separate the discrete time McRuer-Krendel model into two parts: one relating the time delay and the muscular element, the other being the adaptive or the compensating part which is our primary concern. Chapter three discusses the root locus method and a way to close the

loop adaptively. Applying the phase constraint of the root locus method in Chapter 3, we obtain a linear equation for the possible assignments of the adaptive pole-zero pair of the human response model which is suitable for on-line calculations. The adaptation acts as a phase equalizer and makes sure that the phase constraint is satisfied at the desired closed loop location, hence closing the loop. Unfortunately this procedure alone is not sufficient. The stability and error minimization arguments should be added for optimum values, and the adaptation must proceed accordingly. The adaptive pilot model is utilized in Chapter 5, and the extension for the multivariable control case is discussed.

Chapter 4, describes a time series parameter estimation technique using Kalman filters which can be easily modified to estimate transfer functions, parameters of the state and output equations. This chapter can be treated separately since it only deals with parameter estimation. Examples will be given to demonstrate the applications of the algorithm and computational aspects will be discussed.

Finally in Chapter 6, we combine the diagrams and equations for the adaptive pilot and discuss the resulting pilot insertions and compare with the static pilots[9][10][11] previously reported.

2.0 MATHEMATICAL MODELLING OF THE HUMAN RESPONSE

A human is intermittent in his operation, his bandwidth is limited by the time required for decisions and action, his senses are non-linear, and his awareness of output movement is of limited accuracy. However, he has the ability to detect signals in the presence of noise, and his presence can make a system adaptive and self-optimizing. Although his behavior is non-linear, it is not for a long time. There are periods when he acts in a non-linear manner, like the impulsive reactions in case of a sudden emergency, but most of his responses are observed to be linear. This aspect helps modelling the effect of a human in a closed loop system.

In the case of a control system, the basic human output is the control movement of skeletal muscles resulting in limb displacement or application of force. The knowledge of the limb position and force output is due not only to vision but to sense organs in muscles and joints known as the "proprioceptors". The sensory outputs of these organs provide feedback signals which make possible the regulation of skilled muscular movements. This feedback is transmitted by afferent nerve fibers from the muscles to the central nervous system, and after being processed, the control signal is sent to the limbs. Kelley (1968), discusses the neuro-muscular system for manual control purposes. However, very efficient approximate models for engineering analysis are utilized[12].

If the human-control system combination was completely linear, the analysis could have been quite simple. In the case of the human pilot-aircraft, neither the aircraft nor the human pilot present any linear behavior. Although non-linear models can be developed, the analysis of such systems is highly complex, and the results are not much

better than linear models. Another approach is to approximate these non-linear relationships by linear or quasi-linear models.

Despite this non-linear, adaptive human pilot mechanism, many linear and low order models have been successfully developed. Of these models the low order model (13) is the result of a servomechanism model approach of the human operator. This model demonstrated that human operator dynamics in single loop compensatory systems could be described by quasi-linear functions. A study on a variety of controlled element dynamics and random appearing input commands with different bandwidths confirmed the applicability of such a model[6].

There are other complex models relating optimum control theory to the experienced pilot behavior[14][15], or discrete models[16]. The Optimal Control Model (OCM) has better results in the low and high frequencies, but the basic disadvantage of the model is its complexity. The model consists of a Kalman Filter estimator, a predictor, a simplified neuro-muscular equivalent and a linear state feedback capable of multivariable control tasks.

The McRuer-Krendel model[7] has been simulated for the Black Hawk helicopter and for the Harrier AV-8B aircraft, for single and multiple cascaded pilot configurations[9][10][11], and the results confirm the model. Pilot parameters for the model are chosen after extensive aircraft testing for the flight configurations that are being considered in the simulations as an analogy to pilot training.

While the discrete domain model[16] only gives the freedom of choosing the order of the transfer function, the McRuer-Krendel model has adjustable parameters for the adaptive nature of the human pilot. We will transfer this continuous domain model into

the discrete domain, for reasons that will become clear later, and use this model to simulate simple maneuvers in a non-linear aircraft simulation environment.

2.1 The McRuer-Krendel Human Response Model

The McRuer-Krendel model is a single-degree of freedom quasi-linear model based on best fit analysis of experimental pilot data[6][7]. The general form is given by,

$$H_p(s) = K_p e^{-T_D s} \frac{(T_L s+1)}{(T_I s+1)} \left\{ \frac{(T_K s+1)}{(T_{K'} s+1)(T_{N_1} s+1)} \frac{1}{[(s/\omega_N)^2 + 2(\xi_N/\omega_N)s+1]} \right\} \qquad (2\text{--}1)$$

where $H_p(s)$ is the transfer function of the human response, often referred to as the describing function, s is the complex Laplace transform variable, the input is the error signal, while the output is the corresponding control displacement. McRuer and Krendel discuss typical values of the precision model[7]. In order to characterize the random component, a remnant is added to the control displacement as in Figure (6).
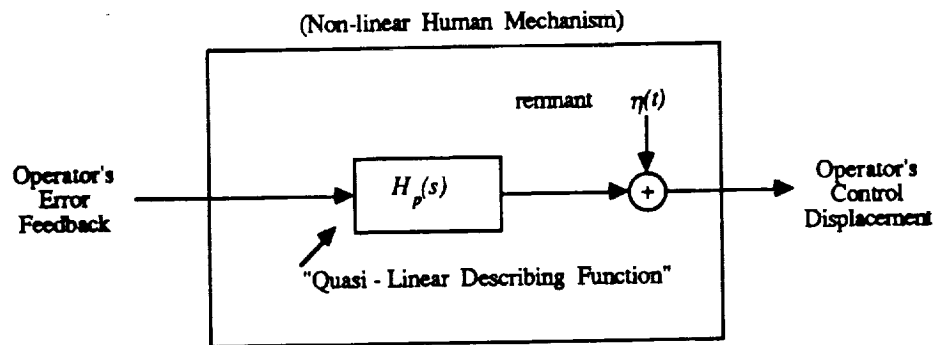
Figure 6. Human describing function model

Although there is no easy way of analyzing the remnant, the model in equation (2-1) can further be simplified to obtain the transfer function,

$$H_p(s) = \frac{K_p e^{-T_D s}(T_L s + 1)}{(T_N s + 1)(T_f s + 1)}$$

(2-2)

where very low and very high frequency accuracy is not necessary. This is a reasonable assumption for the human pilot since, as discussed before, the bandwidth of the closed loop is 3-4 rad/sec (or 0.48-0.64 Hz). In equation (2-2), $e^{-T_D s}$ is the pure transmission time delay within the nerve conduction and stimulation. Although the time delay parameter T_D changes are estimated to be between 0.13-0.23 seconds and even 0.30 for some of the cases, it is not known to exceed 0.30 seconds (see Kelley(1968)). The changes in the time delay can be significant depending on the particular control task but not for a specific control task[17], e.g., the time delay of a driver will be different than that of a pilot, but pilots with similar experience and training will have similar lags. Therefore, we will assume that T_D=0.20 and is constant for the rest of the discussion. The OCM model[14] has a similar argument on the time delay. The term $1/(T_N s + 1)$ is an approximation of the neuro-muscular lag of the arm meaning that the pilot can not move his arm faster than the rate of this pole. The value of T_N is assumed to be constant and approximately 0.10. The remaining term, $K_p(T_L s + 1)/(T_f s + 1)$, is the adaptive part of the model (a time dependent variable gain and a lead-lag compensator) whose parameters are altered by the pilot to the particular flight configuration. The constraints on the model parameters are as follows:

$$0.0 \leq T_L \leq 2.50 \quad (T_L \neq T_N)$$ (2-3a)

$$0.0 \leq T_f \leq 20.0$$ (2-3b)

$$T_N = 0.10$$ (2-3c)

$$T_D = 0.20$$ (2-3d)

The lead-lag compensator part is based on the assumption that the human is required to furnish at least one differentiation and one integration to obtain the desired performance, and the constraints on the parameters, T_L and T_I determine how efficient the integration and differentiation processes are performed by the human. This concept of a human capable of differentiation and integration is a common assumption. The complete model with the remnant added is given in Figure (7).
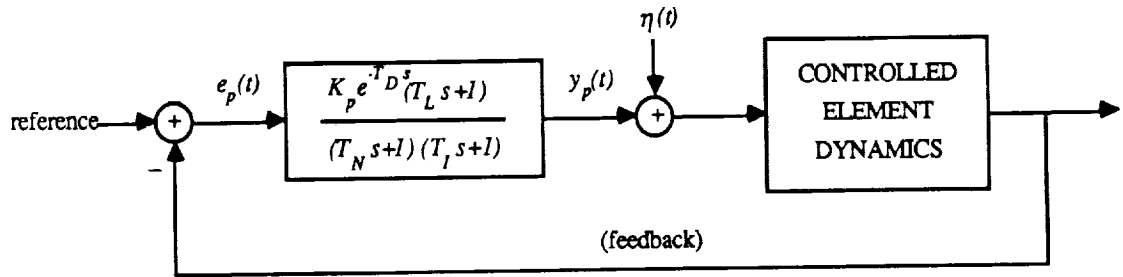
Figure 7. Complete single variable model

The resulting differential equation will be,

$$(T_N T_I)\ddot{y}_p(t) + (T_N + T_I)\dot{y}_p(t) + y_p(t) = K_p T_L \dot{e}_p(t - T_D) + K_p e_p(t - T_D) + \eta(t) \tag{2-4}$$

The quantity $y_p(t)$ is the pilot's control displacement, and the input is the feedback error signal $e_p(t)$. If $T_L \dot{e}_p(t) \gg e_p(t)$, then the output of the model is derived by the rate of the error signal, else if $T_L \dot{e}_p(t) \ll e_p(t)$, then the output is a function of the error signal itself. When they are in the same order, the effect is mixed.

The solution of equation (2-4) defines the modes of the pilot, and the resulting control displacement defines the modes of the closed loop system. Even though there are

a few parameters to be adjusted, the analysis is still not trivial because of the time delay, time-varying pilot parameters and time-varying aircraft dynamics.

Now recall that the external world is sampled for a brief period of time during which the sensing of the feedback component and comparison with respect to a desired motion takes place. It is clear that within this interval another signal can not be processed. The error signal is sensed and held until current information is processed. The total time delay of the decision depends on the pilot's abilities but also on the visual information lag. The compensator network parameters are then selected by the pilot and the location of the pole-zero pair is placed accordingly. Finally there is the input of the neuro-muscular element, and the desired control displacement is sent through the muscles. Unfortunately the desired and commanded controls may differ which greatly affects the pilot's control qualities. Thus the pilot is ready for another sample of the error, but we must note that he is responding to some error signal previous to the present error because of the delay.

The assumption of sampling leads to the model in Figure (8).
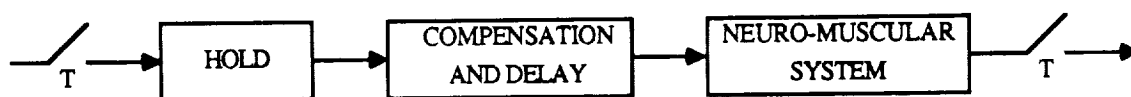
Figure 8. Sampled Human Response Model

Experiments show that it is impossible to deal correctly with every stimulus in a sequence when the stimuli are closer than some time interval from each other (about 0.5 second, Kelley (1968)). This in a way shows that sampling occurs in the human

mechanism because the latter phenomenon can be explained by the sampling theorem where a frequency aliasing occurs due to over-sampling. In other words the human can not respond faster than his bandwidth. Indeed a similar sampled data model has been suggested by McRuer[18] himself, and others have already been studied. However the relative simplicity and the successful simulation results of the McRuer-Krendel model suggest a direct sample-and-hold equivalent of this model for discrete domain analysis. This is legitimate if the bandwidth of the human mechanism is preserved which means that the sampling theorem must be satisfied. Under these conditions, we obtain the discrete time McRuer-Krendel model given by(see Appendix B for derivation):

$$H_p(z^{-1}) = \frac{Kz^{-d}(z^{-1}-\gamma z^{-2})}{(1-\beta z^{-1})(1-\alpha z^{-1})} \tag{2-5}$$

It is not surprising that the structure of the model does not change by sampling. Now the pure transmission delay is represented by z^{-d}, the neuro-muscular component is $1/(1-\beta z^{-1})$ and the adaptive part is $K(1-\gamma z^{-1})/(1-\alpha z^{-1})$. The pole locations are easily found by the relation $z=e^{sT}$. For the zero at γ however, the derivation is not straightforward because sampling relocates the system zeros. We used Greek letters for the discrete model parameters in order not to mix them with the continuous model. The gain K is scaled because of the sampling but that does not have any significance in the design. The zero and the poles of the model are given by,

$$\alpha = e^{(-T/T_I)} \tag{2-6a}$$
$$\beta = e^{(-T/T_N)} \tag{2-6b}$$
$$\gamma = 1 - \frac{(1-\beta)}{1 + \frac{(T_L-T_N)(\alpha-\beta)}{(T_I-T_N)(1-\alpha)}} \tag{2-6c}$$

This is for the case when $T_I \neq T_N$. Otherwise, the partial fraction expansion changes, but we will always avoid the situation $T_I=T_N$ to make the analysis simpler.

Assume that T_p, and thus also α, is fixed, then γ is a function of T_L only. It is easily seen that in that case the local maximum and minimum of the γ is obtained at the limits of T_L, and also that γ is an increasing function of T_L yielding,

$$\gamma_{(T_L=0.0)} \leq \gamma(\alpha) \leq \gamma_{(T_L=2.50)} \tag{2-7}$$

The only drawback to this is that while T_l is changing the possible locations for choosing the zero is changing as well. This is different than the continuous model where pole/zero locations can be assigned independently. The resulting discrete time difference equation is given by,

$$y_p(k) = (\beta+\alpha)y_p(k-1) - (\beta\alpha)y_p(k-2) + Ke_p(k-d-1) - K\gamma e_p(k-d-2) \tag{2-8}$$

The quantity $e_p(k)$ here represents the error information, and $y_p(k)$ is the corresponding pilot control displacement calculated at the discrete times.

The simulation program discussed in Section (1.5) updates the parameters at 0.05 second periods allowing the control inputs to be inputted at these instants. That gives a sampling frequency of 20 Hz. If we recall that the closed-loop bandwidth is desired to be 0.48-0.64 Hz, and the maximum bandwidth of a human pilot is estimated to be 0.96, a sampling frequency of 20 Hz gives a fairly safe region to operate. Furthermore this program is being used by NASA for real time human piloted simulators implying that 20 Hz sampling does not degrade human performance.

Now that T is fixed at 0.05 second, with $T_N=0.10$ and $T_D=0.20$, our model becomes,

$$H_p(z^{-1}) = Kz^{-4}\frac{(z^{-1}-\gamma z^{-2})}{(1-0.6065z^{-1})(1-\alpha z^{-1})} \tag{2-9}$$

For this choice Figure (9) shows the region of the model zeros while α is changing from

minimum to maximum defined by the inequality in equation (2-3b). It is seen that zero location lies inside the unit circle, and since the poles are stable as well, the resulting model is minimal phase. This is regarded to be an advantage because systems with non-minimal phase characteristics may have undesirable responses.

Figure 9. γ_{min} and γ_{max} versus α
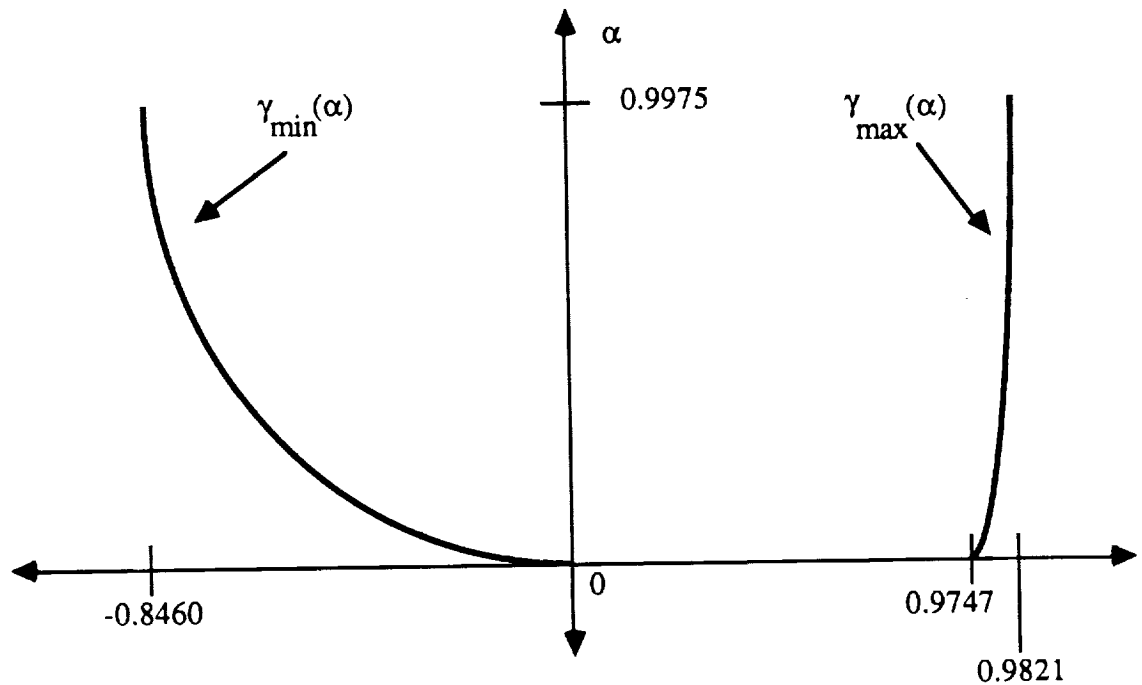
The discrete model has some advantages. First of all, the non-linear pure time delay element $e^{-T_D s}$ is eliminated and replaced by poles at the origin so that the analysis of the root locus is simpler. The pilot is characterized by a difference equation instead of a differential equation which means that any discrete identification method as well as discrete optimization necessary for the adaptation process of the pilot model can be applied. The model turns out to be minimal phase, but one extra constraint is added on the adaptive portion of the model. The parameters of the lead-lag equalization network are to be selected more carefully as a result of the sample and hold equivalent where the

zeros are relocated. Once the pole α is fixed, there is a region where the zero γ can be chosen, but this does not introduce any significant difficulty in the analysis.

2.2 Adaptation Procedure

The adaptation procedure can be divided into four parts: detection, modification, identification and optimization. We will combine detection and identification in one group, and modification and optimization in another.

It is reasonable to assume that a well-trained pilot has an internal representation of the plant dynamics and will be able to identify any changes very rapidly. For a skilled pilot, the identification of the unexpected modes of the system can be in times of order of a reaction time from the time of detection. The detection-identification structure of our model will consist of a linear time-varying plant representation and a parameter estimator which will update the unknown potentialities of the model parameters to desired accuracy constrained by the uncertainties of pilot input with respect to the plant output. For simulation purposes, we will not include the effect of the remnant. We have argued that the system was a compensatory feedback type system, and that only the error signal was available to the pilot. However, the human pilot is capable of monitoring the rate of the error signal[12], namely, $\dot{e}_p(t)$. If we approximate the first of the error signal in the following way,

$$\dot{e}_p(t) = \frac{e_p(t) - e_p(t-T)}{T} = \frac{r(t) - y(t) - (r(t-T) - y(t-T))}{T} \tag{2-10}$$

we can see that the rate of the error signal is proportional to the output. Therefore we argue that we can use the controlled element measurements and the pilot's control

displacement in a parameter estimation scheme which will be the one discussed in Chapter 4.

The second group, modification-optimization involves the proper selection of the lead-lag compensator that will result in a stable response and minimum mean square error. This will not work properly unless the estimate information of the detection-identification is responding to the changes in dynamics properly. If the estimate has some uncertainty in it, which often occurs in the pilot training where the inexperienced pilot over-estimates the next state of the aircraft and pushes the control stick too hard, then the system may become unstable. But this does not mean that the optimization is not working. Of the possible solutions for the lead-lag network parameters, the optimum pair must be found if such a solution exists over the flight envelope that is of question.

If we put together the basic parts of the adaptation, we end up with the model in Figure (10).
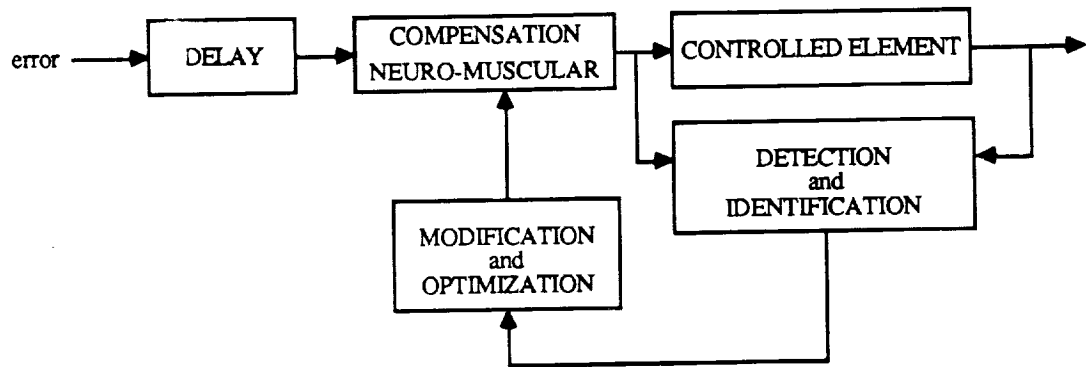
Figure 10. The Adaptation Procedure of the Pilot Model

3.0 CLOSING THE LOOP

In this chapter we will establish the equations for the closed loop pilot-aircraft system. Figure (11) shows the basic configuration of our pilot-in-the-loop model. Notice that this is a single variable closed loop compensatory system. The remaining responses other than the one being controlled are ignored at this point and later will be regarded as the disturbances. This is legitimate if the remaining variables are changing slowly with respect to the controlled element. This can be the case where the pilot is only provided by the pitch angle information and longitudinal stick input to control aircraft's pitch response.
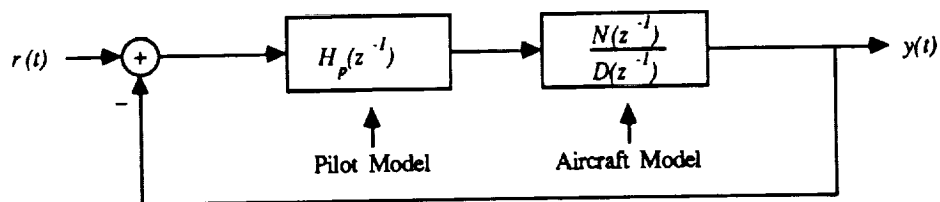
Figure 11. Compensatory single variable pilot control

Before further discussion some assumptions must be made. For the rest of the chapter we will assume the following. Assumptions (a) the controlled element dynamics can be decoupled from the rest of the aircraft responses, (b) there exists a describing function of the human response, and it can be approximated by quasi-linear models, (c) the remnant of the model is approximately zero, (d) the aircraft dynamics and the properties of the

Now we can argue the stability of the system. This is a complicated procedure especially when the aircraft dynamics is changing where the polynomials $N(z^{-1})$ and $D(z^{-1})$ are functions of time. It is important to note that there is no constraint on the order of the open loop aircraft transfer function. It may be impossible for the pilot to identify all the modes of the controlled element except for the ones that lie inside his bandwidth. The pilot adaptation involves an internal representation of the open loop system but not highly sophisticated. The pilot is watching the modes that are perceptible to him which leads to the conclusion that the model of the open loop that is sensed by the pilot is a low order approximation of the system. The approximation should be valid for low frequency regions or approximately $0.1 < \omega < 20$ rad/sec[19]. The parameters of this pilot-decided model are updated, if any discrepancies occur, and if the pilot is experienced enough to sense these changes.

The closed loop system is stable if and only if the roots of $\Delta_{CL}(z^{-1})=0$ lie inside the unit circle. The method of root locus becomes useful for such an analysis where the closed loop poles are plotted as a function of the variable component of the equation. In the case of a linear system the loci are plotted as a function of the open loop gain. Unfortunately, there is more than one variable in equation (3-4). To proceed, we will investigate the properties of the closed loop system only when the pilot parameters are changing. For that purpose we re-write the loci equation in terms of the pilot gain. This is obtained by equating equation (3-4) to zero and solving for pilot gain K, which results,

$$K=K(z^{-1})=-\frac{D(z^{-1})(1-\beta z^{-1})(1-\alpha z^{-1})}{N(z^{-1})z^{-d}(z^{-1}-\gamma z^{-2})} \tag{3-5}$$

All of the closed loop poles must satisfy equation (3-5).The order of the closed system is strictly determined by the order of the open loop transfer function. The constraints are on

the closed loop bandwidth and the corresponding phase margin. Then if z_{CL} is one of the closed loop poles, $K(z_{CL}^{-1})$ must be a real number since the gain can not be complex. But the z-transform variable z^{-1} is complex, so although the polynomials $N(z^{-1})$ and $D(z^{-1})$ have real coefficients. The result of equation (3-5) may not necessarily be a real number and those satisfying the latter argument define the root-locus of the closed loop system. Equivalently, we end up with the basic phase constraint of the root locus method which says that the gain in equation (3-5) must be real, or the complex argument of the gain must be zero, namely,

$$\angle K(z^{-1}) = \begin{cases} \pm (2n+1)180 & \text{for } K>0 \\ \pm (2n)180 & \text{for } K<0 \end{cases} \qquad n=0,1,2,\ldots \qquad (3\text{--}6)$$

The case of K being negative is necessary as we will investigate later in Chapter 6 that the relative airspeed of the R is decreasing by the increasing nozzle angle. If the pilot is required to increase the speed of the aircraft, then he must provide a negative gain.

Now that we have characterized the closed loop poles both as a function of the pilot parameters and the dynamics of the controlled element, we will relate the root locus method to the adaptive portion or the lead-lag equalization network of the McRuer-Krendel human response model in the discrete domain.

Let us re-write equation (3-5) in the following way by separating the pilot determined part from the others which he can not influence, such as time delay, the neuro-muscular lag, and the controlled element dynamics,

$$K(z^{-1}) = \left\{ -\frac{D(z^{-1})(1-\beta z^{-1})}{N(z^{-1})z^{-(d+1)}} \right\} \frac{(1-\alpha z^{-1})}{(1-\gamma z^{-1})} \qquad (3\text{-}7)$$

In equation (3-7), terms inside of the braces denote the non-reachable part for the pilot, and the remaining term which involves the discrete pole-zero pair α-γ is the equalization of the pilot which he alters for optimum flying conditions or equivalently optimum closed loop pole locations that are dominated by the non-reachable term or at least by the available amount of information on this term.

The adaptation is known to occur in the pilot mechanism, and we can explain such an adaptation by the phase requirement necessary to satisfy the phase constraint of the root locus defined in equation (3-7) at the desired closed loop pole location. In other words, the pilot changes the closed loop poles by the proper selection of his adaptive pole-zero pair and gain according to the variations of equation (3-7).

Assume that,

$$K_f(z^{-1}) = -\frac{D(z^{-1})(1-\beta z^{-1})}{N(z^{-1})z^{-(d+1)}} \qquad (3\text{-}8)$$

which reduces equation (3-7) to,

$$K(z^{-1}) = K_f(z^{-1})\frac{(1-\alpha z^{-1})}{(1-\gamma z^{-1})} \qquad (3\text{-}9)$$

As is usually done in bode plot analysis, we treat the magnitude and phase of the equation (3-9) in two different equations because this simplifies the analysis. For phase analysis, the equation (3-9) reduces to,

$$\angle K(z^{-1}) = \angle K_f(z^{-1}) + \angle \left(\frac{1 - \alpha z^{-1}}{1 - \gamma z^{-1}} \right) \qquad (3\text{--}10)$$

Let us examine the adaptive part $(1-\alpha z^{-1})/(1-\gamma z^{-1})$ separately since we do not have any influence on the other terms. We can find the phase angle supplied by α and γ to the equation (3-10). We can write

$$\frac{1 - \alpha z^{-1}}{1 - \gamma z^{-1}} = \frac{z - \alpha}{z - \gamma} \qquad (3\text{--}11)$$

Then the phase contribution of α and γ can be seen from the graphical representation of $(z-\alpha)$ and $(z-\gamma)$ in the complex plane as in Figure (12).
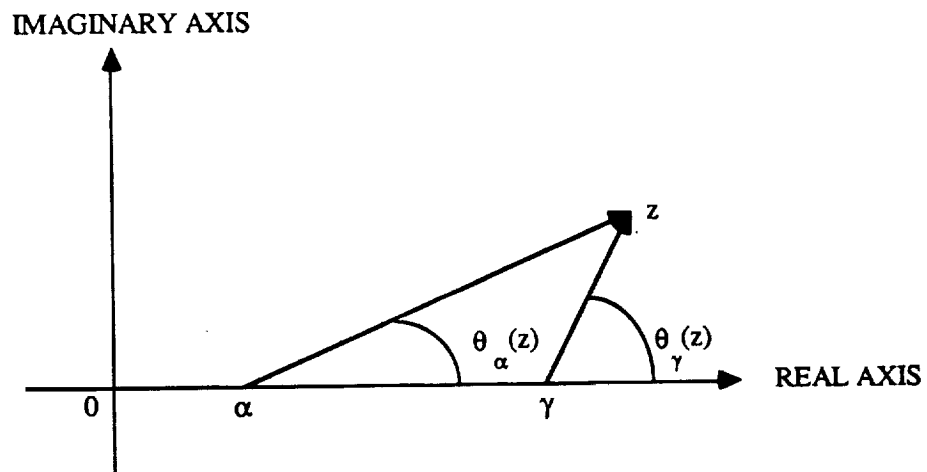
Figure 12. Graphical representation of the adaptive part

where, z is any desired pole location to be included in the loci. Then

$$\angle\left(\frac{1-\alpha z^{-1}}{1-\gamma z^{-1}}\right)=\theta_\alpha(z^{-1})-\theta_\gamma(z^{-1}) \qquad (3\text{-}12)$$

$\theta_\alpha(z^{-1}),\theta_\gamma(z^{-1})$ are as defined in Figure (12). By representing the closed loop behavior of the system with the root locus plot of the closed loop pole locations, the procedure of controlling the aircraft like the human pilot is now reduced to the appropriate assignment of α and γ that will satisfy equation (3-10). By the following definitions

$$\angle K(z^{-1})=\theta_K(z^{-1}) \qquad (3\text{-}13a)$$
$$\angle K_f(z^{-1})=\theta_f(z^{-1}) \qquad (3\text{-}13b)$$

equation (3-10) becomes,

$$\theta_K(z^{-1})-\theta_f(z^{-1})=\theta_\alpha(z^{-1})-\theta_\gamma(z^{-1}) \qquad (3\text{-}14)$$

Provided that $\angle K(z^{-1})$ and $\angle K_f(z^{-1})$ are known, the equation (3-14) can be solved. Although the equation looks like a linear equation, because of the possible set of assignments of α and γ, further analysis must be done. This can also be seen from Figure (12), α and γ can move right or left while still keeping a constant phase angle $(\theta_\alpha(z^{-1})-\theta_\gamma(z^{-1}))$.

If the quantity $\theta_\alpha(z^{-1})-\theta_\gamma(z^{-1})$ is negative, then the pole lags the zero (Figure (13.a)). Conversely if $\theta_\alpha(z^{-1})-\theta_\gamma(z^{-1})$ is positive then the pole leads the zero (Figure (13.b)). Once α and γ are fixed the corresponding gain is calculated from equation (3-9) by evaluating the right hand side at $z=z_{CL}$, z_{CL}, being the desired closed loop pole. Then, by taking the magnitude of each side of the equation (3-9),

$$|K(z_{CL}^{-1})|=|K_f(z_{CL}^{-1})|\frac{|(1-\alpha z_{CL}^{-1})|}{|(1-\gamma z_{CL}^{-1})|} \qquad (3\text{-}15)$$

α   γ   γ   α

(a)   (b)
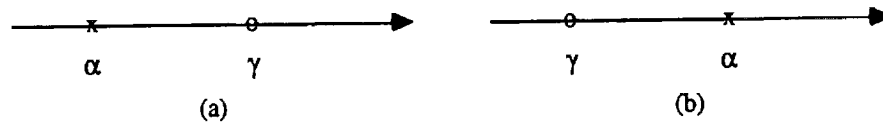
Figure 13. Possible pole/zero assignments

There may be more than one possible choice of the α-γ pair for the same task forcing other constraints for the assignment process. Just as the human pilot does, we must pick the pair that will result in the minimum error signal and a stable closed system. This is the optimization process. Unfortunately, the pilot-aircraft combination can not be guaranteed to be stable though an experienced pilot will try to maintain the opposite. But if instability occurs, this must be sensed, and the closed loop pole must be relocated. This is also necessary if the open loop transfer function has resonances at the pilot desired closed loop pole which makes the control very "touchy" so that the pilot must exert a considerable amount of force on the controls. Therefore the closed loop pole must be relocated within the allowable limits if possible. In the next section, we will define the limits of the desired closed loop system poles both in the continuous and the discrete domains to combine the Root Locus criterion with the closed loop poles.

3.2 Closed Loop Poles

In the introduction section, we indicated that the pilot's flying qualities can be determined by the closed loop bandwidth. We also related this bandwidth constraint into the undamped natural frequency and the damping ratio of the resulting closed loop transfer function. Now we will relate the region defined by

$$3.0 \leq \omega_n \leq 4.0 \quad \text{rad/sec} \tag{3-16a}$$
$$0.5 \leq \xi \leq 0.8 \tag{3-16b}$$

to the closed loop poles.

The second order, dominant complex conjugate poles are given by,

$$s = -\xi \omega_n \pm j\sqrt{1-\xi^2}\,\omega_n \tag{3-17}$$

applying the region defined in equation (3-16a) and (3-16b), we can plot the resulting s-domain poles as in Figure (14). The transformation $z=e^{sT}$, maps the poles in equation (3-17) to the z-domain poles as,

$$z = e^{-\xi \omega_n T}\left[cos(\sqrt{1-\xi^2}\,\omega_n T) \pm j sin(\sqrt{1-\xi^2}\,\omega_n T) \right] \tag{3-18}$$

The discrete poles change as the sampling time changes along with the resulting region of the desired closed loop poles. For $T=0.05$, the region of desired closed loop poles is given in Figure (15).

Therefore, we will assume that an experienced pilot adapts to the flight configuration in such a way that the dominant closed loop pole lies in these regions. And since it is the dominant pole, the bandwidth of the system is determined by this pole. For simulation purposes we will supply the desired closed loop pole to our model so that the

nominal value is used for most of the configurations, and the on-line adaptation scheme may change the precise location depending on the open loop transfer function, especially the behavior of the open loop transfer function at the pre-decided closed loop pole. If the system already has resonances at that pole, then the pilot must re-locate the closed loop pole within the regions of s-domain poles as in Figure (14) or equivalently z-domain poles as in Figure (15).

(-2.00,3.60)

jω

(-1.50,2.60)

(-3.20,2.40)

(-2.40,1.80)

0

σ
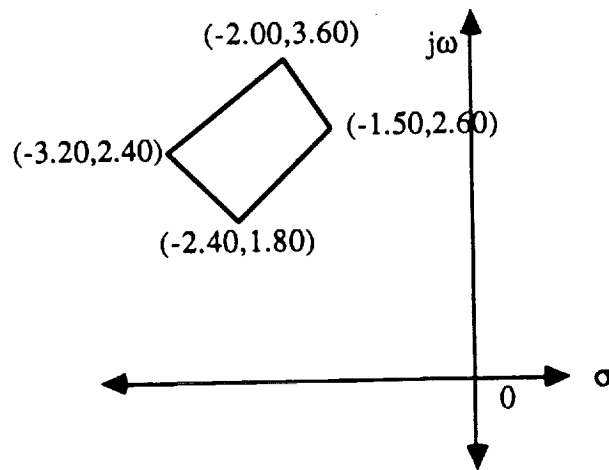
Figure 14. Closed loop poles in s-domain

Imaginary

unit circle

(0.89,0.16)

(0.92,0.12)

(0.85,0.10)

Real

(0.88,0.08)
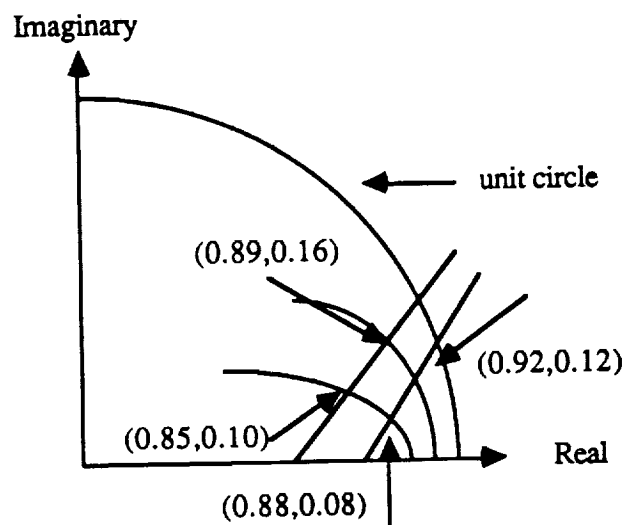
Figure 15. Closed loop poles in z-domain (T=0.05)

So far we have defined the behavior of the closed loop control system and related the Root Locus criterion to the adaptive part of our human response model. Although we have accomplished a desired result, it took a lot of assumptions to be able to get to this point. Unfortunately this is not sufficient. Now we will assume that the pilot's representation of the open loop aircraft dynamics can be modelled by a discrete difference equation based on the sampled available data of the input-output relation of the aircraft response. This is the identification part of the adaptive pilot model. We must also note that pilot does not know the aircraft dynamic equations nor the equations of motion exactly. He reasons on the information supplied and observed. For that purpose in the next chapter we will introduce a parameter estimation scheme based on discrete measurements.

4.0 ESTIMATION SCHEME

Kalman filter modelling is widely used in stochastic control. The idea is to model the system in question by a state and a measurement equation. The model can be fictitious but as long as it has the general form,

$$x_{k+1} = F_k x_k + G_k u_k + B_k w_k \qquad (4\text{–}1a)$$

$$y_k = C_k^T x_k + J_k u_k + D_k v_k \qquad (4\text{–}1b)$$

the theory can be applied. The unknown or unmeasurable states of the system are estimated with the information of input/output measurements and previous estimates. The basic assumptions on w_k and v_k are as follows: w_k and v_k are independent, zero mean, white-gaussian, random noises, and

$$E[w_k w_j^T] = Q_k \delta_{k-j} \qquad (4\text{–}2a)$$

$$E[v_k v_j^T] = R_k \delta_{k-j} \qquad (4\text{–}2b)$$

where $E[f]$ denotes the expected value of the variable f. If the noises are not white, the theory is still available by adding extra states to the state equation that characterize the spectrum of the noise by the innovations approach provided that the frequency spectrum of the noises are known[20].

Both Anderson[21] and Goodwin-Sin[22] discussed a state model for the parameter estimation purposes where all the unknown plant parameters are put in the state equation in the following way,

$$\theta_{k+1} = \theta_k + w_k \qquad (4\text{–}3)$$

and any measurement of the known plant characteristics are modelled by the measurement equation,

$$z_k = H_k^T \theta_k + v_k \tag{4-4}$$

We have found this model approach to be quite effective after extensive simulation on discrete and sampled data systems. The convergence rates are found to be faster than the Recursive Least Square (RLS) estimator schemes we tried, and the estimates agreed with the parameters of the simulated system. By appropriate selection of the noise covariances of this filter, the RLS filter can also be obtained. The basic assumptions on w_k and v_k apply. Once the estimation is put into the form of a Kalman filter, all the properties of the Kalman filter theory can be used such as the best linear estimator property of the Kalman filter and the convergence of the estimates.

If the unknown plant parameters and plant measurements can be put into the formulation,

$$\theta_{k+1} = \theta_k + w_k \tag{4-5a}$$

$$z_k = H_k^T \theta_k + v_k \tag{4-5b}$$

we can use the following Kalman filter equations for the estimation of the plant dynamics, given as,

$$K_k = P_k H_k [H_k^T P_k H_k + R_k]^{-1} \tag{4-6a}$$

$$\hat{\theta}_{k+1} = \hat{\theta}_k + K_k[z_k - H_k^T \hat{\theta}_k] \tag{4-6b}$$

$$P_{k+1} = P_k - K_k H_k^T P_k + Q_k \tag{4-6c}$$

No restrictions on the order of the state vector and the amount of measurements are required. The filter is started with the initial conditions on the covariance matrix and

estimates, namely with $P_0, \hat{\theta}_0$. The estimates are updated by the equations (4-6a), (4-6b) and (4-6c) at each measurement to be taken at discrete sampling frequencies.

The choice of R_k and Q_k are the preliminary determinations on how the filter will behave. The covariance of the measurement noise v_k determines the quality of the measurements. For example if $R_k=0$, then there is no measurement noise. The choice of $Q_k=0$ drops the state equation to

$$\theta_{k+1} = \theta_k \qquad (4-7)$$

which means that the system is a Linear Time Invariant (LTI) system. This can also be observed from the covariance update in equation (4-6c). The value of Q_k is added to the covariance so that it does not vanish by converging to zero. If the covariance matrix is zero, then the estimate can not change an undesirable situation. By keeping Q_k non-zero, the filter can estimate the parameters of time-varying systems. P_0 and Q_k are usually assumed to be diagonal matrices, namely, $P_0=p_0 I$ and $Q_k=\rho_k I$, p_0 is some big positive number while ρ_k is some small positive number.

We will now investigate different types of configurations for the estimation process.

4.1 Applications

4.1.1 SISO Case

Suppose the input and output relationship of a discrete system can be given by the following difference equation,

$$y_k = \sum_{i=1}^{n} a_i(k) y_{k-i} + \sum_{j=d}^{m+d} b_j(k) u_{k-j} \tag{4-8}$$

Then choose,

$$\theta_k = [a_1(k) \ldots a_n(k) b_d(k) \ldots b_{m+d}(k)]^T \tag{4-9a}$$
$$H_k = [y_{k-1} \ldots y_{k-n} u_{k-d} \ldots u_{k-m-d}]^T \tag{4-9b}$$

The resulting filter equations are given by,

$$K_k = P_k H_k [H_k^T P_k H_k + R_k]^{-1} \tag{4-10a}$$
$$\hat{\theta}_{k+1} = \hat{\theta}_k + K_k [y_k - H_k^T \hat{\theta}_k] \quad \text{with } \hat{\theta}_0 \tag{4-10b}$$
$$P_{k+1} = P_k - K_k H_k^T P_k + Q_k \quad \text{with } P_0 \tag{4-10c}$$
$$H_{k+1} = [y_k \ldots y_{k-n+1} u_{k-d+1} \ldots u_{k-m-d+1}]^T \tag{4-10d}$$

It is easily seen that if $R_k=1$ and $Q_k=0$, the above filter is exactly the RLS estimator. Unfortunately the estimator can not be run off-line because the vector H_k, or the regressor, is a function of the previous measurements of the system input and output.

4.1.2 MIMO Case

Assume that a MIMO discrete system can be characterized by the following difference equation,

$$y_k^p = \sum_{l=1}^{L} \sum_{i=1}^{n_l} a_i^{pl}(k) y_{k-i}^l + \sum_{l=1}^{M} \sum_{j=d_l}^{m_l+d_l} b_j^{pl}(k) u_{k-j}^l \qquad p=1 \ldots L \tag{4-11}$$

where there are L outputs and M inputs, i^{th} output and j^{th} input are y_k^i, u_k^j, respectively. We have two choices to model this system: we can put all the unknown parameters in one big state equation, or we can separate the state equations into smaller parts of each representing the unknown parameters for one output equation. Although it looks hard to put into words, it is easier to see by the following definitions,

$$\theta_k^p = [a_1^{p1}(k) \cdot \cdot a_n^{p1}(k)\ a_1^{p2}(k) \cdot \cdot a_n^{p2}(k) \ldots a_1^{pL}(k) \cdot \cdot a_n^{pL}(k)$$

$$b_d^{p1}(k) \cdot \cdot b_{m+d}^{p1}(k)\ b_d^{p2}(k) \cdot \cdot b_{m+d}^{p2}(k) \ldots b_d^{pL}(k) \cdot \cdot b_{m+d}^{pL}(k)]^T \tag{4-12a}$$

$$p=1 \ldots L$$

$$H_k = [y_{k-1}^1 \cdot \cdot y_{k-n}^1\ y_{k-1}^2 \cdot \cdot y_{k-n}^2 \ldots y_{k-1}^L \cdot \cdot y_{k-n}^L$$

$$u_{k-d}^1 \cdot \cdot u_{k-m-d}^1\ u_{k-d}^2 \cdot \cdot u_{k-m-d}^2 \ldots u_{k-d}^L \cdot \cdot u_{k-m-d}^L]^T \tag{4-12b}$$

where $d=\min(d_1 \ldots d_L)$, $n=\max(n_1 \ldots n_L)$, $m=\max(m_1 \ldots m_L)$. This suggests that there are L separate estimators, each having the same form but calculated independently. Now recall that the original Kalman gain equation and covariance update equation involve only H_k. So by appropriate assumptions, the gain and covariance update equations of these separate estimators can be calculated only once and used for the estimate updates, only if the initial covariances are the same for all of the estimators, but this value is re-definable and one can assume that all the initial uncertainities are the same. Goodwin and Sin (1984) discuss such a simplification.

The final form of the equations is as follows,

$$K_k = P_k H_k [H_k^T P_k H_k + R_k]^{-1} \tag{4-13a}$$

$$\hat{\theta}_{k+1}^l = \hat{\theta}_k^l + K_k [y_k^l - H_k^T \hat{\theta}_k^l] \quad \text{with } \hat{\theta}_0^l \quad l = 1 \ldots L \tag{4-13b}$$

$$P_{k+1} = P_k - K_k H_k^T P_k + Q_k \quad \text{with } P_0 \tag{4-13c}$$

$$H_{k+1} = [y_k^1 \cdot \cdot y_{k-n+1}^1 \ y_k^2 \cdot \cdot y_{k-n+1}^2 \ldots y_k^L \cdot \cdot y_{k-n+1}^L$$
$$u_{k-d+1}^1 \cdot \cdot u_{k-m-d+1}^1 u_{k-d+1}^2 \cdot \cdot u_{k-m-d+1}^2 \cdots u_{k-d+1}^L \cdot \cdot u_{k-m-d+1}^L]^T \tag{4-13d}$$

4.1.3 Estimating the Parameters of STATE-OUTPUT Equations

It is sometimes necessary to have some information of the parameters of state and output matrices of a time-varying plant. Such an application may be the adaptive-optimal control. At each sample by the current values of the time-varying state and output equation parameters, the discrete Ricatti equation is solved, and the solution is used for the control of the system.

Assume that a time-varying discrete system can be modelled by the following n-state, m-input state equation:

$$x_{k+1} = F_k x_k + G_k u_k \tag{4-14}$$

Given the state and the input measurements, x and u we wish to estimate the parameters of the state and input matrices, F and G. Let us re-write the equation (4-14) in terms of x_k, as,

$$x_k = F_{k-1} x_{k-1} + G_{k-1} u_{k-1} \tag{4-15}$$

Then the lth state equation will be,

$$x_k^l = \sum_{i=1}^{n} f_{li}(k-1) x_{k-1}^i + \sum_{j=1}^{m} g_{lj}(k-1) u_{k-1}^j \tag{4-16}$$

or if,

$$\theta_k^l = [f_{l1}(k-1) \ldots f_{ln}(k-1) g_{l1}(k-1) \ldots g_{lm}(k-1)]^T \tag{4-17a}$$

$$H_k = [x_{k-1}^1 \ldots x_{k-1}^n u_{k-1}^1 \ldots u_{k-1}^m]^T \tag{4-17b}$$

$$x_k^l = H_k^T \theta_k^l \quad l=1 \ldots n \tag{4-17c}$$

Then we can use the same argument of MIMO case to have the following equations for the estimation of the unknown parameters:

$$K_k = P_k H_k [H_k^T P_k H_k + R_k]^{-1} \tag{4-18a}$$

$$\hat{\theta}_{k+1}^l = \hat{\theta}_k^l + K_k [x_k^l - H_k^T \hat{\theta}_k^l] \quad \text{with } \hat{\theta}_0^l \quad l=1 \ldots n \tag{4-18b}$$

$$P_{k+1} = P_k - K_k H_k^T P_k + Q_k \quad \text{with } P_0 \tag{4-18c}$$

$$H_{k+1} = [x_k^1 \ldots x_k^n u_k^1 \ldots u_k^m]^T \tag{4-18d}$$

In the same way the p-output equation

$$y_k = C_k x_k + D_k u_k \tag{4-19}$$

can be put into a parameter estimation scheme structure by the following definitions,

$$\theta_k^i = [c_{i1}(k) \ldots c_{in}(k) d_{i1}(k) \ldots d_{im}(k)]^T \tag{4-20a}$$

$$H_k = [x_k^1 \ldots x_k^n u_k^1 \ldots u_k^m]^T \tag{4-20b}$$

$$y_k^i = H_k^T \theta_k^i \quad i=1 \ldots p \tag{4-20c}$$

to have the filter equations,

$$H_k = [x_k^1 \ldots x_k^n u_k^1 \ldots u_k^m]^T \tag{4-21a}$$

$$K_k = P_k H_k [H_k^T P_k H_k + R_k]^{-1} \tag{4-21b}$$

$$\hat{\theta}_{k+1}^i = \hat{\theta}_k^i + K_k [y_k^i - H_k^T \hat{\theta}_k^i] \quad \text{with } \hat{\theta}_0^i \quad i=1 \ldots p \tag{4-21c}$$

$$P_{k+1} = P_k - K_k H_k^T P_k + Q_k \quad \text{with } P_0 \tag{4-21d}$$

4.2 Computational Aspects

Let us examine the gain and covariance update equations and how to implement them since the parameter update is relatively easier to handle with respect to the others. Recall equations (4-6a) and (4-6c):

$$K_k = P_k H_k [H_k^T P_k H_k + R_k]^{-1} \tag{4-22a}$$

$$P_{k+1} = P_k - K_k H_k^T P_k + Q_k \tag{4-22b}$$

They have the common expression $P_k H_k$. If we rename this quantity with a temporary variable, T_k, then equations become,

$$T_k = P_k H_k \tag{4-23a}$$

$$K_k = T_k [H_k^T T_k + R_k]^{-1} \tag{4-23b}$$

$$P_{k+1} = P_k - K_k T_k^T + Q_k \tag{4-23c}$$

The efficiency of an algorithm is often judged by the number of operations necessary to carry one update of the parameters. Assume that the order of the state vector is N. Table (1) shows the required operations of each equation in the estimator.

To summarize, for each application of the Kalman filter parameter estimator scheme, Table (2) shows the total number of operations. The latter argument includes the

effect of a symmetric covariance matrix which obviously reduces the necessary operations.

Table 1. Number of operations for the Kalman Filter Parameter Estimator

Equation	(*,/)	(+,-)
$T_k = P_k H_k$	N^2	$N(N-1)$
$K_k = T_k[H_k^T T_k + R_k]^{-1}$	$2N$	N
$\hat{\theta}_{k+1} = \hat{\theta}_k + K_k[z_k - H_k^T \hat{\theta}_k]$	$2N$	$2N$
$P_{k+1} = P_k - K_k T_k^T + Q_k$	$N(N+1)/2$	$N + N(N+1)/2$
Total	$1.5N^2 + 4.5N$	$1.5N^2 + 3.5N$

Table 2. Total operations for the Kalman Filter Parameter Estimators

TYPE	N	(*,/)	(+,-)
SISO	$n+m$	$1.5N^2 + 4.5N$	$1.5N^2 + 3.5N$
MIMO	$Ln+Mm$	$1.5N^2 + (2.5+2L)N$	$1.5N^2 + (1.5+2L)N$
STATE	$n+m$	$3.5N^2 + 2.5N$	$3.5N^2 + 1.5N$
OUTPUT	$n+m$	$1.5N^2 + (2.5+2p)N$	$1.5 + (1.5+2p)N$

To demonstrate the algorithm, we will take the case of SISO and apply the filter (see Appendix C). Now we will simplify the above equations where P_k is replaced by a linear array of length $N(N+1)/2$ to take the advantage of its symmetry. Consider the following mapping,

$$P = \begin{bmatrix} p_{11} & & & \\ p_{21} & p_{22} & & \\ p_{31} & p_{32} & p_{33} & \\ \vdots & & & \end{bmatrix}$$

$$P_{LINEAR} = \begin{bmatrix} p_{11} & p_{21} & p_{22} & p_{31} & p_{32} & p_{33} & \cdots \end{bmatrix}$$

The location of the equivalent linear array is found from the symmetric array's indices by the following equation,

$$P(i,j) = \begin{cases} P_{LINEAR}(i \times (i-1)/2 + j) & \text{if } i \geq j \\ P_{LINEAR}(j \times (j-1)/2 + i) & \text{else} \end{cases} \qquad (4\text{--}24)$$

Notice that although we are introducing extra arguments to be calculated, the necessary storage is reduced from N^2 to $N(N+1)/2$ for the covariance matrix P_k, and the remaining $N(N-1)/2$ storage can be used for the temporary variable T_k ($N(N-1)/2 \geq N$ for $N \geq 3$). Furthermore equation (4-24) requires only integer operations as opposed to the floating point calculations which are the most time consuming operations.

Let us examine the evaluation of T_k. The lth component of T_k is given by,

$$t^l = \sum_{i=1}^{N} P[l,j] \times H[j].$$

So starting from the first element, the following sequences relate the referred indices of the covariance matrix to the index of the linear equivalent covariance array,

l	sequence
1	(1, 2, 4, 7,11,16, ...)
2	(2, 3, 5, 8,12,17, ...)
3	(4, 5, 6, 9,10,18, ...)
4	(7, 8, 9,10,14,19, ...)
5	(11,12,13,14,15,20, ...)
6	(16,17,18,19,20,21, ...)
⋮	

Then we can simplify this procedure by a recursive sequence formulation, $s(i,j)$, because when it comes to evaluate the covariance matrix one needs the exact locations of the matrix indices and that can be simplified.

The first column is given by,

$$s(l,1) = s(l-1,1)+l-1, \quad s(0,1) = 1.$$

So $s(1,1)=1+1-1=1$, $s(2,1)=1+2-1=2$, $s(3,1)=2+3-1=4$, and so on. In the same formulation, the rows are given by,

$$s(l,k) = \begin{cases} s(l,k-1)+1 & 1 \leq k \leq l \\ s(l,k-1)+k-1 & k > l \end{cases}.$$

Thus for the third row, as an example, $s(3,1)=4$. Then $s(3,2)=4+1=5$, $s(3,3)=5+1=6$, $s(3,4)=6+4-1=9$, $s(3,5)=9+5-1=13$, etc..

If a similar argument is made on the evaluation of the covariance, which is rather simple after the recursive sequence is formulated, the algorithm can be simplified by taking the recursivity and the linear array formulation into account (see Appendix D).

Finally, we wish to consider the real time application of the above algorithms. It is certain that, as in every "current estimator", after the measurements are taken, a certain computation time must be taken into consideration. Only after the necessary calculations are made, a new estimate is available, and that might be a disadvantage where on-line adaptation is to be applied to the system.

Consider the SISO case of section (4.1.1). Suppose that the Kalman gain K_k was already calculated before the measurements are taken. Then the estimates can be updated just after the measurements with a small time delay for the necessary calculations. This is possible if the regressor H_k is not a function of the current values of the input and output, namely y_k and u_k, which implies that $d \geq 1$. In that case we have the following filter equations:

$$\hat{\theta}_{k+1} = \hat{\theta}_k + K_k[z_k - H_k^T\hat{\theta}_k] \tag{4-25a}$$

$$P_{k+1} = P_k - K_kH_k^TP_k + Q_k \tag{4-25b}$$

$$\text{update } H_{k+1} \tag{4-25c}$$

$$T_{k+1} = P_{k+1}H_{k+1} \tag{4-25d}$$

$$K_{k+1} = T_{k+1}[H_{k+1}^TT_{k+1} + R_{k+1}]^{-1} \tag{4-25e}$$

The time indices of the gain equation are increased and placed properly after the covariance update equation.

Now assume that H_k has terms involving the current values of input u_k, then partition the matrices in such a way that most of the calculations can be done before u_k is available.

The following are the equations emphasizing the latter argument:

$$T_k = T_k + P_k \begin{bmatrix} u_k \\ 0 \end{bmatrix}$$

$$\delta_k = \delta_k + \begin{bmatrix} u_k \\ 0 \end{bmatrix} T_k + R_k$$

$$K_k = T_k \delta_k^{-1}$$

$$\varepsilon_k = z_k - [u_k \quad 0]\hat{\theta}_k - \varepsilon_k$$

$$\hat{\theta}_{k+1} = \hat{\theta}_k + K_k \varepsilon_k$$

$$P_{k+1} = P_k - K_k T_k^T + Q_k$$

$$H_{k+1} = [0 \quad y_k \cdots y_{k-n+1} u_k \cdots u_{k-m+1}]^T$$

$$T_{k+1} = P_{k+1} H_{k+1}$$

$$\varepsilon_{k+1} = H_{k+1}^T \hat{\theta}_{k+1}$$

$$\delta_{k+1} = H_{k+1}^T T_{k+1}$$

In other words the above simplification ignores the effect of u_k in the equations until it becomes available.

4.3 Examples

Consider the second order sampled data system ($T=0.05$ sec) characterized by the difference equation,

$$y_k = a_1(k)y_{k-1} + a_2(k)y_{k-2} + b_1(k)u_{k-1}$$

where the parameters $a_1(k)$, $a_2(k)$ and $b_1(k)$ are to be estimated based on input-output measurements. Figures (16), (17) and (18) show the Kalman Filter (with $Q_k = 10^{-20}I$, $P_0 = 10^3 I$, $\hat{\theta}_0 = 0$), together with the RLS (with $P_0 = 10^3 I$, $\hat{\theta}_0 = 0$) results for a Gaussian random sequence input (persistent excitation). No measurement noise is

assumed. The same system is simulated by a step input and the results are given in Figures (19), (20), (21).

It is observed that, for the persistent excitation case, the Kalman Filter follows the step changes in the parameters, and converges to the actual parameter values. However, for the case where the system is derived by a step input, the estimates have offset values, but the number of discrete frequencies in the input sequence strictly affect the number of identifiable paremeters[23]. Nevertheless, the Kalman Filter follows the changes in each case where the RLS estimator fails to respond to the parameter changes in both of the cases. Furthermore, a simple analysis shows that, the resulting transfer function given by the Kalman Filter estimates for the step input matches the actual transfer function for low frequency regions.

Consider the following system (ball-in-the-hoop) given by the state equation,

$$
\begin{bmatrix} \dot{\theta}(t) \\ \ddot{\theta}(t) \\ \dot{\Psi}(t) \\ \ddot{\Psi}(t) \end{bmatrix} = F \begin{bmatrix} \theta(t) \\ \dot{\theta}(t) \\ \Psi(t) \\ \dot{\Psi}(t) \end{bmatrix} + G\ u(t)
$$

where

$$
F = \begin{bmatrix} 0.0 & 1.0 & 0.0 & 0.0 \\ 0.0 & -1.7518 & -3.936 & 0.0 \\ 0.0 & 0.0 & 0.0 & 1.0 \\ 0.0 & -0.6029 & -75.66 & 0.0 \end{bmatrix}
$$

$$
G = \begin{bmatrix} 0.0 \\ 29.094 \\ 0.0 \\ 100.14 \end{bmatrix}
$$

The system is sampled at T=0.10 sec., and excited by a step input to identify the parameters of the state and input matrices. Five state measurements were taken (see Table (3)).

Table 3. State measurements of "ball-in-the-hoop" system

Time	$\theta(t)$	$\dot{\theta}(t)$	$\Psi(t)$	$\dot{\Psi}(t)$
0.00	0.000000	0.000000	-1.000000	0.000000
0.10	0.154597	2.978369	-0.601010	7.439874
0.20	0.570984	6.789393	0.302242	9.448706
0.30	1.176426	5.223810	1.055641	4.641170
0.40	1.915283	7.950068	1.115215	-3.537536
0.50	2.764527	9.048253	0.431920	-9.266817

The estimates of the state and input matrices are given in (Appendix E) where the Kalman Filter was used as a parameter estimator. The final estimates (t=0.50) match the parameters of the equivalent sampled data system. Also note that the order of the covariance matrix is 5(=4+1), not 20(=4^2+4).
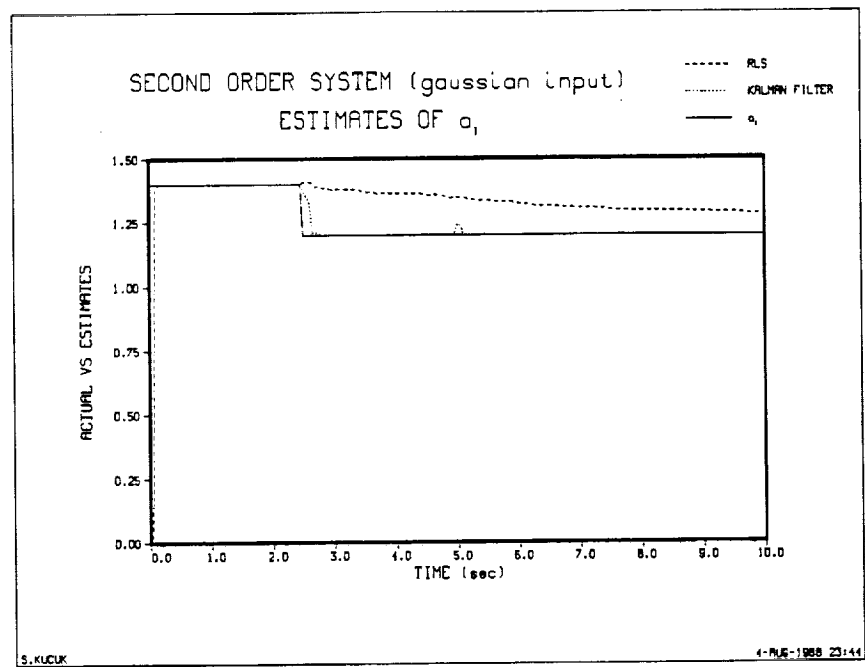
Figure 16. Kalman Filter vs RLS estimate of a_1, (Gaussian input)
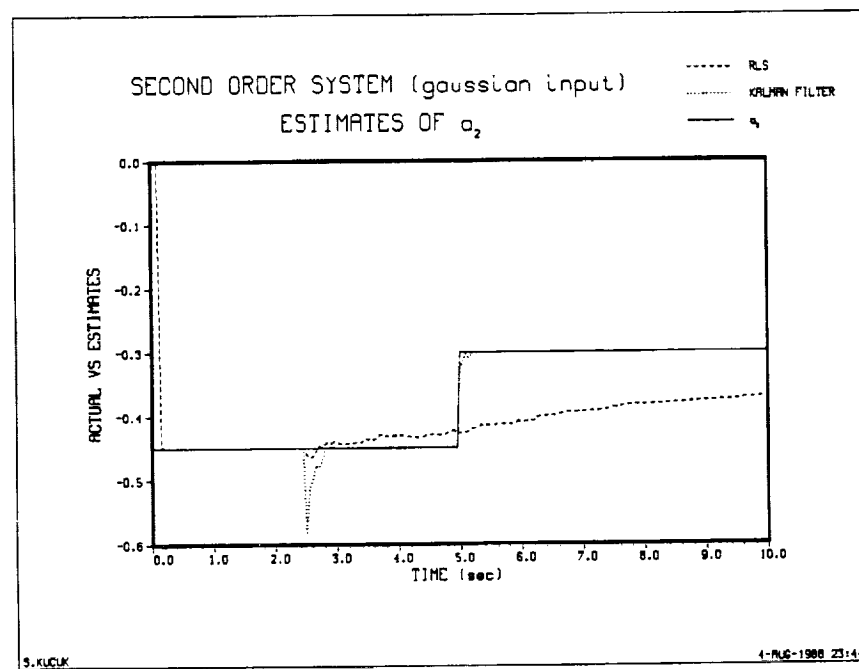
Figure 17. Kalman Filter vs RLS estimate of a_2, (Gaussian input)
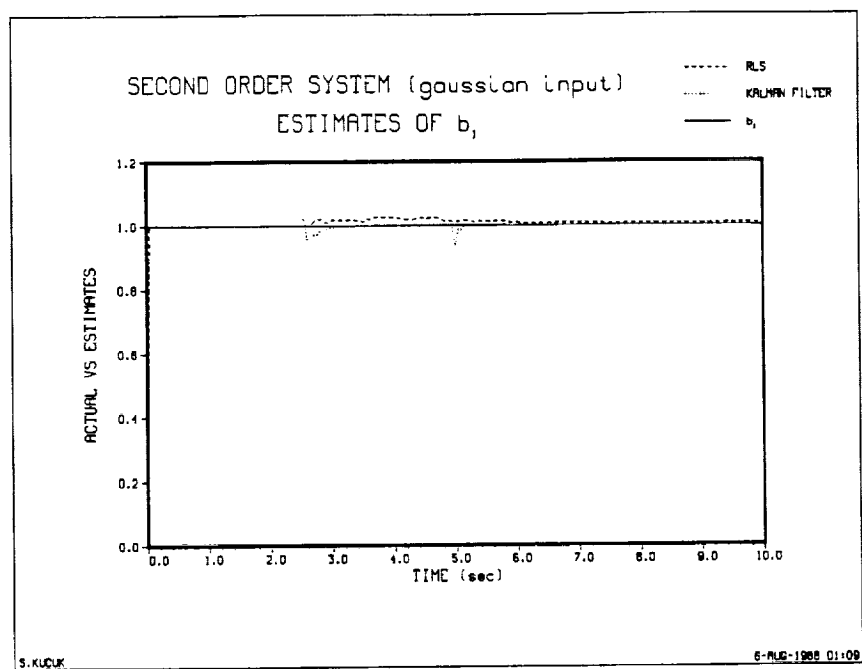
Figure 18. Kalman Filter vs RLS estimate of b_1, (Gaussian input)
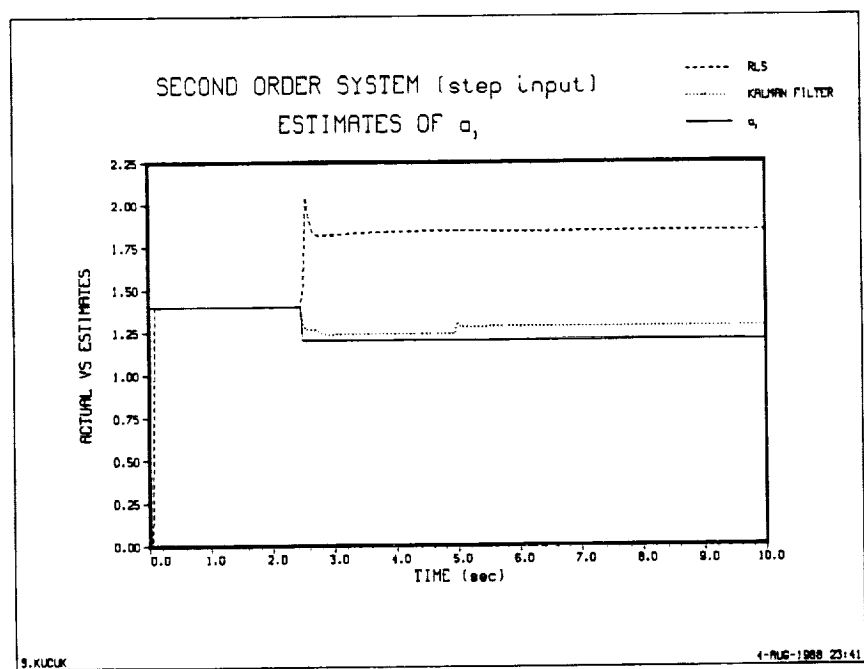
Figure 19. Kalman Filter vs RLS estimate of a_1, (Step input)
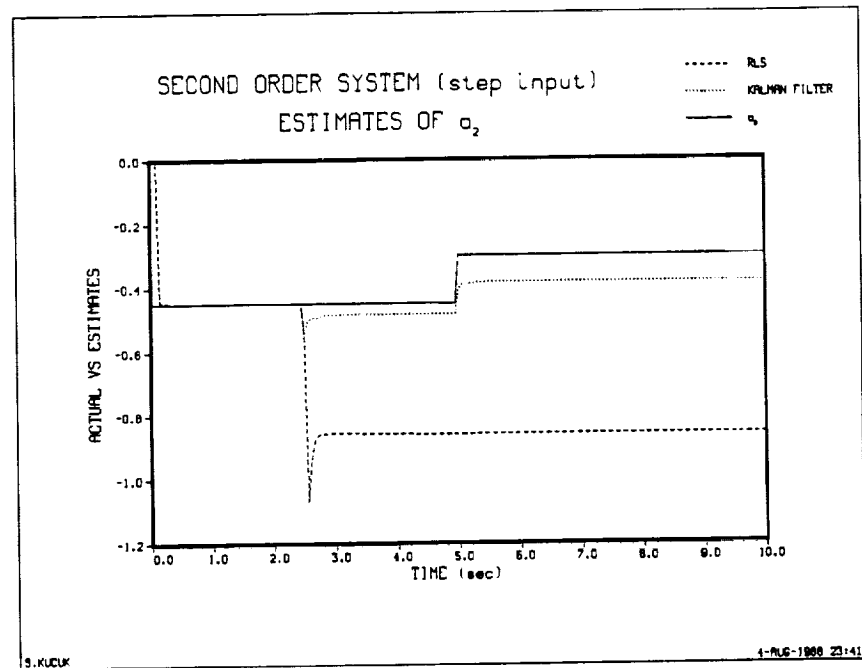
Figure 20. Kalman Filter vs RLS estimate of a_2, (Step input)
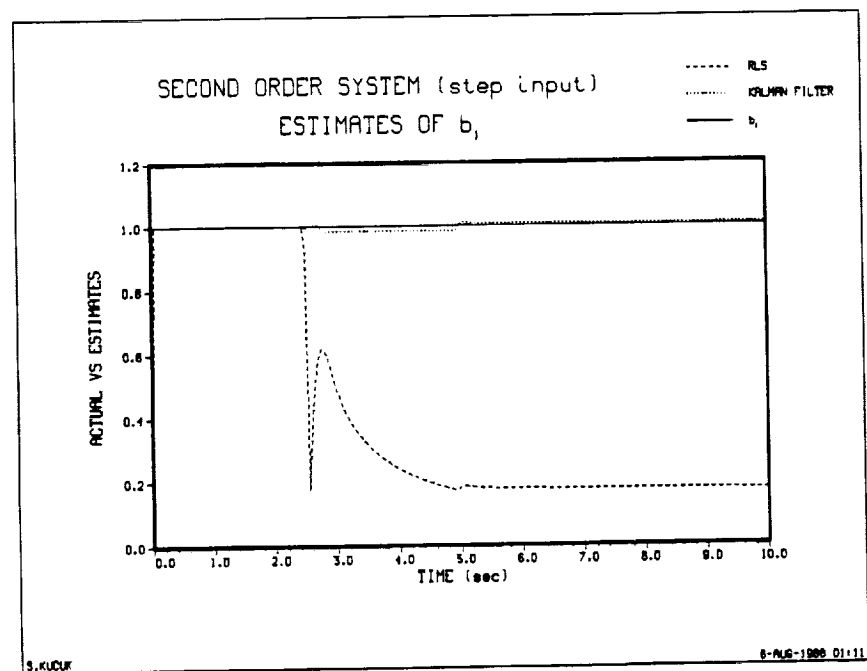
Figure 21. Kalman Filter vs RLS estimate of b_1, (Step input)

5.0 THE ADAPTIVE PILOT MODEL

In this chapter we will combine the adaptive pilot model with the discrete McRuer-Krendel human describing model derived in Chapter 2, the Root Locus criterion and the closed loop operating regions defined in Chapter 3, and the estimation scheme discussed in Chapter 4.

In Section (2.3), the adaptation process was divided into two groups. The first was the detection and identification. The adaptive model that will be developed, will have a discrete time difference equation for the identification which is derived by the detector. The detector monitors the control displacement of the pilot and the rate of the error signal which is proportional to the controlled element's output value. This can be through the instrumentation or through the senses or a combination. If there is any uncertainity in the detection, like trying to observe visual feedback in the dark, the identification must be done accordingly to include the effect of measurement error.

The most important part of the adaptation procedure is the modification and optimization, although we can not separate any of the parts of the adaptation because any failure of one will directly affect the whole procedure. In Chapter 3, we related the closed loop human-aircraft modes to the adaptive pole-zero pair of the human response model as a function of the controlled element dynamics. The closed loop bandwidth has a nominal value which the pilot knows from his experience. He knows that if the controls are pushed faster than some value, which he must have estimated by that time, then the aircraft will be responding in a "sluggish" way or the responses will be too fast where there may be oscillations or the forces on the aircraft may be dangerous. If he fails to

react slower than some value, then the aircraft may fail to respond in time for the proper action. Thus the pilot knows what to do when it comes to maneuvering the aircraft. The responses can not be too slow or too fast but must be in the proper operating region. Any optimization must be within this region. If the aircraft denies any attempt to operate in that region, the pilot must decide to relocate the operating region as safely as possible.

Keeping these facts in mind, our modification procedure must do the appropriate selection of the closed loop bandwidth, equivalently the dominant closed loop poles. The key element will be the necessary pilot gain required to perform a certain maneuver. If the pilot gain is bigger than some value, then closed loop pole must be changed. This can be related to the gain equation (3-15) of Section (3.1). The pilot gain is proportional with the magnitude of the denominator dynamics and inversely proportional with the numerator dynamics of the controlled element. A big gain then indicates that the controlled element has some resonances at the desired closed loop frequencies. Relating the latter argument to the root locus is the case where the pole and the open loop system zero of the plant are very close to each other.

On the other hand, if the required pilot gain is too small, this indicates that the plant has already modes at the desired closed loop location. This might be dangerous because the pilot can not maintain control. The aircraft responds, but the pilot is not totally in charge.

Therefore in any of the above cases, the judgment must be made on the desired operating poles. Once the selection does not contradict the limits of the region, then the necessary phase required from the adaptive pole-zero pair is determined. The rest is the optimal solution for the pole and zero that will satisfy the phase constraint and minimize

the error signal. The corresponding procedure defining our adaptive pilot model is given in Figure (22).
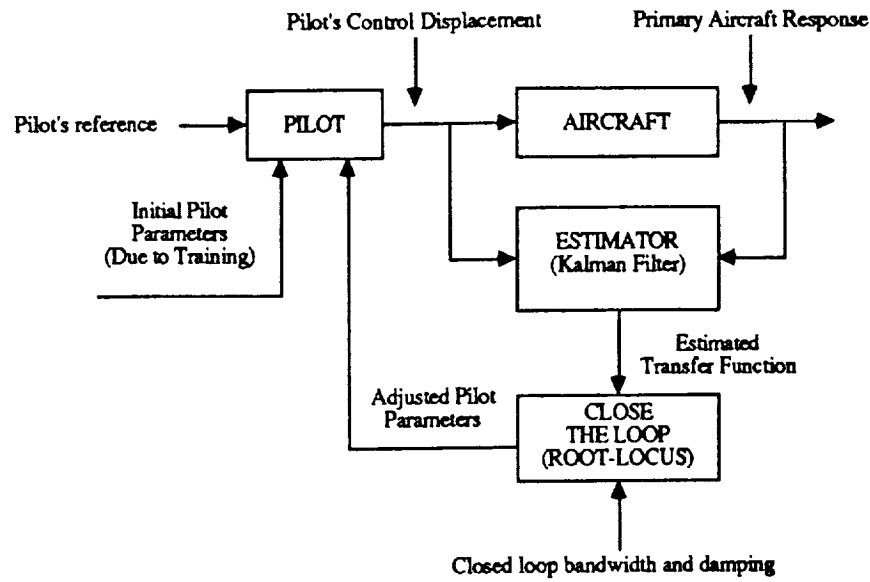
Figure 22. The Adaptive Pilot Model

Let us examine the processes in the adaptive model. As soon as the error signal is active, the adaptation begins. The error signal is held until the current information is processed and the control is applied. The error is then delayed because of the pilot's visual lags. The current estimate of the controlled element dynamics from the Kalman filter estimator is used to get information on the frequency content at the desired closed loop pole. This pole is the nominal operating value. Since we related the adaptation to the root locus criterion, the estimate of the open loop transfer function is used to evaluate the value of equation (3-8). This gives the part of the phase necessary which is not determined by the pilot in equation (3-9). Then the type of gain is selected depending on

the relative change of the primary response variable. The difference gives the phase that must be provided by the adaptive pole-zero of the human response mechanism, but first the absolute magnitude of the gain must be checked to make sure that pilot does not use the limits of the controls, or he does not have to provide extensive gain to move the controls. If the latter occurs, then this requires the pole-relocation procedure. Until the gain is in the allowable limits, the closed loop pole is moved in the operating region. Then the phase required by the pole and zero pair is fixed. The rest is the optimization problem. The values of the zero and pole are searched that will minimize the error signal and at the same time supplying the desired phase difference to close the loop at the desired closed loop pole. After the adaptive part of the human response is evaluated, the output is sent to the neuro-muscular equivalent of the model which sends the appropriate commands through the nerves to the muscles to perform the desired task. Finally the adaptive model is ready to process another error signal, and this goes on until the steady state is reached or the desired maneuvering is fulfilled.

The problem now is to give the model some initial knowledge to start the algorithm. This is the analogy to pilot training. The adaptive model needs some initial values of the model parameters so that they will be used until adaptation is necessary or the estimators converge to give reliable estimates of the controlled element dynamics. Nevertheless, this is a primitive attempt to describe pilot training. A real pilot, depending on the scenario, would not only adjust the initial values of parameters ($H_p(s; t=t_0)$), but also start the control sequence properly ($\{u_p(t); t_0 \leq t \leq T_f\}$). Unfortunately, we do not have the starting control sequence, but an expert system would.

The initial parameters are calculated, as we mentioned earlier, by aircraft testing at the desired flight envelope and using low order approximations to design the pilot

parameters via root locus techniques. These are used as the static part of the pilot model which are subject to change. This is actually what happens in real pilot control. The pilot has a pre-determined idea of how the aircraft will behave at that operating region. So he moves the controls depending on this information. But if he fails to succeed in the maneuvering, by monitoring the input-output relationship, he adjusts to the changing environment. The flowchart in Figure (23) demonstrates the adaptation algorithm.

To conclude this chapter we will mention the multivariable manual control case. The pilot actually resorts to controls depending on the configuration and he uses the best combination possible to maintain the controllability, stability and the performance. This means that he can, and will, use more than one control at a time; for example while in the coordinated turn he uses the longitudinal and lateral sticks by one hand, the rudder pedals by his feet, and the throttle or nozzle settings by the other hand whenever necessary. We will simulate this multivariable control case by having more that one single variable loop, each closing the loop from the primary response variable to the corresponding pilot input. The multivariable pilot loops are shown in Figure (24). This seems to be a good approximation where the pilot is required to fulfill simple maneuvers over the aircraft speed, altitude or the angular positioning. Although the single variable loops do not affect each other directly, one's output will change the other through the dynamic equations. Furthermore we will add constraints about the behavior of the aircraft state for the optimization problem of each one of the adaptive loops so that better results can be obtained. In the next chapter, we will give some examples on how to design the static pilots and simulate them in the Harrier AV-8B environment to perform simple tasks. The control loops will be multivariable loops. We will compare the static pilots by the adaptive pilots and discuss the results.
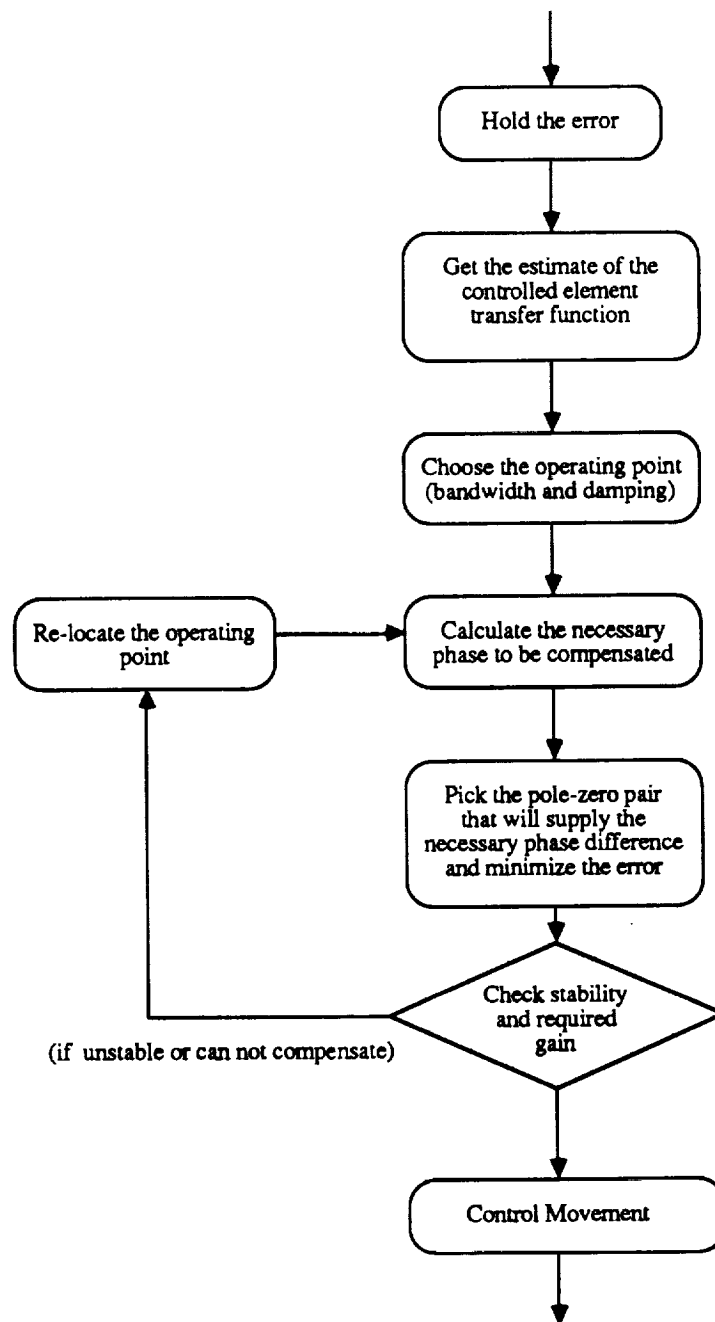
Figure 23. Flowchart of the adaptive pilot model
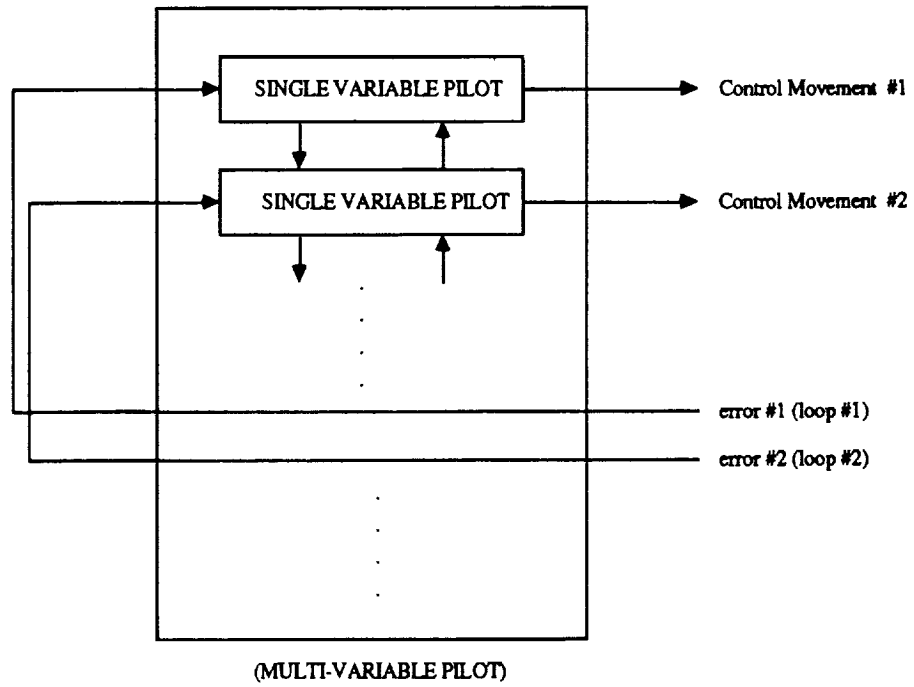
Figure 24. Multivariable pilot configurations

6.0 PILOT INSERTIONS

6.1 Selection of the control sets

An analysis of the Harrier AV-8B control system suggests the following: since the aircraft is symmetric, any movement of the longitudinal stick (to the elevator or stabilizer) creates longitudinal motions. Engine nozzle angle, which is the most important aspect of thrust vectoring, a unique feature of the Harrier AV-8B, is also symmetric. There are four nozzles, having two symmetric openings on each side of the aircraft, but not creating any lateral moments since only forward and downward components of the force changes in the equations of motion. Thrust, which affects the magnitude of the forces at the nozzles, must also have longitudinal effects since it is only adding force in the direction of the main thrust vector. Therefore the longitudinal pilot is characterized by controlling the stabilizer (longitudinal stick), engine throttle setting and nozzle angle setting. We will now investigate the primary variables of the longitudinal control set which means that by checking the responses of the aircraft, the primarily affected states from the control input are to be selected.

Let us examine the stabilizer first by testing the longitudinal stick through impulses. These tests will be taken from a trimmed flight condition which is very important. A trimmed aircraft is in equilibrium, and there are no accelerations (except the turbulances or changes in the relative wind) so that at this configuration small perturbation analysis can be performed. The length of the window is also important. As we mentioned earlier, the short period responses of the aircraft are perceptible to the

pilot. Furthermore since these tests are taken without a pilot in the loop, just the insertion of the required input sequence to the control units, the aircraft will go out of the trim conditions because of the disturbed motion unless new trim settings are determined. To summarize, we first trim the aircraft and then insert impulses to the controls one at a time and observe the aircraft responses within a small time window of three or may be four seconds length. This time interval will define the response of the aircraft shortly after the pilot has commanded. Also we will avoid numerator dynamics whenever possible in order to obtain simple all-pole transfer functions.

Consider the initial aircraft parameters, $(\Phi,\Theta,\Psi)=(0.0°,6.0°,0.0°)$, at 20.0 knots, with nozzles directed at 81.77°, 100 ft. above sea level. This is a low speed configuration in the transition region to the high speed mode where nozzle angles are close to vertical, pointing downwards, which means that most of the thrust is used for the lifting of the aircraft. This is an advantage of the Harrier AV-8B aircraft. By directing the nozzle angles, it can fly at very low speeds without any difficulty.

Figures (25), (26), (27) and (28) show the pitch, pitch velocity, altitude and the airspeed responses of the Harrier AV-8B for the longitudinal stick impulse. The stick movement changes the elevator (stabilizer) angle. There is also the effect of front and aft RCS valves, but we will consider the combined effect since the pilot observes these total changes in the responses.

Altitude change is almost negligible. The speed drop is approximately 0.1 knots per second, but this is also a side effect of pitching up. The pitch angle of the aircraft increases the vertical lift component of the thrust at the same time decreasing the forward thrust vector which as a result drops the forward velocity. This causes the relative speed

of the aircraft to drop significantly. Similarly, if the aircraft was pitching down, with only the stabilizer, then the speed would tend to increase.

The primary response of the stabilizer, and the main purpose, is the control of the pitch angle. This seems trivial because by adjusting the elevator angle, equivalently by directioning the "nose" of the aircraft, pitching moments are applied thus changing the pitch angle. If the pilot needs to pitch-up, he must pull the longitudinal stick. Conversely he pushes the stick to pitch-down. So the primary response is the pitch angle, and the remaining changes in altitude, forward and downward velocities, angle of attack are disturbances to be regulated for the case of the longitudinal stabilizer input.

From the control point of view, the pitch velocity response can be approximated by a first order pole which reduces the transfer function from the longitudinal stick to the pitch rate to be,

$$\frac{\delta_e(s)}{\theta(s)} \propto \frac{1}{s+a\{\theta,\delta_e\}} \tag{6-1}$$

The pitch angle is then given by the pure integration of the pitch rate:

$$\frac{\delta_e(s)}{\theta(s)} \propto \frac{1}{s(s+a\{\theta,\delta_e\})} \tag{6-2}$$

Next we will analyze the nozzle angle setting. Figures (29), (30), (31) and (32) show the airspeed, altitude, pitch angle and the pitch rate responses for a positive impulse on the nozzle angles. Slowing of the aircraft is reasonable since increasing nozzle angle means more power for lifting as in the case of a pitch-up command. While the pitch angle and altitude do not change too much, we notice a step-like response in the airspeed. The primary response then is observed to be the airspeed and this assumption confirms with

the Harrier AV-8B pilots. In fact, it seems obvious that by changing the effective angle of the main thrust vector, all the body axis forces of the aircraft change, and it is the fastest way to change the speed. However, the nozzle setting can also be used to control the altitude since by changing the downward speed component, the altitude can be adjusted. Also changes in nozzle angle setting applies pitching moments to be regulated.

The speed response can be approximated by a step within the region of our interest, resulting,

$$\frac{\delta_{\theta_j}(s)}{v_{eq}(s)} \propto -\frac{1}{s} \qquad (6\text{--}3)$$

Once again the other responses will be the regulating set. We must mention that the pilot may wish to control the aircraft, say the pitch angle, through the controls of the nozzle angles. That is possible, but we are only trying to model the most common configurations of the aircraft control mechanism. Of course the latter case can be modelled as a separate mode, and transfer functions can be obtained. However, it will not be a regular scheme.

In Section (1.2) we mentioned that the throttle setting is the most common input for altitude control. If the altitude is being controlled, then the feedback is from the altitude response. Otherwise, if the constraints are on the rate of the altitude, then the feedback is taken from the altitude rate response of the aircraft. Figures (33), (34), (35) and (36) show the rate of the altitude, altitude, pitch angle, and the airspeed results for a positive throttle impulse which controls the flow of the fuel to be combusted in the engine. Unlike the nozzle angle control, no noticeable effect can be seen in the pitch or the speed and that is the main reason for its use in altitude control. The approximated transfer functions are as follows:

$$\frac{\delta_{TH}(s)}{h(s)} \propto \frac{1}{s^2+2\xi\{h,\delta_{TH}\}\omega_n\{h,\delta_{TH}\}s+\omega_n^2\{h,\delta_{TH}\}} \qquad (6\text{--}4a)$$

$$\frac{\delta_{TH}(s)}{h(s)} \propto \frac{1}{s(s^2+2\xi\{h,\delta_{TH}\}\omega_n\{h,\delta_{TH}\}s+\omega_n^2\{h,\delta_{TH}\})} \qquad (6\text{--}4b)$$

A second order response is observed in the altitude rate, and altitude is the pure integral of this signal. Once again if the desired command is a change in the altitude, then altitude will be the feedback element. On the other hand, if the primary concern is on the rate of climb or descent, then the rate of the altitude is used in the feedback control.

The lateral control set is the lateral stick, which includes the effect of ailerons, and the RCS valves, and the rudder operated separately from the lateral stick through the pedals. The same aircraft with the initial rates is subjected to a positive impulse input at the ailerons, and Figures (37), (38), (39) and (40) show the corresponding roll angle, roll rate, yaw angle and the yaw rate responses. The primary response in this case is the roll angle. Transfer functions are estimated to be,

$$\frac{\delta_a(s)}{r(s)} \propto \frac{1}{s+a\{r,\delta_a\}} \qquad (6\text{--}5a)$$

$$\frac{\delta_a(s)}{\Phi(s)} \propto \frac{1}{s(s+a\{r,\delta_a\})} \qquad (6\text{--}5b)$$

The sideslip, yaw, yaw rate and roll angle changes are given in Figures (41), (42), (43) and (44) for a positive rudder pedal impulse. The sign of the rudder pedal input in this case implies the right or left pedal movements. Notice the change of the sideslip angle. Zero sideslip is very important, and it must be fulfilled whenever possible because it changes the aerodynamic behaviour of the aircraft. From outside of the aircraft the vehicle seems to slide in a direction not parallel to the fuselage. The wind then is exerted by an angle to the aircraft.

The primary response of the rudder is the sideslip angle for coordinating a turn and yaw angle for heading adjustments which can be approximated by the transfer functions given by:

$$\frac{\delta_r(s)}{\beta(s)} \propto \frac{1}{s(s+a\{\beta,\delta_r\})} \tag{6-6a}$$

$$\frac{\delta_r(s)}{\Psi(s)} \propto \frac{(s+b\{\Psi,\delta_r\})}{s^2(s+a\{\Psi,\delta_r\})} \tag{6-6b}$$

Thus we have examined all the controls supplied to the Harrier AV-8B pilot. However, there are also the assisting devices provided to the pilot like the SAS switch. The SAS unit adds a single pole to the mechanism and closes a feedback loop to the control unit before it is connected to the pilot stick input. This is a very limited control. In most of the cases the effect of the SAS control is within a 5% range so that it does not interfere with the pilot control so the pilot has full authority on the aircraft. But in cases where the pilot does not hold the stick continuously and incremental adjustments must be made to compensate the phugoid or the spiral mode, the SAS becomes quite useful. Although it can not hold the current configuration of the aircraft for a long period because of its limited authority, the SAS devices are used commonly at low speeds by the pilots. For that reason we will assume that the SAS is fully engaged in our simulations while using the Harrier AV-8B simulation program provided by NASA-Lewis. The above responses used for the approximate transfer function analysis were also taken with the SAS switch activated. Let us add that the SAS unit is inoperative at high speeds and high speed configuration is a very sensitive operating region. Therefore we will insert our pilot models to the simulation program at low speed operating conditions.
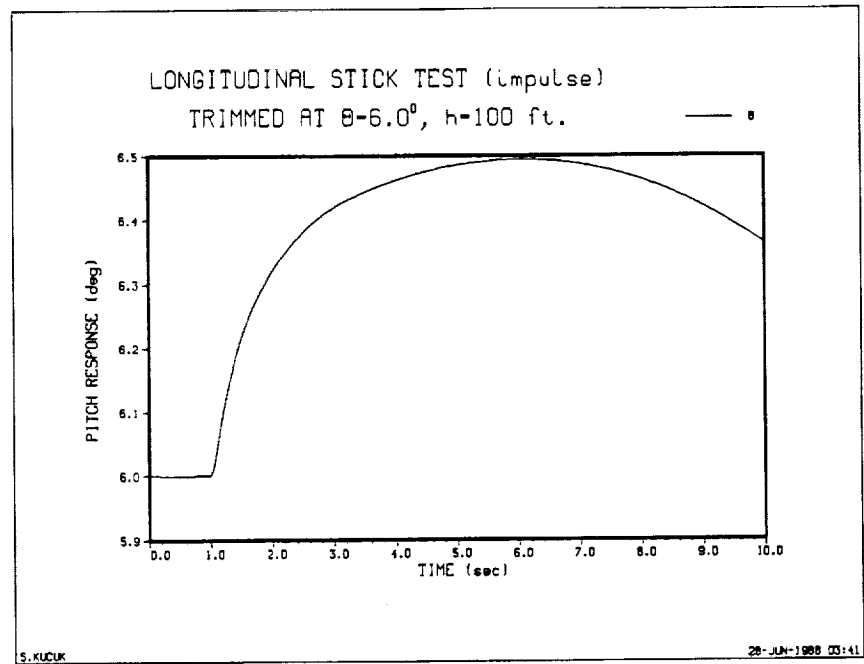
Figure 25. Pitch response to a longitudinal stick impulse
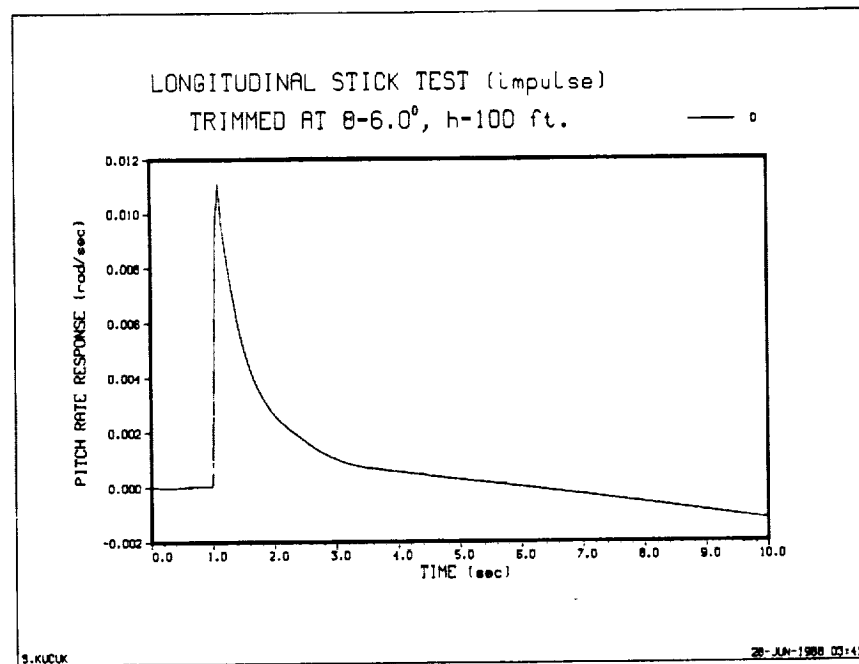
Figure 26. Pitch rate response to a longitudinal stick impulse
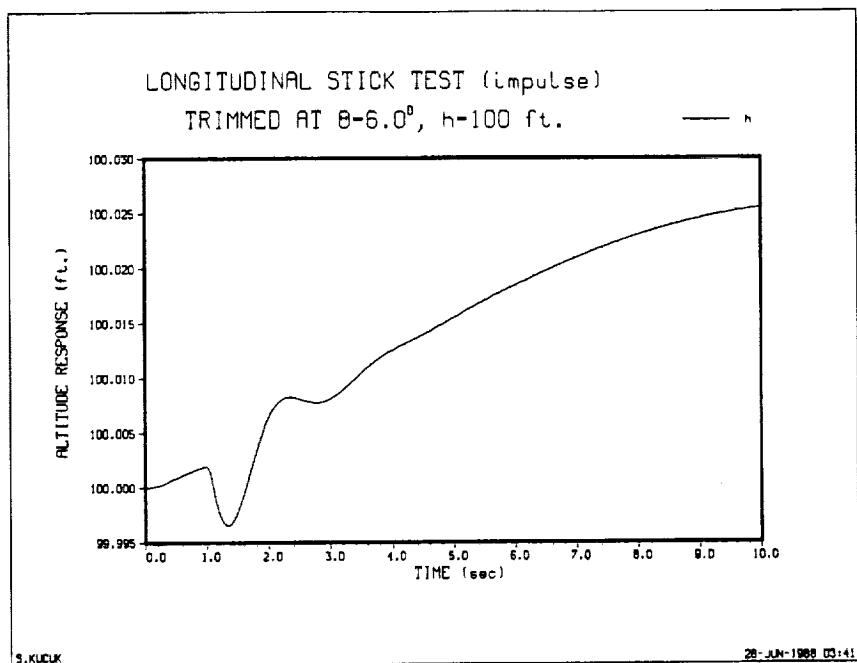
Figure 27. Altitude response to a longitudinal stick impulse
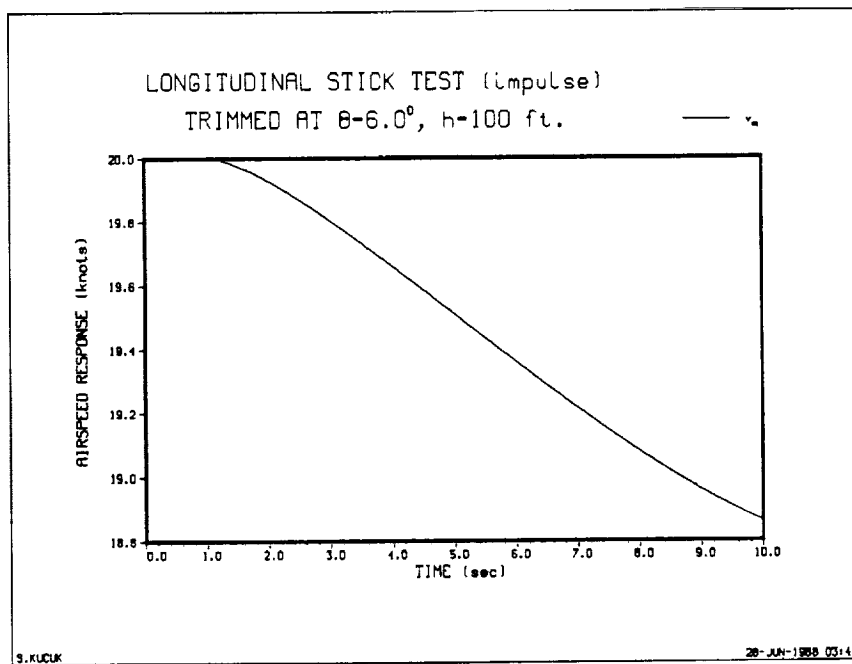
Figure 28. Airspeed response to a longitudinal stick impulse
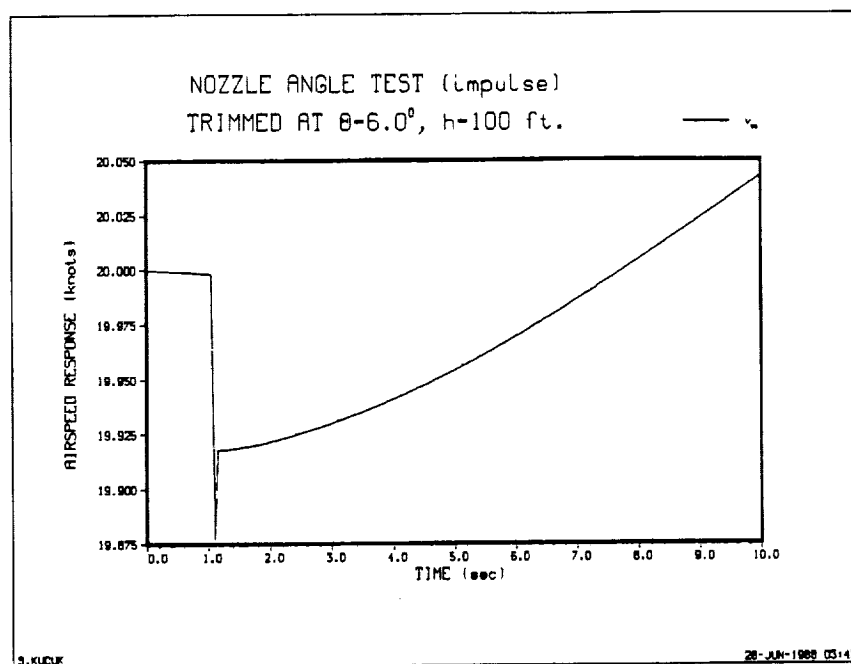
Figure 29. Airspeed response to a nozzle setting impulse
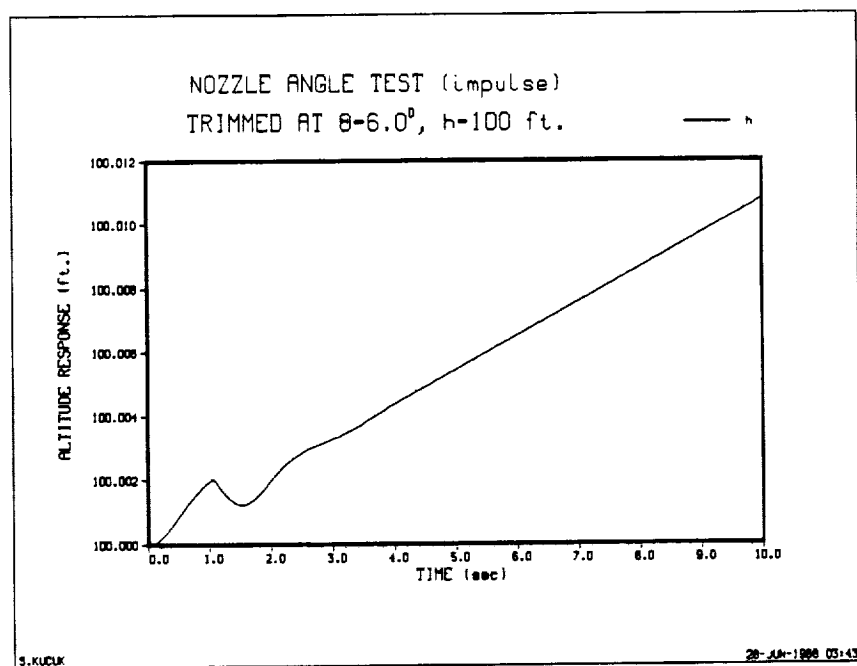
Figure 30. Altitude response to a nozzle setting impulse
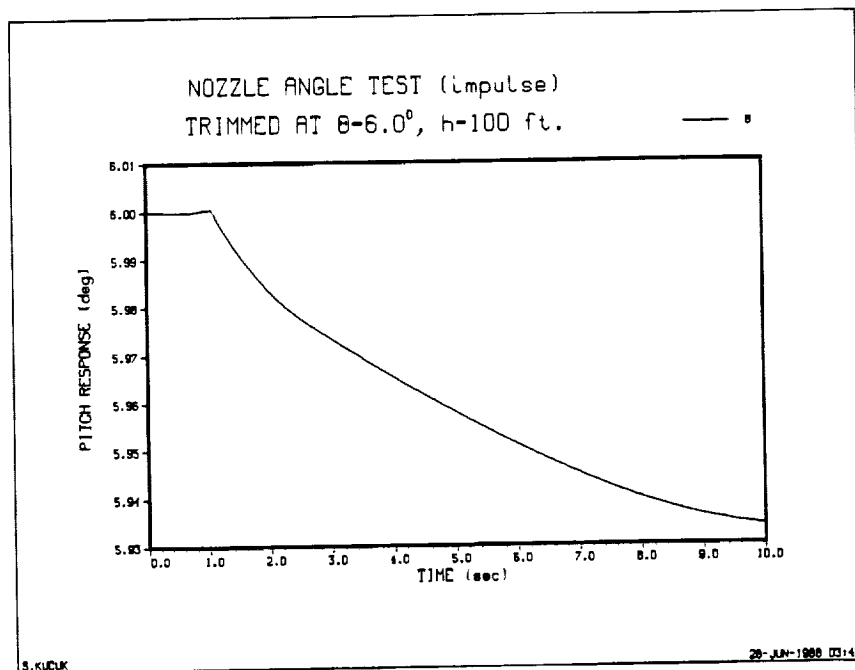
Figure 31. Pitch response to a nozzle setting impulse
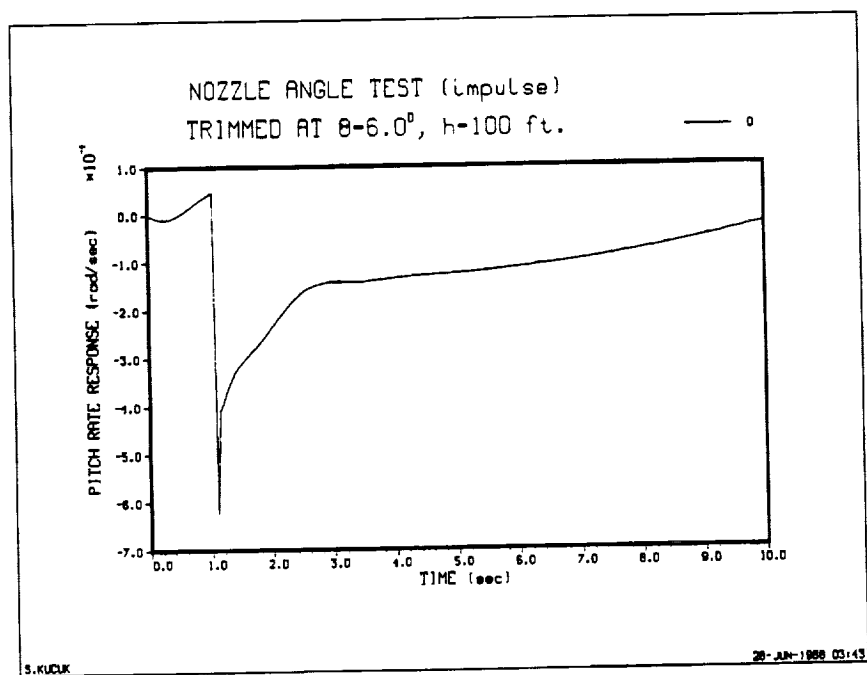
Figure 32. Pitch rate response to a nozzle setting impulse
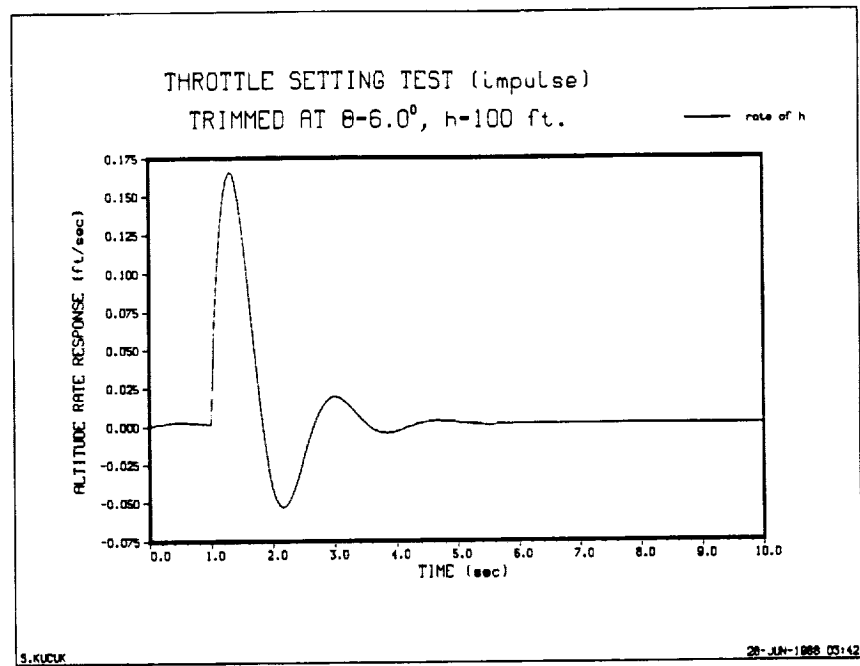
Figure 33. Altitude rate response to a throttle setting impulse
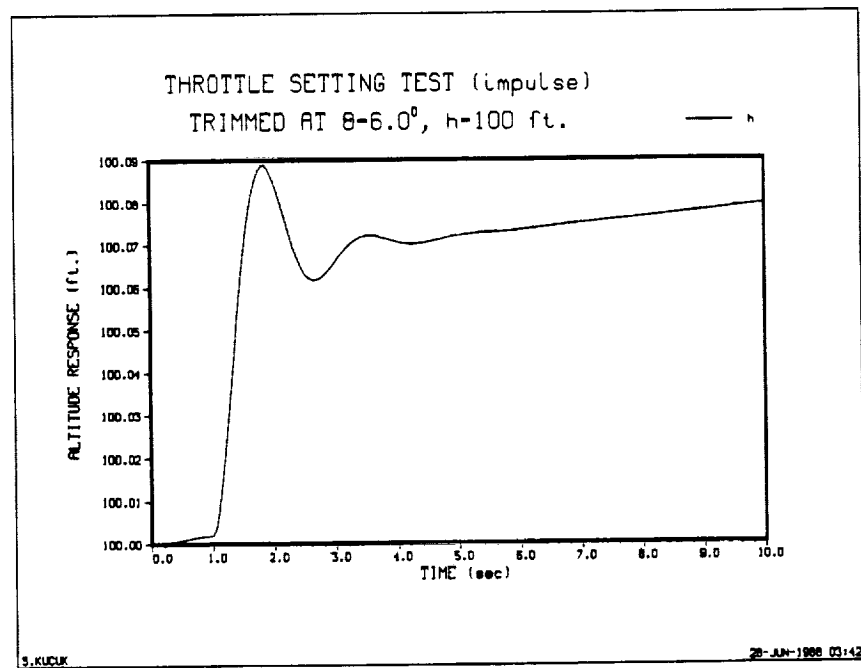
Figure 34. Altitude response to a throttle setting impulse
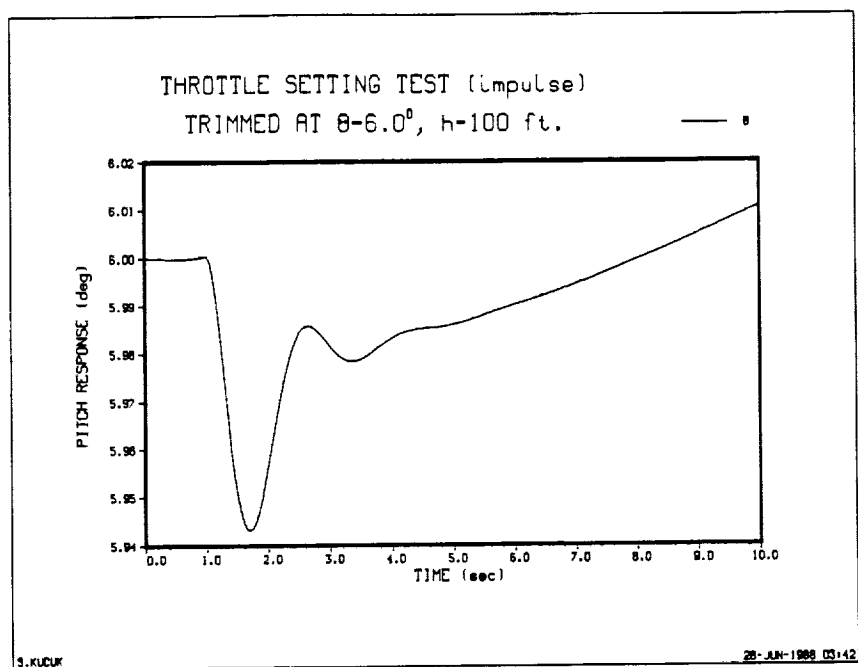
Figure 35. Pitch response to a throttle setting impulse
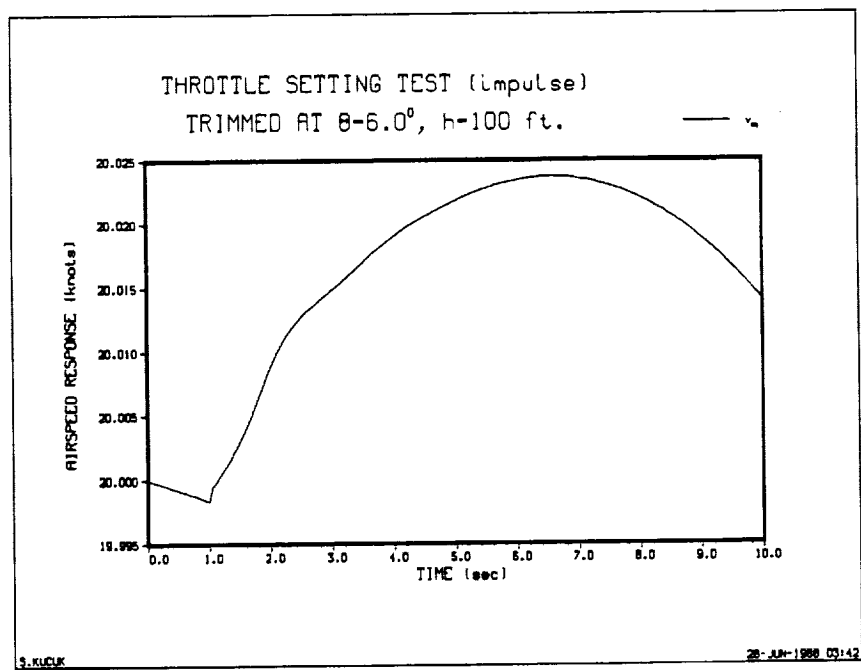
Figure 36. Airspeed response to a throttle setting impulse
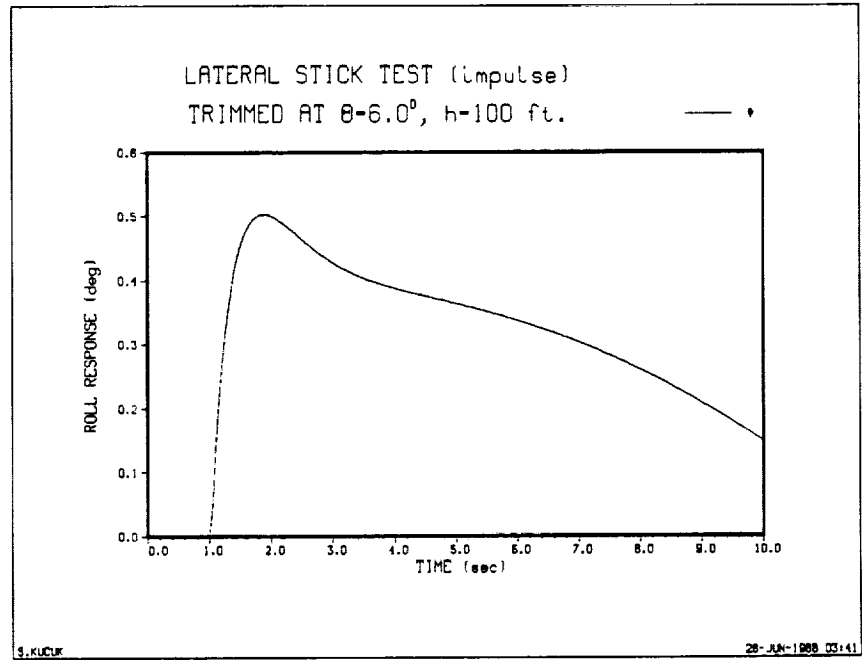
Figure 37. Roll response to a lateral stick impulse
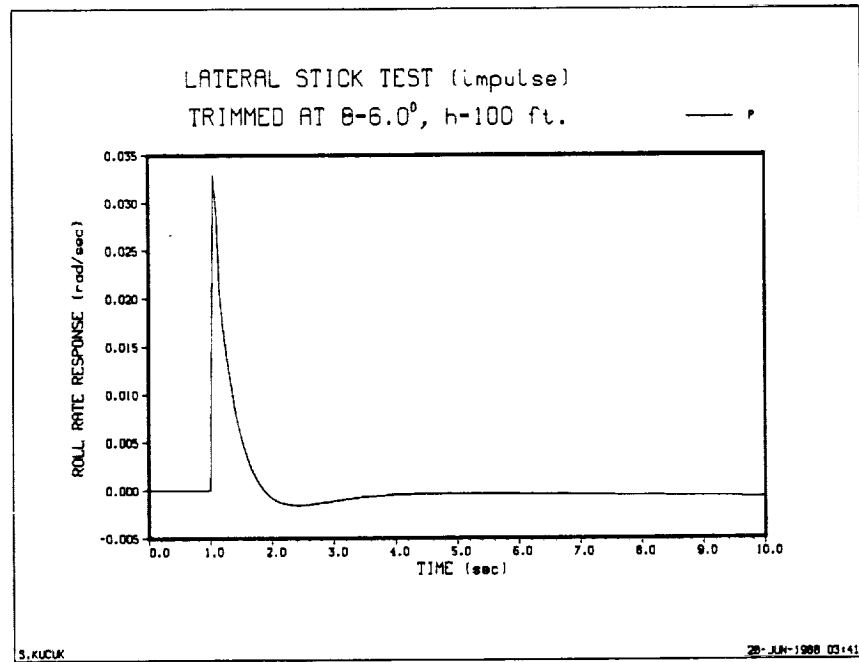
Figure 38. Roll rate response to a lateral stick impulse
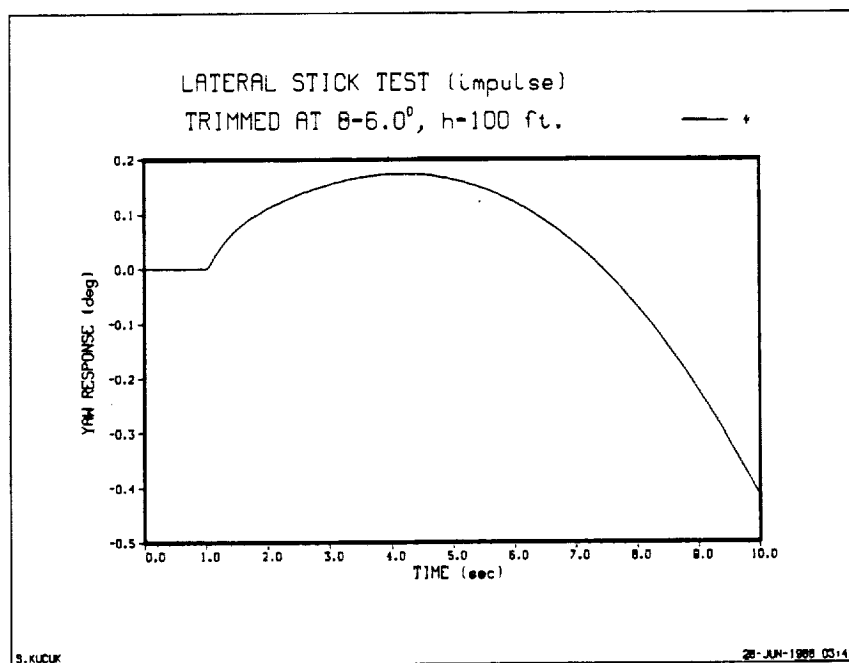
Figure 39. Yaw response to a lateral stick impulse
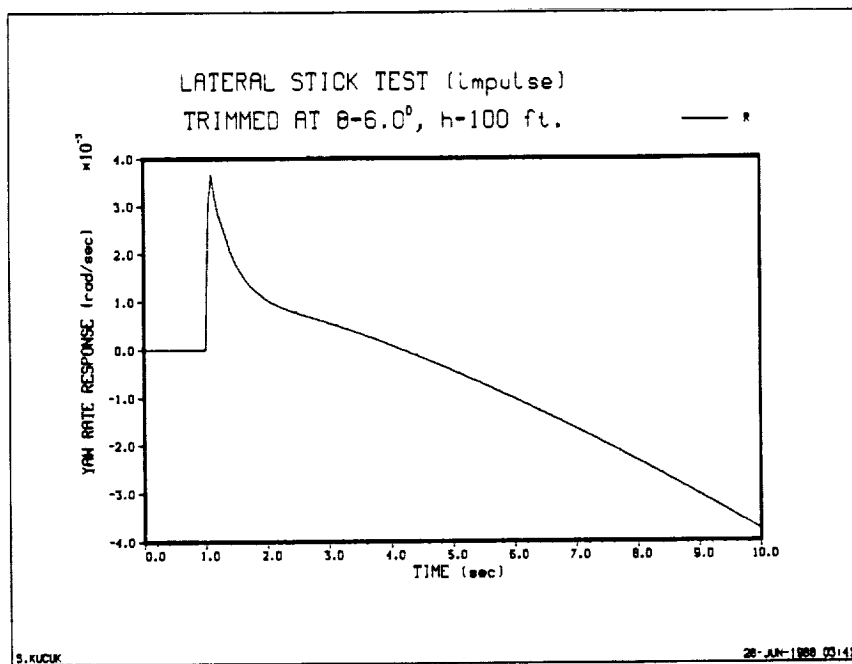
Figure 40. Yaw rate response to a lateral stick impulse
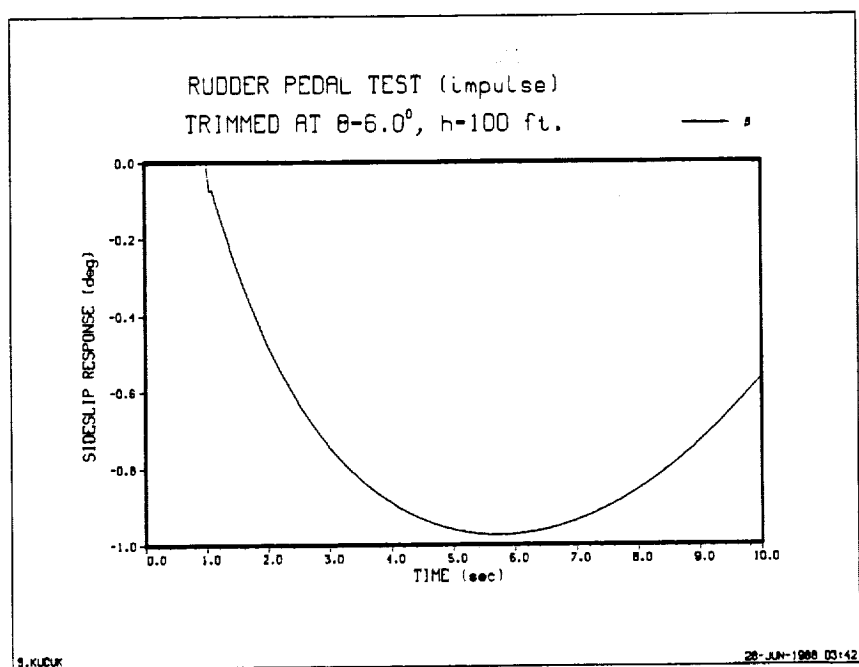
Figure 41. Sideslip response to a rudder impulse
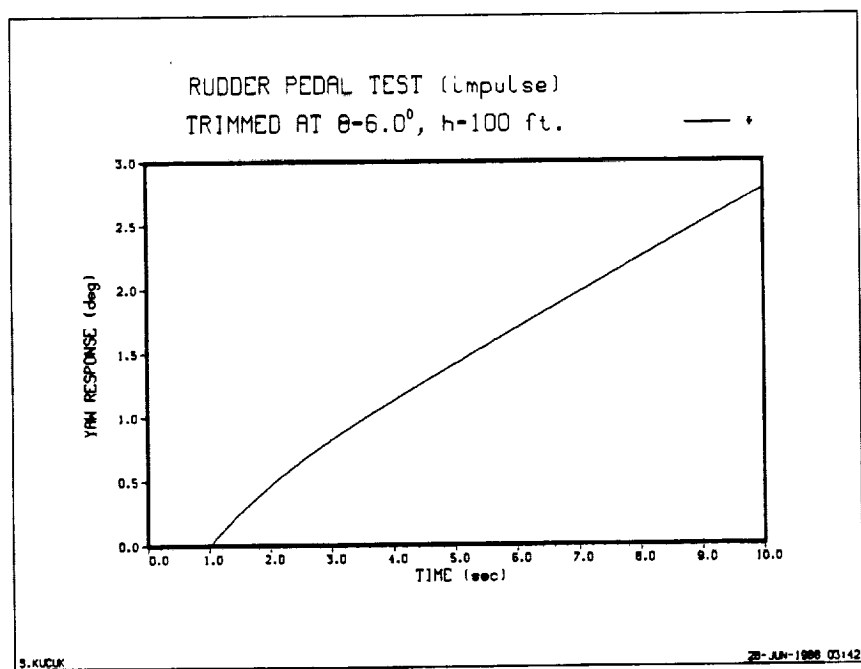
Figure 42. Yaw response to a rudder impulse
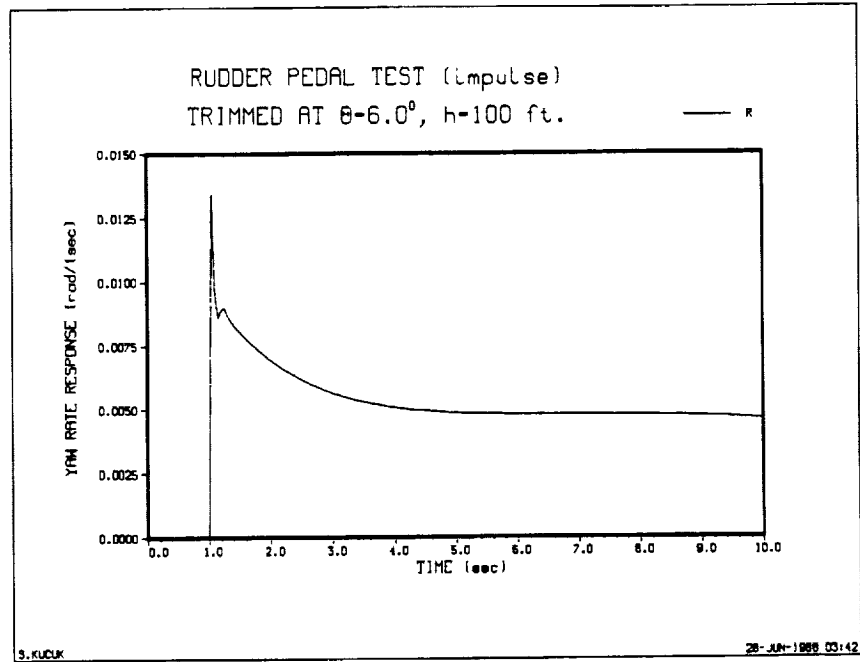
Figure 43. Yaw rate response to a rudder impulse
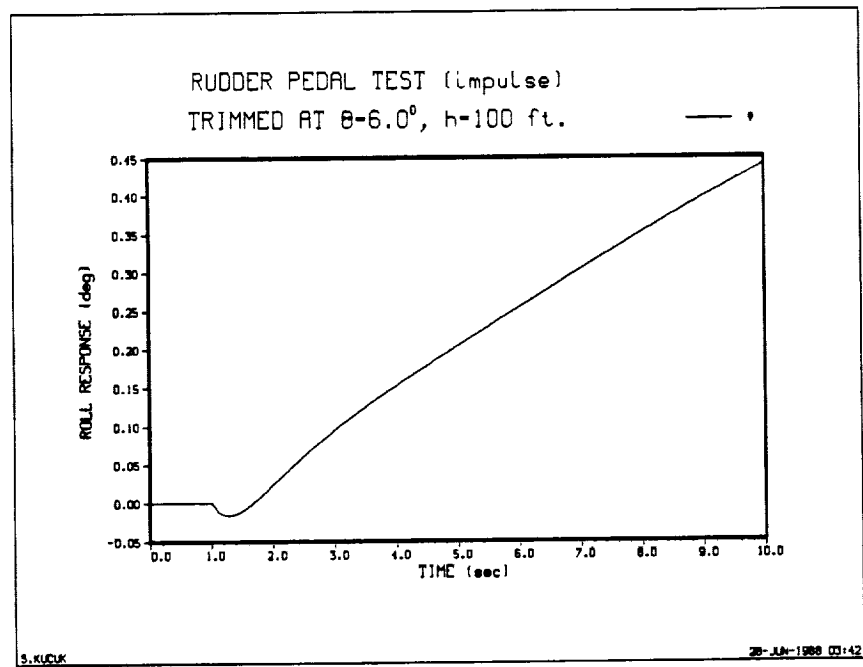
Figure 44. Roll response to a rudder impulse

6.2 Static Pilot Runs

As mentioned earlier, the static pilot parameters are calculated off-line using the time and frequency data of the trimmed aircraft at the desired initial flight conditions. The selection of the static pilot parameters will also affect the adaptive pilot since the experience of the adaptive pilot is provided by the static pilot. We will later illustrate this by varying the activation time of the adaptive pilot which is the adaptive pilot of Chapter 5.

The Harrier AV-8B is trimmed at 25 knots with the initial angular positioning $(\Phi,\Theta,\Psi)=(0.0°,6.50°,0.0°)$ at 100 ft. above sea level. The same analysis of Section (6.1) is applied to the impulse response data, and the following discrete pilot parameters in equations (6-7a), (6-7b), (6-7c), (6-7d) and (6-7e) are calculated to close the longitudinal stick through the pitch angle, lateral stick through the roll angle, rudder pedals through the heading, nozzle angle setting through the airspeed and the throttle setting through the altitude, respectively. Equations (6-7a), (6-7d) and (6-7e) define the longitudinal directional pilot. Equations (6-7b) and (6-7c) define the lateral directional pilot.

$$H^{\delta}_{\Theta}e(z^{-1})=0.2z^{-4}\frac{(z^{-1}-0.94z^{-2})}{(1-0.6065z^{-1})(1-0.7778z^{-1})} \qquad (6\text{-}7a)$$

$$H^{\delta}_{\Phi}a(z^{-1})=0.69317z^{-4}\frac{(z^{-1}-0.93z^{-2})}{(1-0.6065z^{-1})(1-0.22475z^{-1})} \qquad (6\text{-}7b)$$

$$H^{\delta}_{\Psi}r(z^{-1})=0.54017z^{-4}\frac{(z^{-1}-0.94z^{-2})}{(1-0.6065z^{-1})(1-0.45535z^{-1})} \qquad (6\text{-}7c)$$

$$H^{\delta}_{\Theta_j}(z^{-1})=-0.4z^{-4}\frac{(z^{-1}-0.605z^{-2})}{(1-0.6065z^{-1})(1-0.6z^{-1})} \qquad (6\text{-}7d)$$

$$H^{\delta}_{h}TH(z^{-1})=1.46997z^{-4}\frac{(z^{-1}-0.965z^{-2})}{(1-0.6065z^{-1})(1-0.87952z^{-1})} \qquad (6\text{-}7e)$$

First, the longitudinal pilot was commanded a +10° pitch response and required to hold the speed of the aircraft. Almost downward pointing nozzles will cause a significant loss in the speed by pitching-up so the constraint on the relative speed of the aircraft becomes essential. Figures (45) and (46) show the pitch angle and the airspeed responses of the aircraft. The loop associated with the pitch angle is type-1, so the steady state error is almost zero, but the speed loop is type-0. This is why there is approximately 10 knots drop in the speed even though the pilot was required to hold the speed at 25 knots. To overcome this situation, the pilot's adjustable pole can be shifted as close as to $z=1$, so that the error is minimal, but a type-1 loop in the speed causes a very sluggish response. Any oscillations in this loop must be avoided. For that reason, we will ignore this steady state error. A following argument is that, if the pilot senses the final value of the speed, he can always change his reference so that the gap can be compensated. The pilot's performance is shown in Figures (47) and (48). The latter are the corresponding control movements of the pilot models to obtain the responses of Figures (45) and (46).

In the next scenario, the altitude pilot is activated to achieve a +10 ft. altitude command after t=5.0 sec. The resulting pitch angle, speed, and the altitude responses of the aircraft for the three-variable pilot model are given in Figures (49), (50) and (51). The corresponding control movements are shown in Figures (52), (53) and (54). This example shows how efficient the single variable loops act as a complete multi-variable pilot model.

Let us examine this simulation. First the pitch pilot receives a command to adjust the pitch angle of the aircraft and acts on the longitudinal stick. The change in the aircraft state is sensed by the nozzle and altitude pilots and they act on the controls to regulate these changes caused by the pitch pilot. Then at t=5.0 sec., the altitude pilot receives an

increase in altitude command by 10 ft. and acts on the throttle as a primary control mechanism not to regulate. The changes in throttle affect the aircraft state once again, and the pitch pilot and nozzle pilot react to regulate the disturbed motion caused by the altitude pilot until the steady state is reached.

In addition to the pitch, altitude, and speed loops, we will add to the above case a coordinated heading change maneuver where the heading of the aircraft is to be adjusted with rudder movements while the longitudinal stick holds the pitch angle, the lateral stick minimizes the roll angle, and the throttle setting is used to maintain the altitude of the aircraft. Also the nozzle angle setting will be used to regulate the aircraft speed. Therefore, this maneuver requires all of the five main control mechanisms to be used.

The pilot is required to change his heading by +5° in approximately 5 seconds, after t=10.0 sec. Another constraint becomes effective for this case where the disturbed roll of the aircraft, due to the yaw-roll coupling, must be regulated although small in magnitude. The pitch, yaw, roll, speed and altitude responses for the above simulation are given in Figures (55), (56), (57), (58) and (59). The corresponding control movements of the pilots are given in Figures (60), (61), (62), (63) and (64).
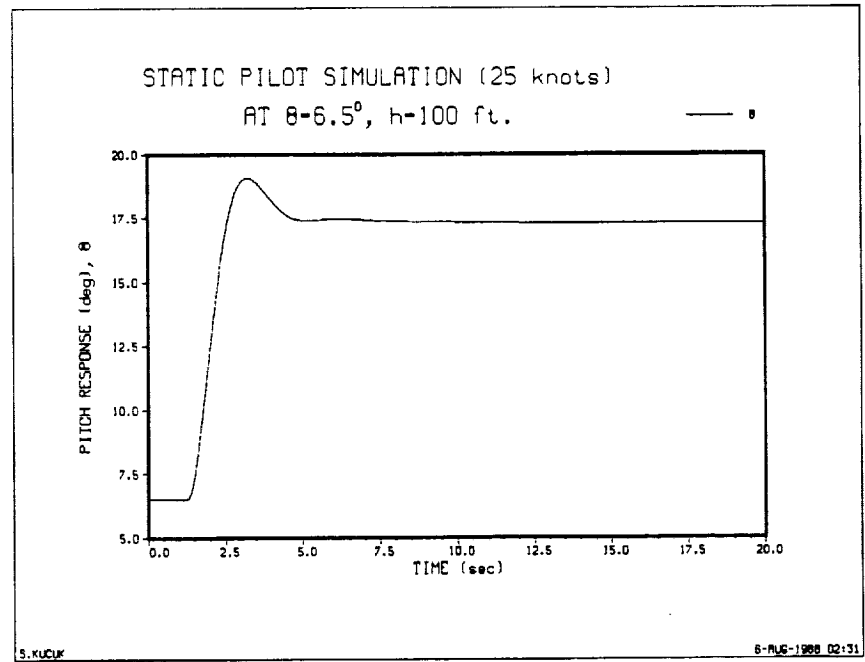
Figure 45. Pitch response, two-pilot configuration
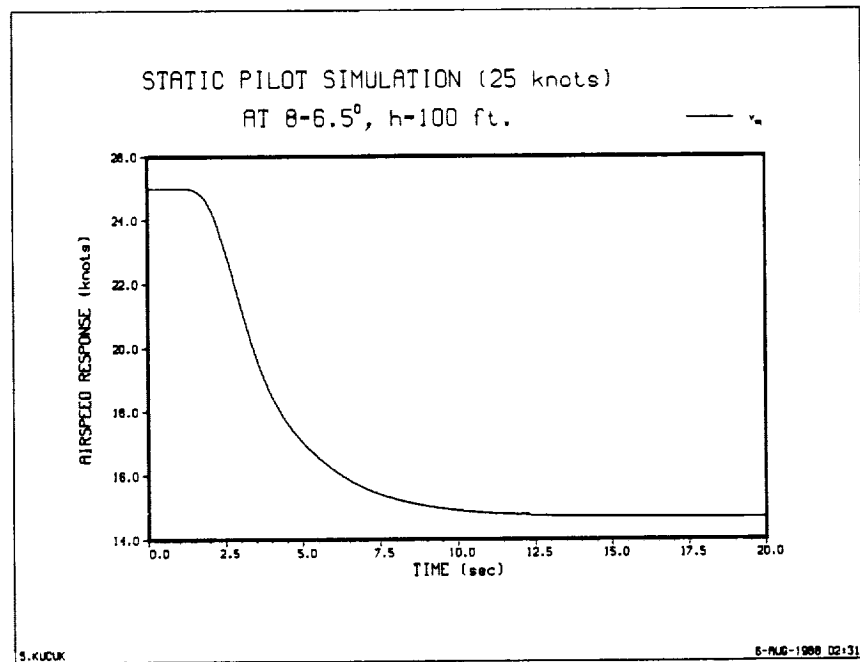
Figure 46. Airspeed response, two-pilot configuration
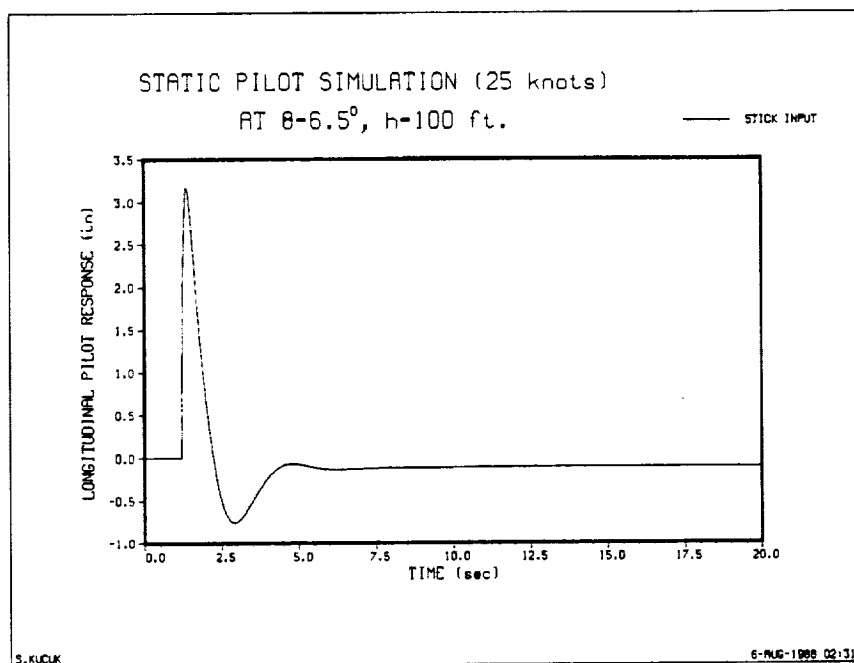
Figure 47. Longitudinal stick pilot response, two-pilot configuration
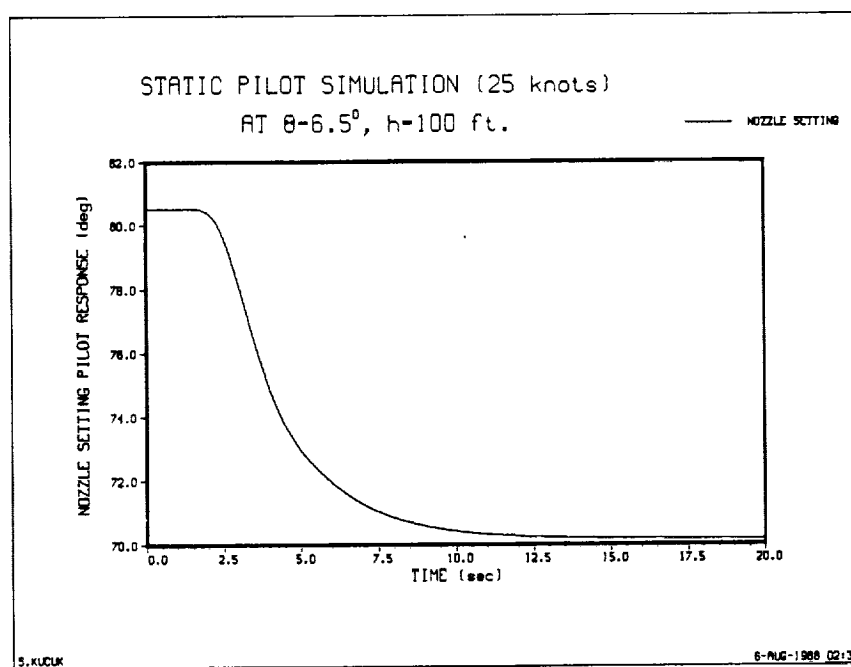
Figure 48. Nozzle setting pilot response, two-pilot configuration
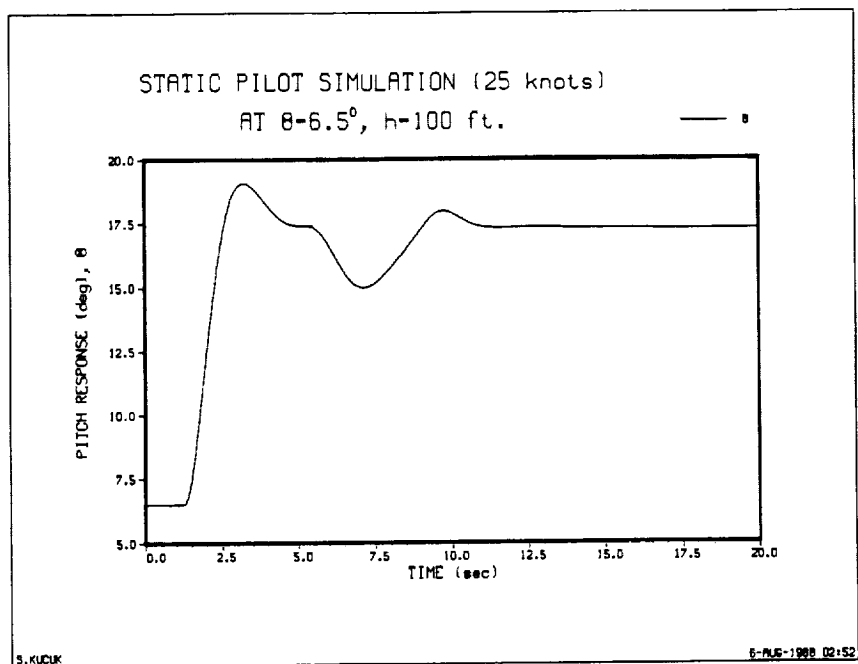
Figure 49. Pitch response, three-pilot configuration
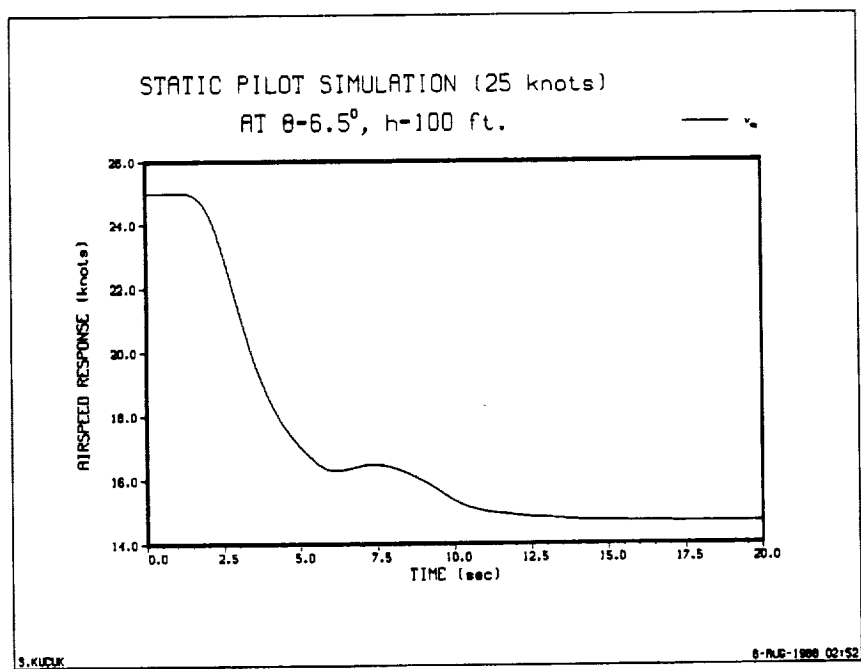
Figure 50. Airspeed response, three-pilot configuration
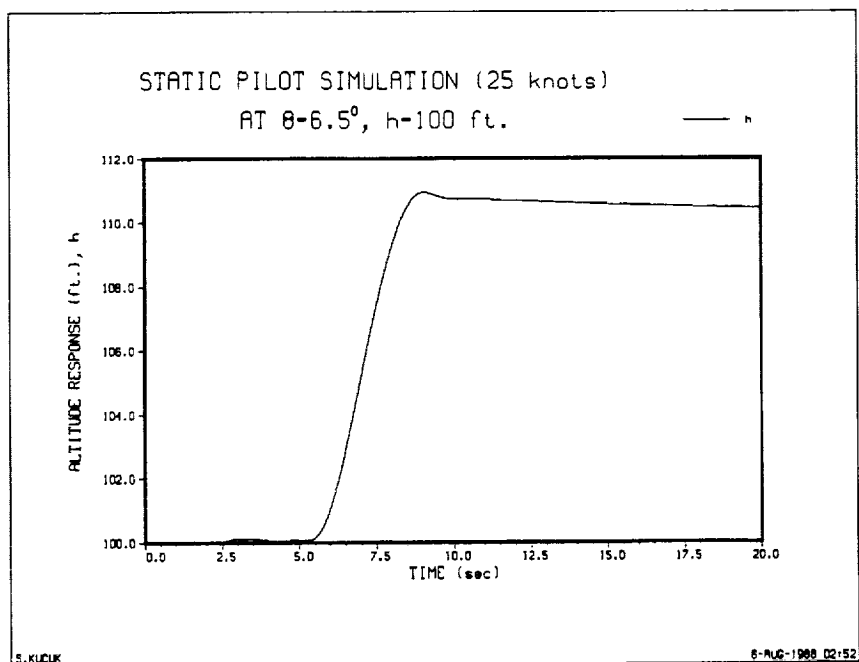
Figure 51. Altitude response, three-pilot configuration
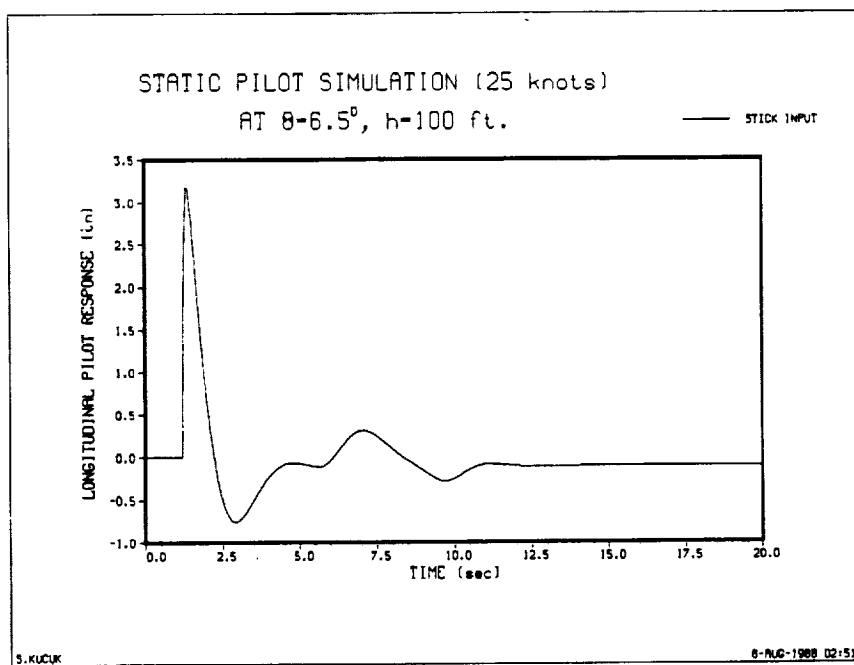
Figure 52. Longitudinal stick pilot response, three-pilot configuration
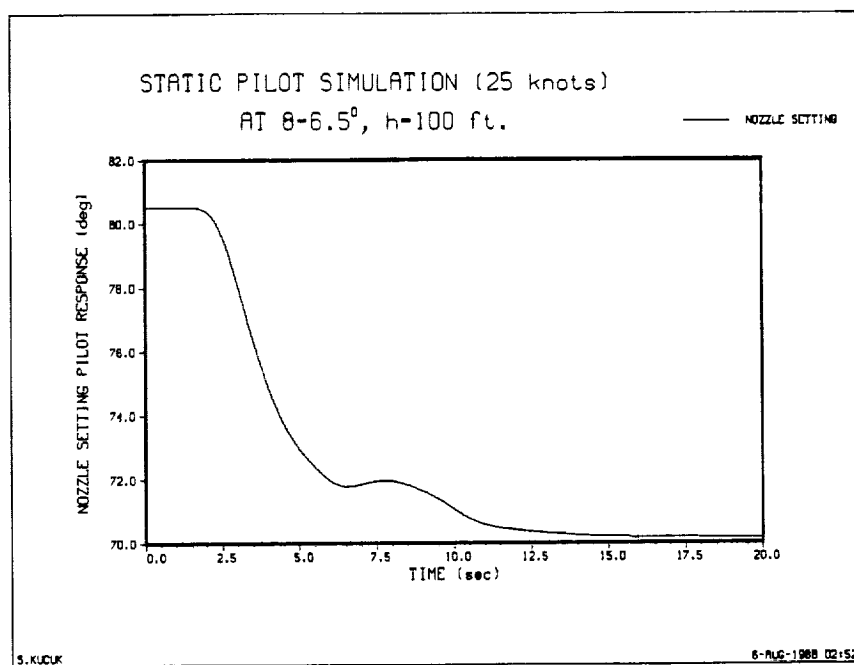
Figure 53. Nozzle setting pilot response, three-pilot configuration
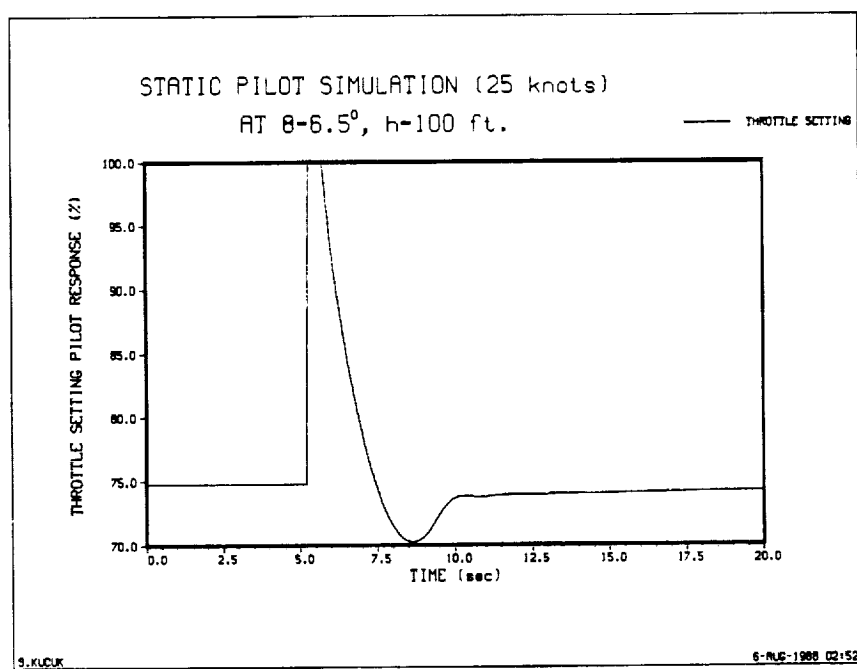
Figure 54. Throttle setting pilot response, three-pilot configuration
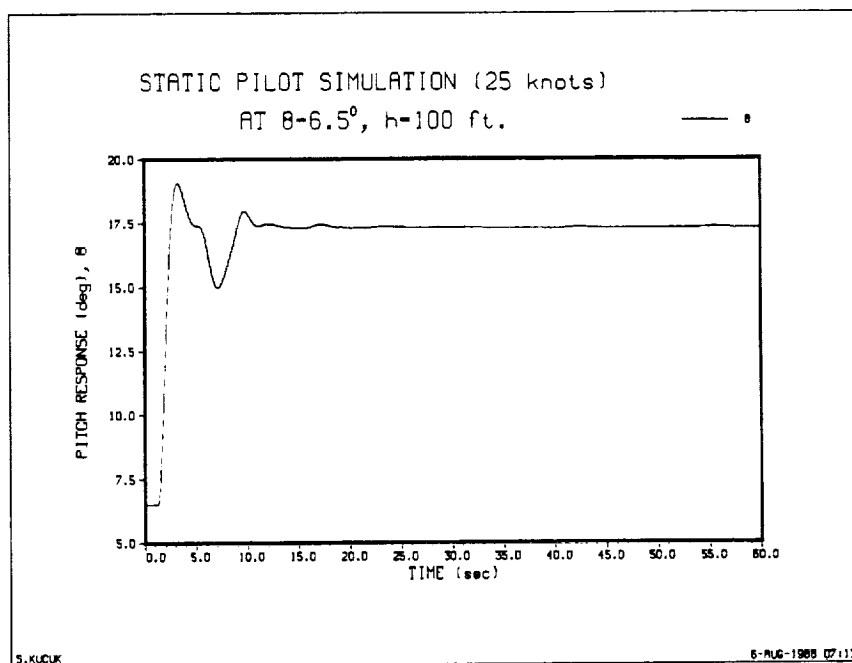
Figure 55. Pitch response, five-pilot configuration
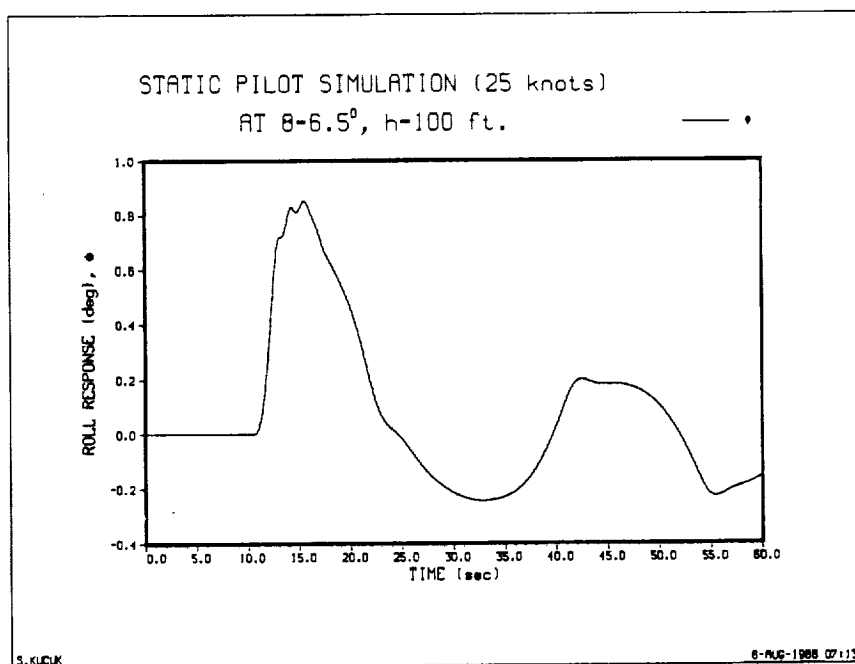
Figure 56. Roll response, five-pilot configuration

C·2
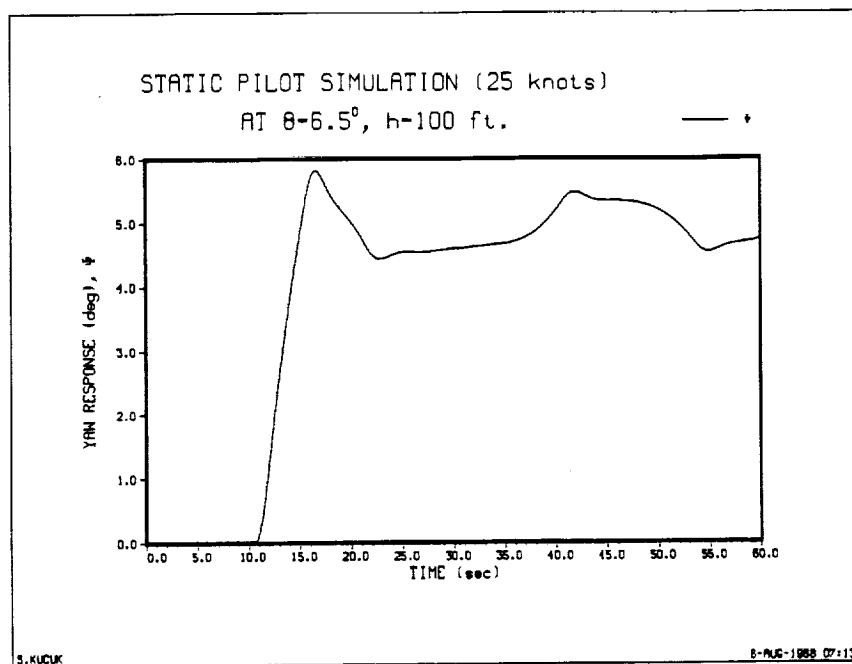
Figure 57. Yaw response, five-pilot configuration
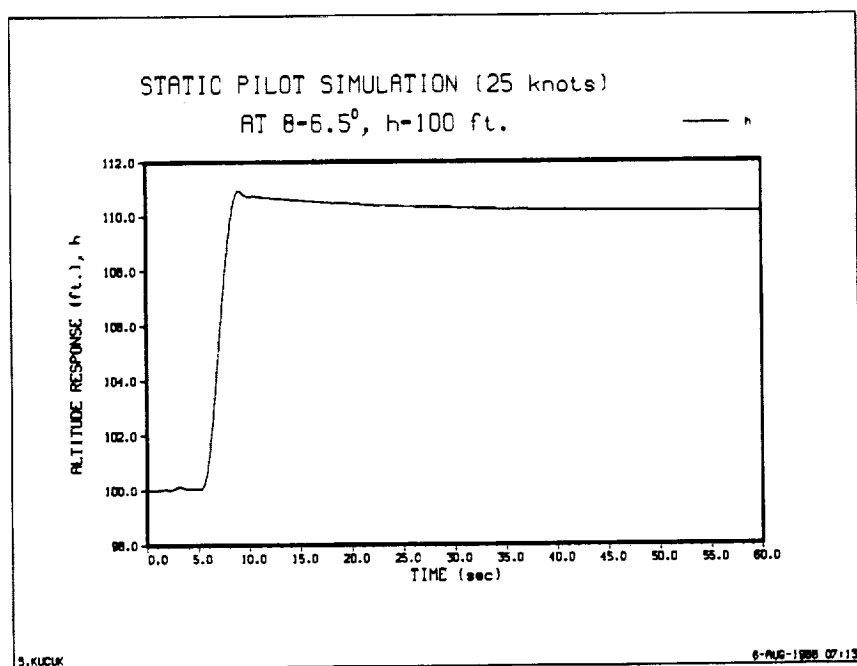
Figure 58. Altitude response, five-pilot configuration
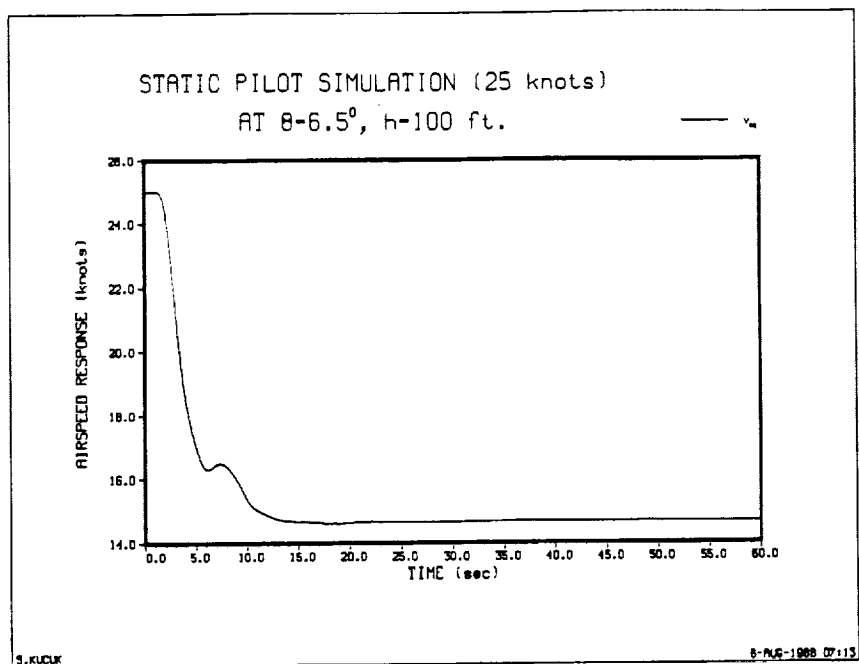
Figure 59. Airspeed response, five-pilot configuration
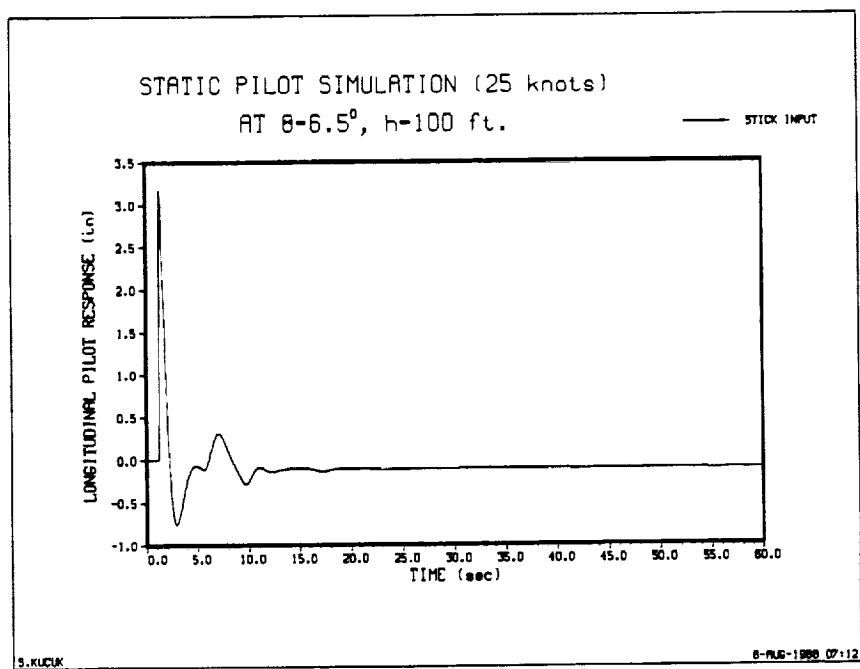
Figure 60. Longitudinal stick pilot response, five-pilot configuration
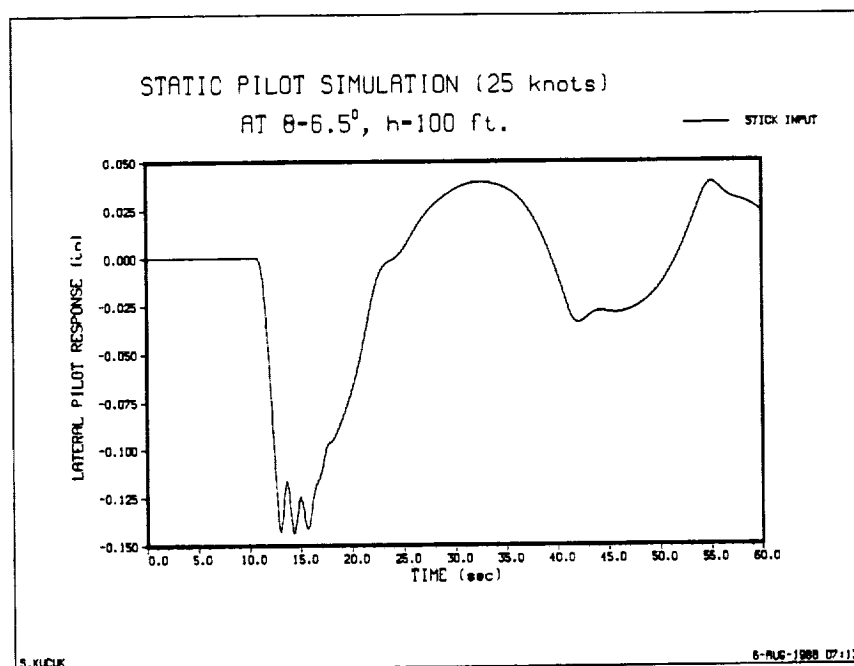
Figure 61. Lateral stick pilot response, five-pilot configuration
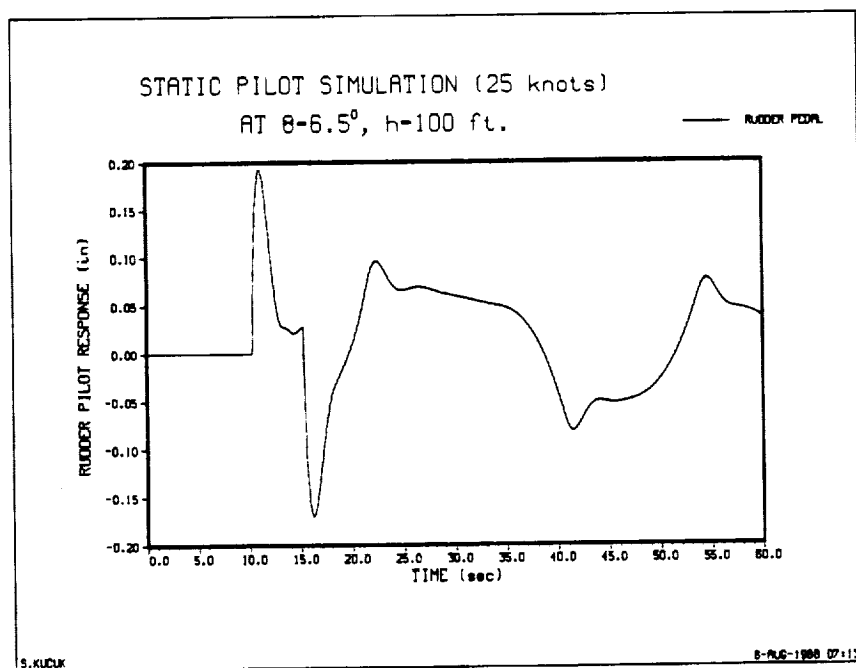
Figure 62. Rudder pedal pilot response, five-pilot configuration
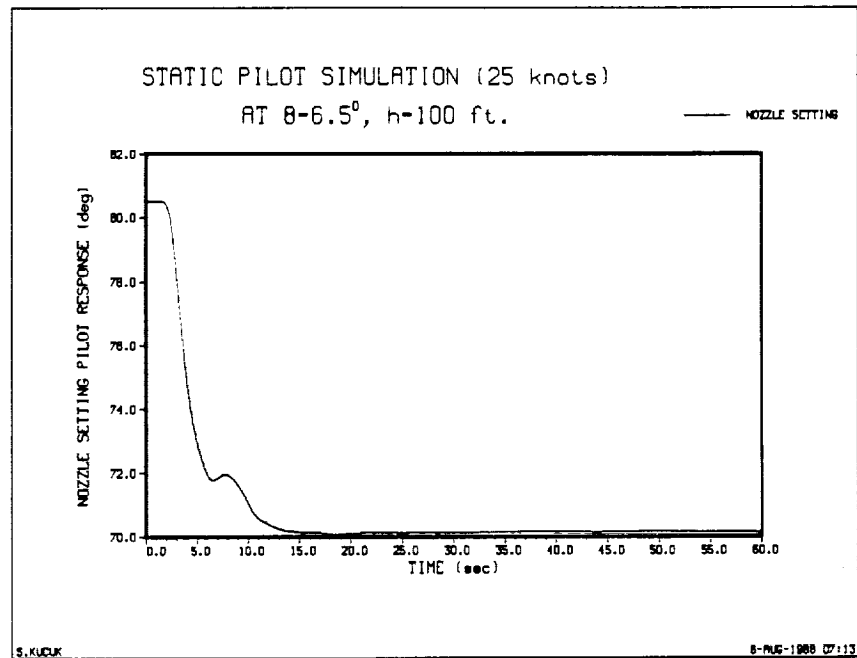
Figure 63. Nozzle setting pilot response, five-pilot configuration
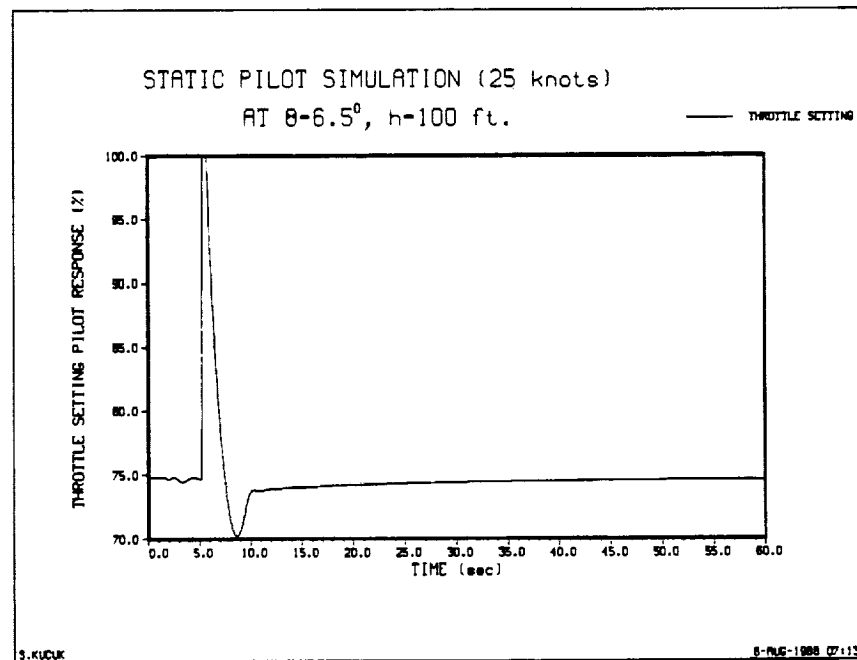
Figure 64. Throttle setting pilot response, five-pilot configuration

6.3 Adaptive Pilot Runs

Now that we have simulated and verified the static pilots, we will investigate the behavior of the adaptive pilot model. In order to simulate the adaptive pilot model, we chose $z_{CL}=0.90\pm j0.10$ to be the desired dominant close loop operating poles corresponding to a damping ratio of 0.6676 and an undamped natural frequency of 2.973 rad/sec which is in the middle of the "best" rated region of Figure (2). Recall that the adaptive pilot compensates the necessary phase to close the loop at $z_{CL}=0.90\pm j0.10$. For that reason, the model relocates the adjustable pole/zero pair of the discrete human response model of equation (2-5), in such a way that the phase contribution of the pole and zero gives the necessary compensation. We also mentioned that there is no unique solution to this problem. Therefore, our criterion was based on the location of the adjustable pole, α. The pole, α, is moved towards the origin $z=0$, as a function of the required phase. The zero, γ, is then chosen accordingly, and a table look-up was designed to store the values of the pole/zero values for specific conditions. Therefore, in the simulation, after the information of the phase be to compensated is available, the model searches the table to find the appropriate values of α and γ. Although there is no proof to the latter argument, we have mentioned that an experienced pilot is almost deterministic in his responses, knowing how to react and when to react at various configurations as is our model.

Figures (65), (66), (67) and (68) show the pitch angle and speed responses of the aircraft, longitudinal stick and nozzle setting movements of the adaptive pilot model where the adaptation starts at t=5.0 sec. The adjusted pole/zero and gains of the pilot model are given in Figures (69), (70), (71), and (72). Three numerator and three denominator coefficients are used in the identification process of the adaptive pilot model

where the controlled element dynamics is estimated. A rather interesting behavior is observed in the adaptive model's output. As soon as the adaptation starts, the model applies very rapid, approximately symmetric, push-and-pull type of movements to the controls until it can identify the information related with the controls. This is not an actual "learning" process, in the sense that the model acts deliberately on the controls to identify the system modes, but it is a result of the current information available to the model. Suppose that a human is given an adjustment stick that is attached to a spring-mass system where he is subjected to a control task to find the equilibrium value of the stick that will balance the mass. If he has no idea of what to do, the first response of the human will be to move the stick forward and backward, simultaneously, until the desired action is performed. The same situation applies to a human guiding a car, for example. For heading maneuvers, the human knows the boundaries of the steering wheel. To make a right turn, in his first attempt, he may push the wheel more than the optimum value, but if such a case happens he will pull the wheel back, rather in a panic, rapidly correcting his action. Although it is hard to prove such an argument, we find a close relationship between the learning process of a human and the output of the adaptive model. However, we must also note that this type of learning may be dangerous in some of the cases.

Also, when compared with the same static, two-pilot configuration in Figures (45), (46), (47) and (48) the adaptive pilots performed better. Especially, the nozzle setting pilot, has better steady state response where it is required to hold the speed of the aircraft due to pitch changes. The static pilot stabilized at approximately 15 knots while the adaptive pilot converged to a steady state value of approximately 23 knots.

Figures (73), (74), (75), (76), (77), (78), (79), and (80) show the results when the adaptive pilots are activated at t=2.0 sec. This case clearly shows the importance of the

static pilot performance. If the adaptive pilot is not given sufficient time to converge its parameters, the adaptation results are not better than the static pilots. In the absence of a decisionmaking, adaptive pilot will not perform efficiently.

However, once the adaptive pilot parameters converge, the pilot can respond to maneuvers, and his performance can be compared with the performance of the static pilot. Figures (81) through (118) compare the adaptive and the static pilot performances for five different scenarios.

Figures (81), (82), (83), and (84) show a pitch-up response followed by a speed-up and a pitch-down maneuver performed by the adaptive and the static pilots. Notice that in both pitch and the speed loops the adaptive pilot has better steady state errors. The longitudinal stick and the nozzle angle setting pilots are adaptive after t=5 sec.

Figures (85), (86), (87), (88), (89), (90), (91), (92), (93), and (94) show a +10° pitch-up followed by a coordinated +5° heading change with a +10ft. altitude change maneuver and at the same time the speed of the aircraft is to be regulated by the nozzles. The aircraft is constrained to have a 0° roll angle to coordinate the heading change. The longitudinal stick and the rudder pedal pilots are adaptive after t=5 sec. and t=15 sec. respectively.

Figures (95), (96), (97), (98), (99), (100), (101), and (102) show a pitching, yawing, and a speed-up with 0° rolling maneuver where all the loops are closed with the adaptive pilots. The longitudinal stick and the nozzle angle pilots become adaptive after t=5 sec. while the rudder pedal and the lateral stick pilots are adaptive after t=25 sec. and t=28 sec. respectively.

Figures (103), (104), (105), (106), (107), (108), (109), and (110) show a rolling based maneuver with 0° heading constraint. Figures (111), (112), (113), (114), (115), (116), (117), and (118) show a similar scenario where the adaptation times are given by t=5 sec. for the longitudinal stick and the nozzle setting pilots, t=40 sec. and t=43 sec. for the rudder pedal and the lateral stick pilots, respectively.
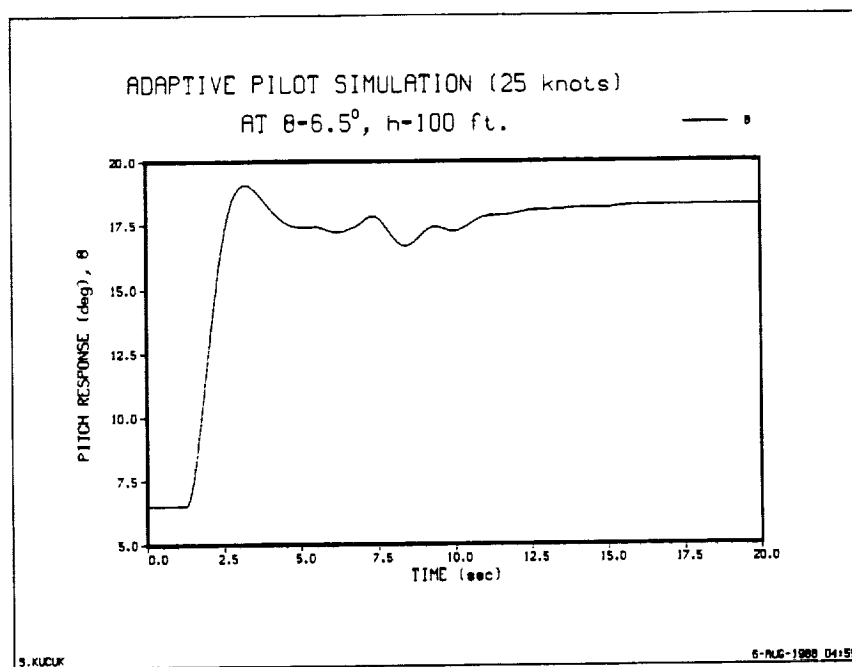
Figure 65. Pitch response, two-pilot configuration, adaptive after
t=5 sec
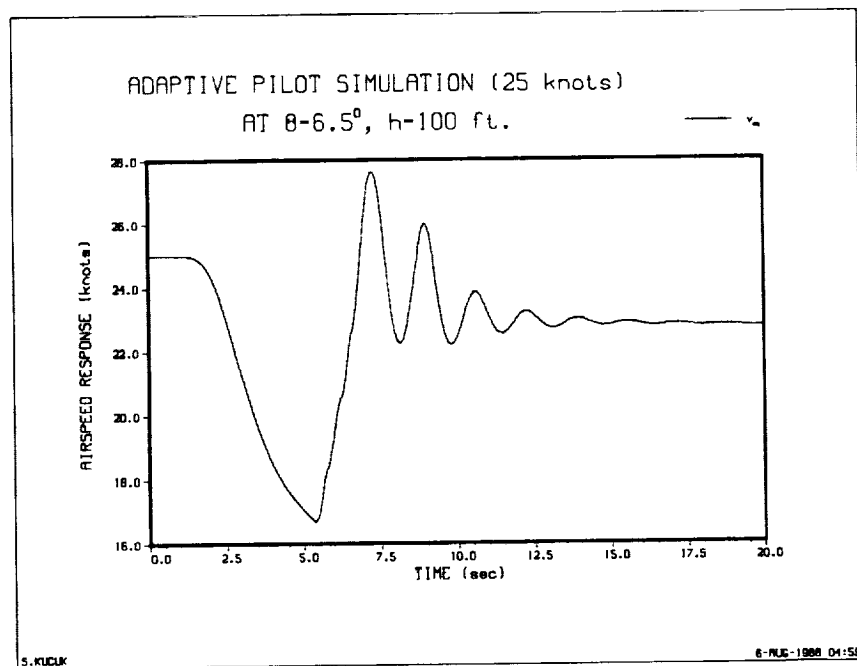
Figure 66. Airspeed response, two-pilot configuration, adaptive after t=5 sec
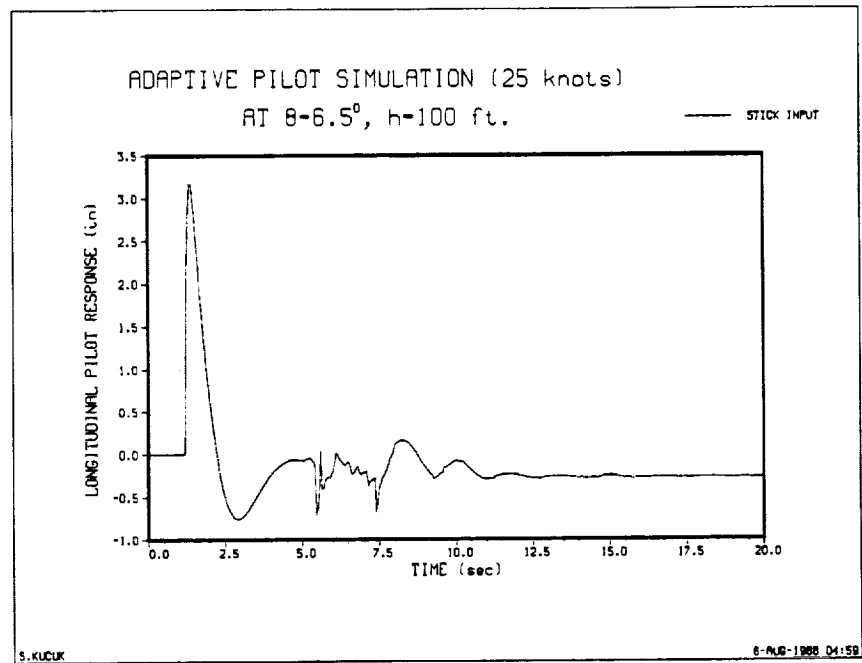
Figure 67. Longitudinal stick pilot response, two-pilot configuration, adaptive after $t=5$ sec
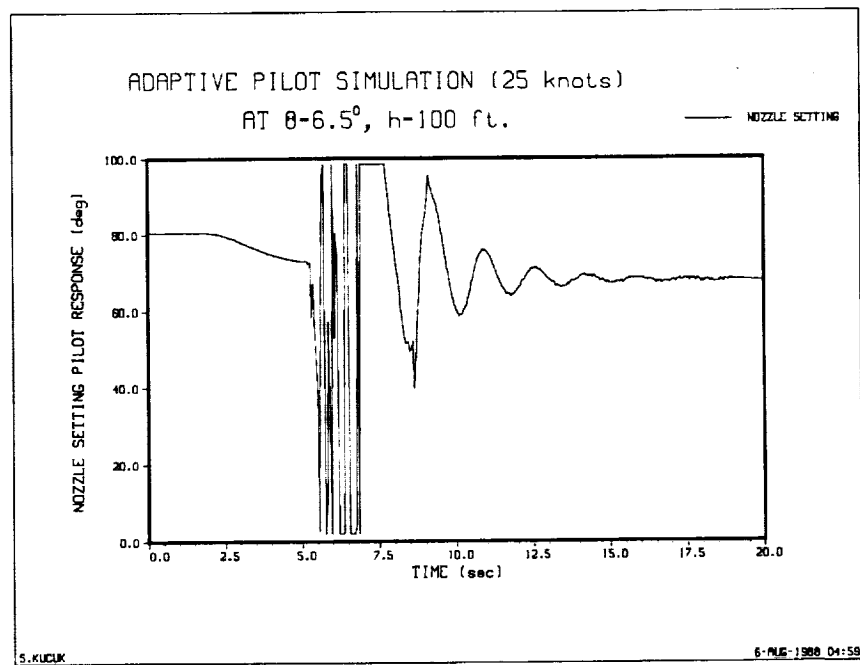
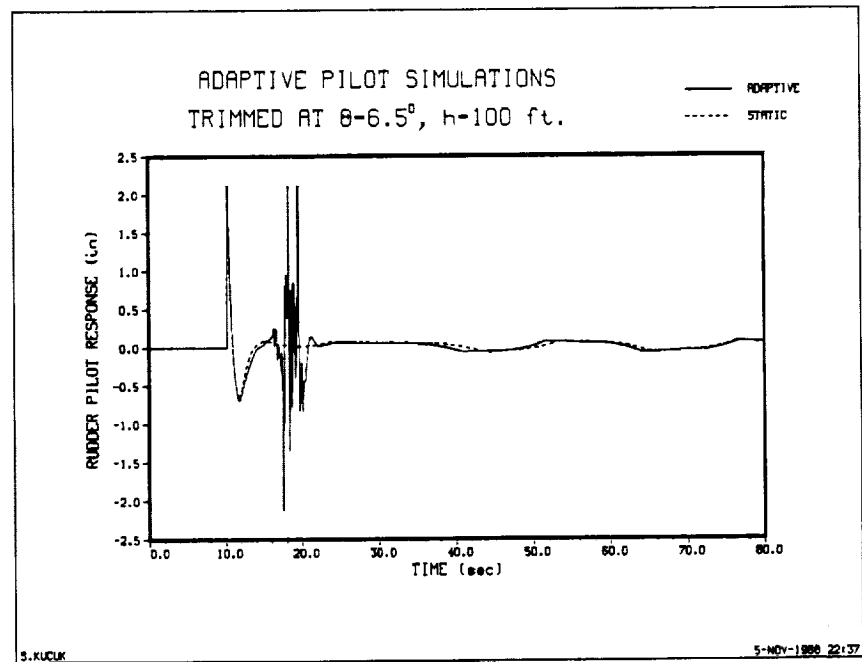**Figure 68.** Nozzle setting pilot response, two-pilot configuration, adaptive after $t=5$ sec
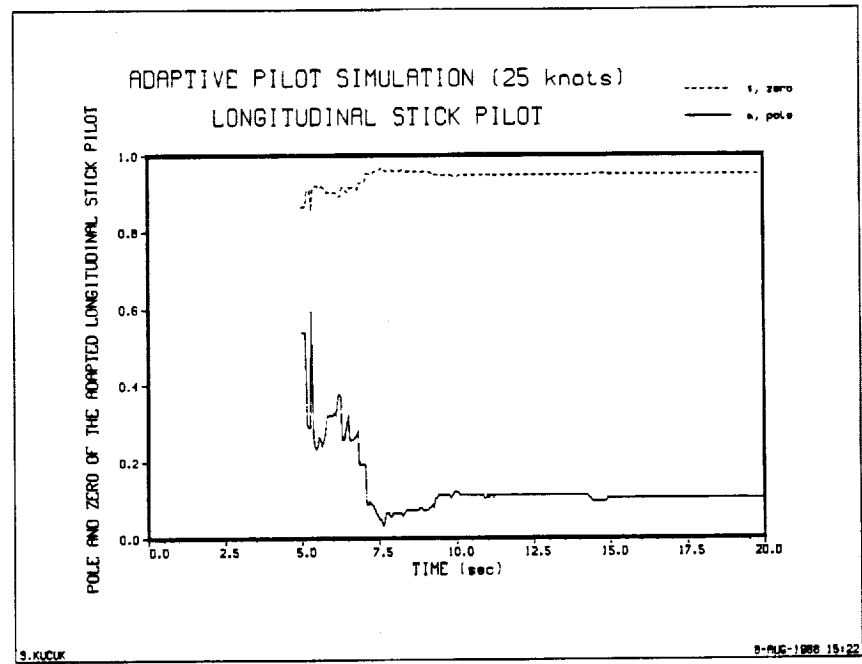
Figure 69. Longitudinal stick pilot, adapted pilot pole/zero, two-pilot configuration, adaptive after $t=5$ sec
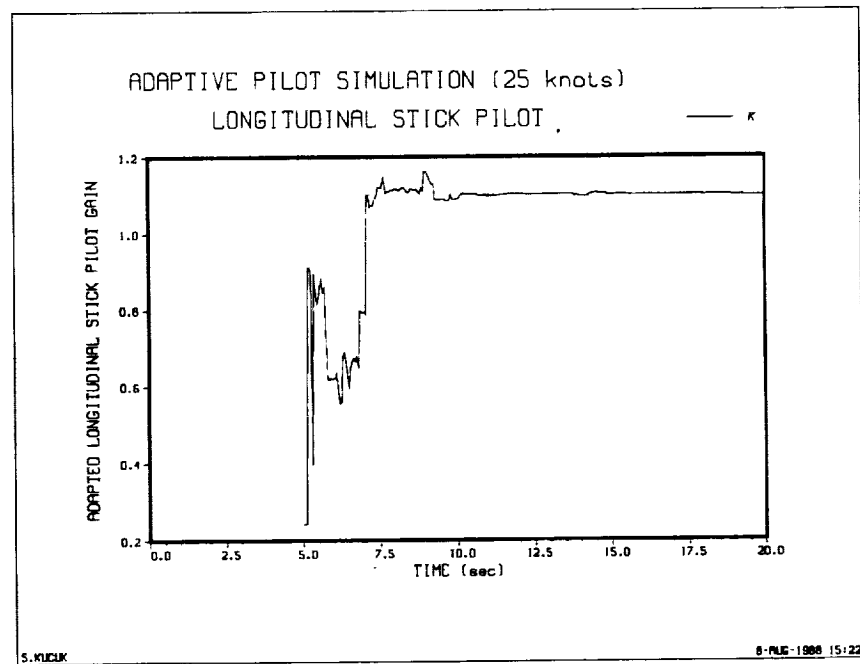
Figure 70. Longitudinal stick pilot, adapted pilot gain, two-pilot configuration, adaptive after $t=5$ sec
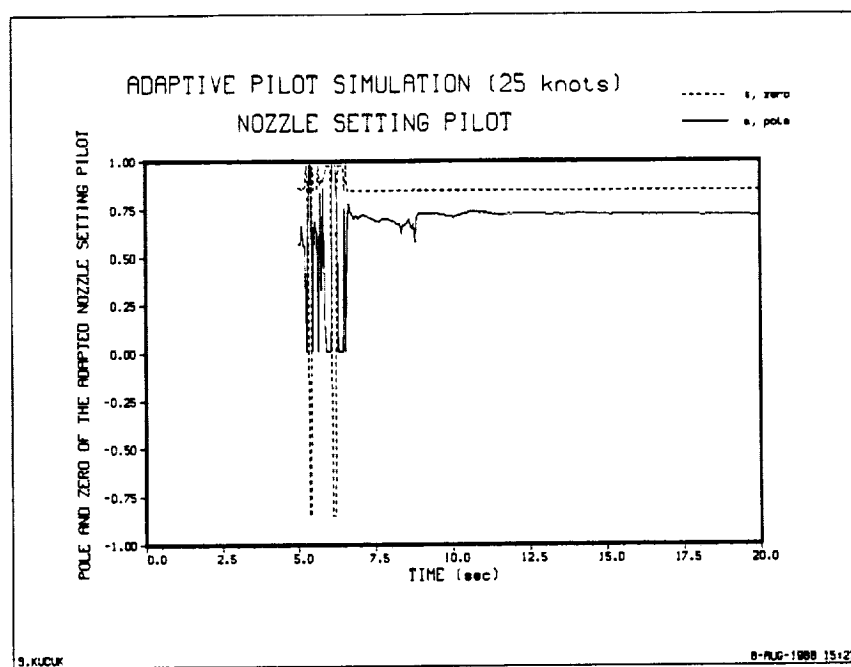
Figure 71. Nozzle setting pilot, adapted pilot pole/zero, two-pilot configuration, adaptive after t=5 sec
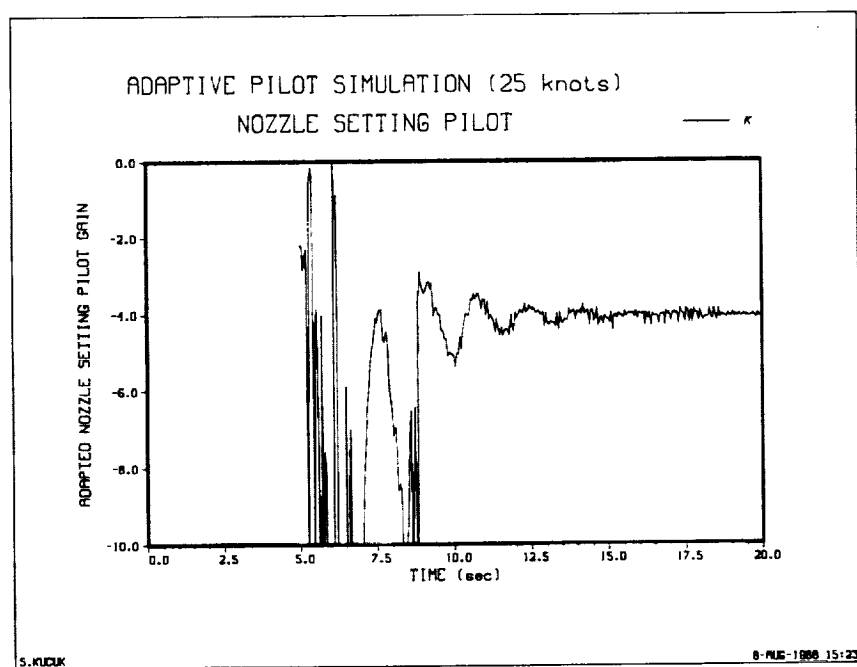
Figure 72. Nozzle setting pilot, adapted pilot gain, two-pilot configuration, adaptive after t=5 sec
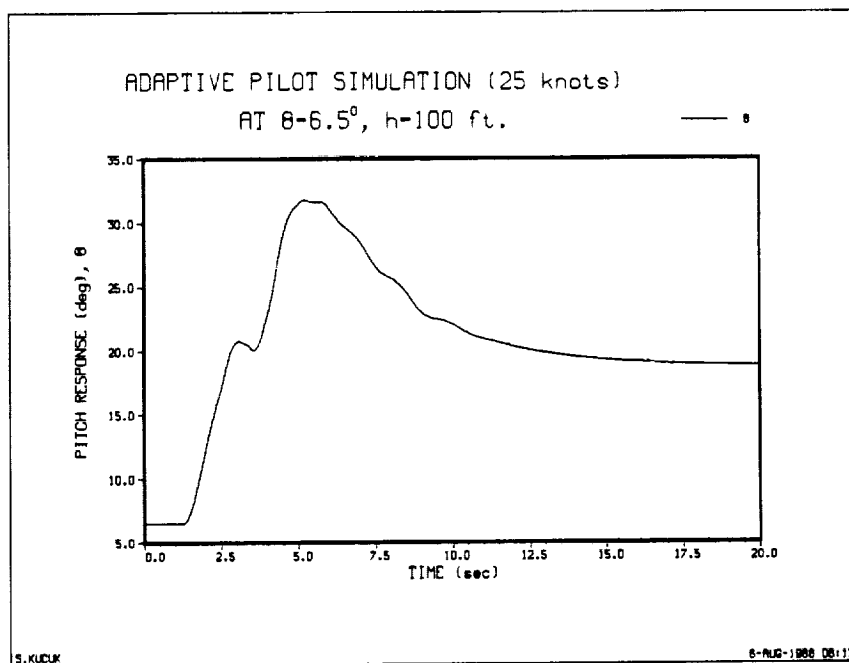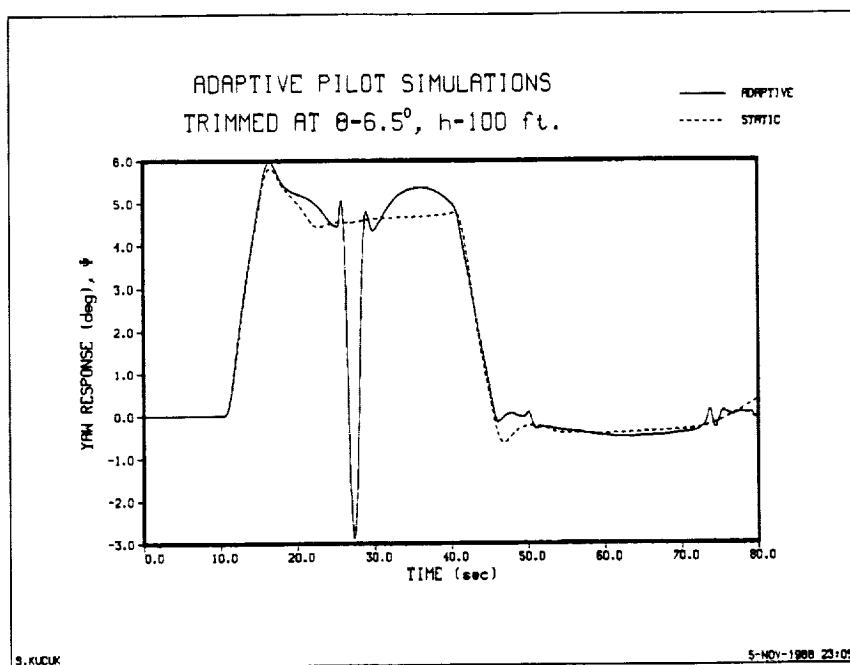
Figure 73. Pitch response, two-pilot configuration, adaptive after
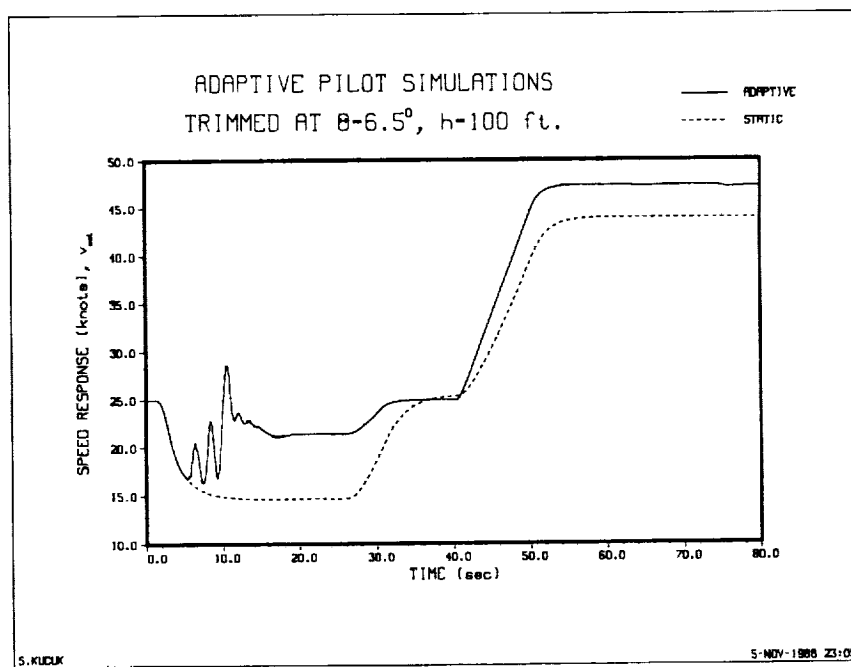*t*=2 sec
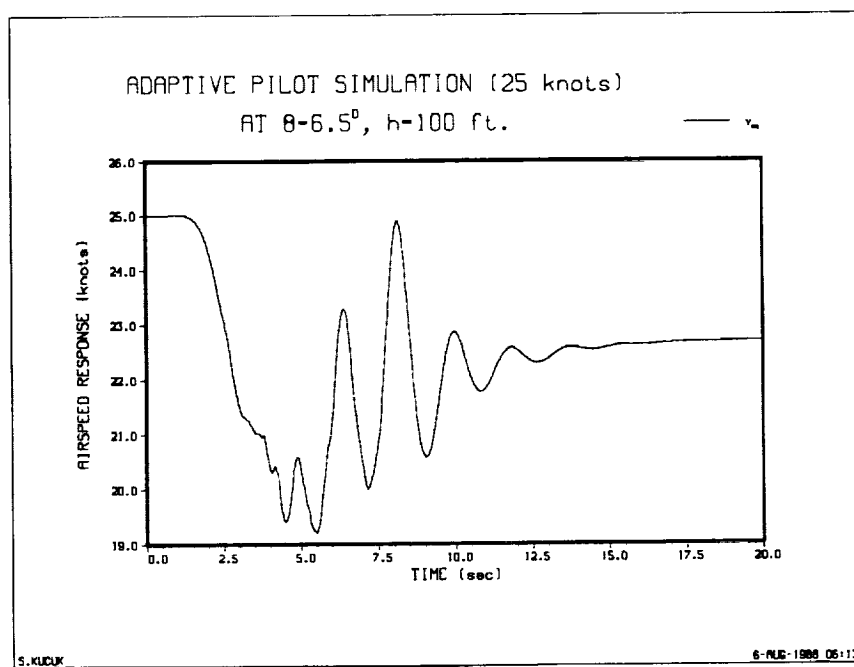
Figure 74. Airspeed response, two-pilot configuration, adaptive
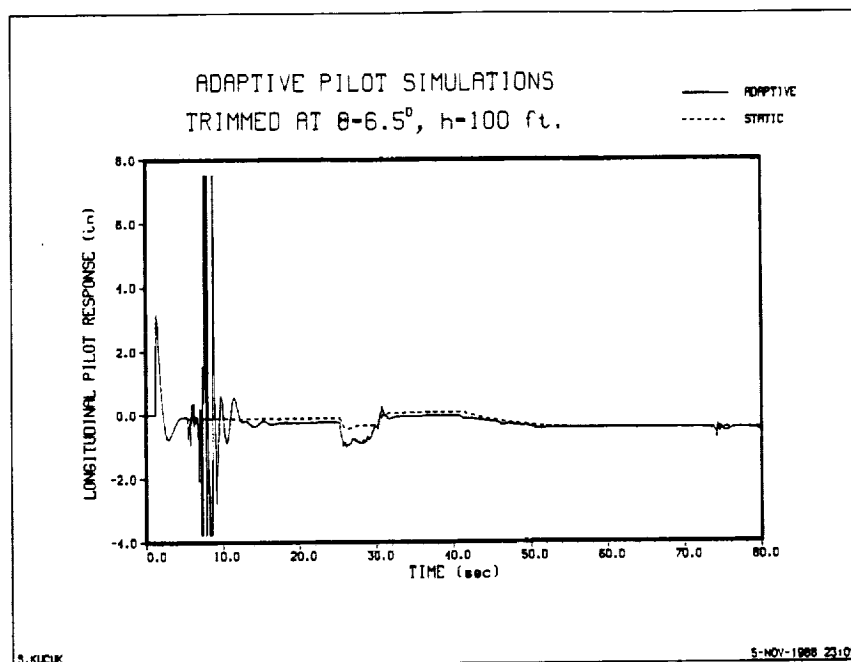after *t*=2 sec
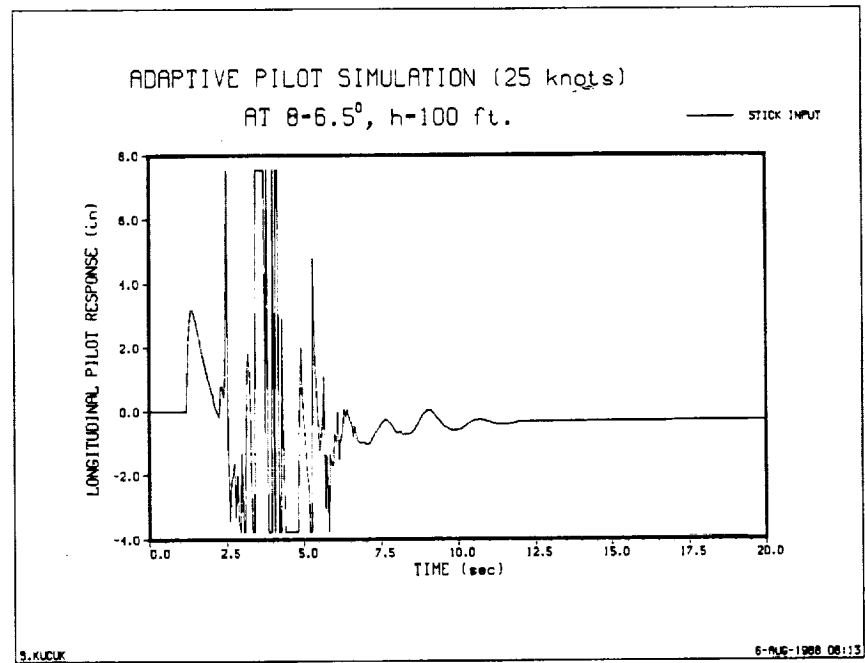
Figure 75. Longitudinal stick pilot response, two-pilot configuration, adaptive after *t*=2 sec
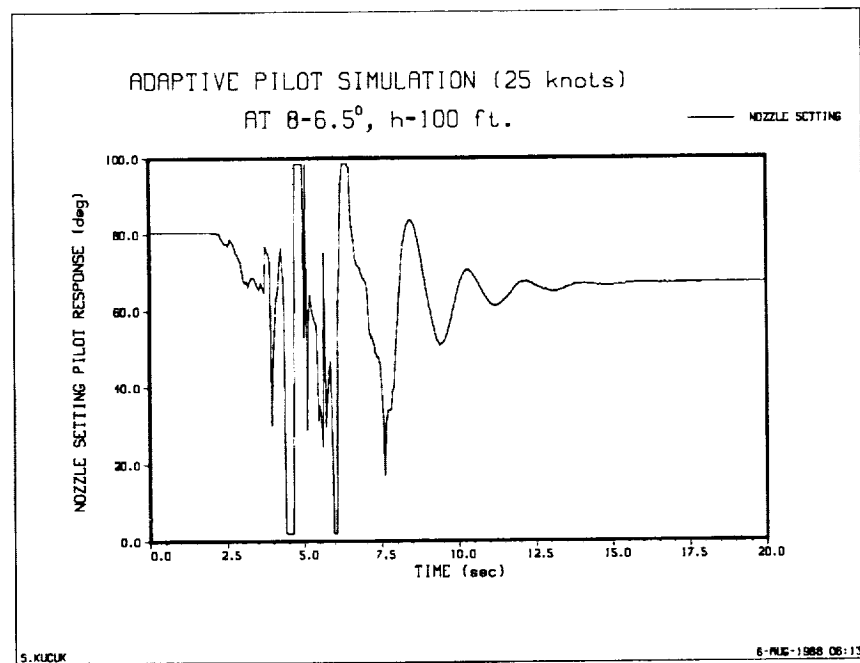
Figure 76. Nozzle setting pilot response, two-pilot configuration, adaptive after *t*=2 sec
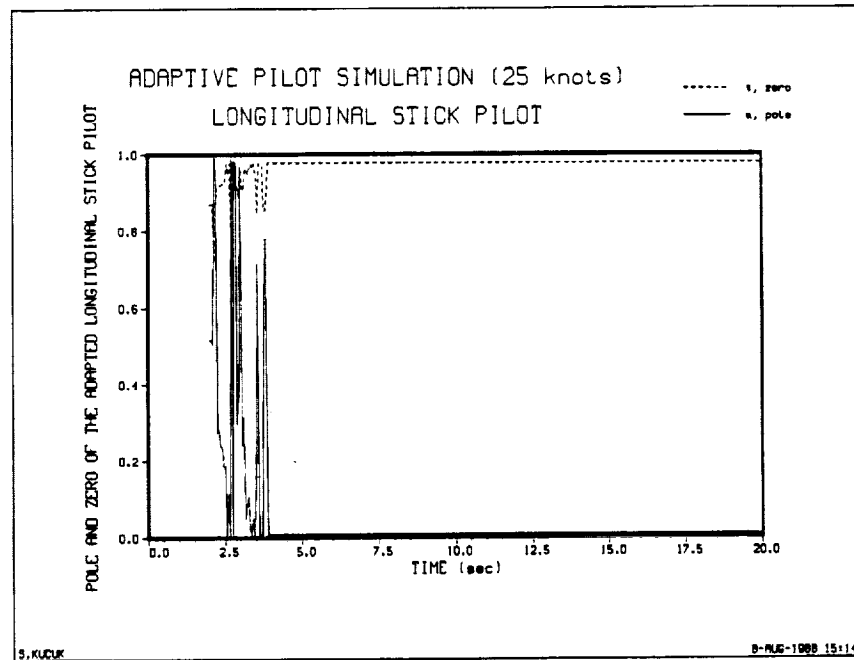
Figure 77. Longitudinal stick pilot, adapted pilot pole/zero, two-pilot configuration, adaptive after *t*=2 sec
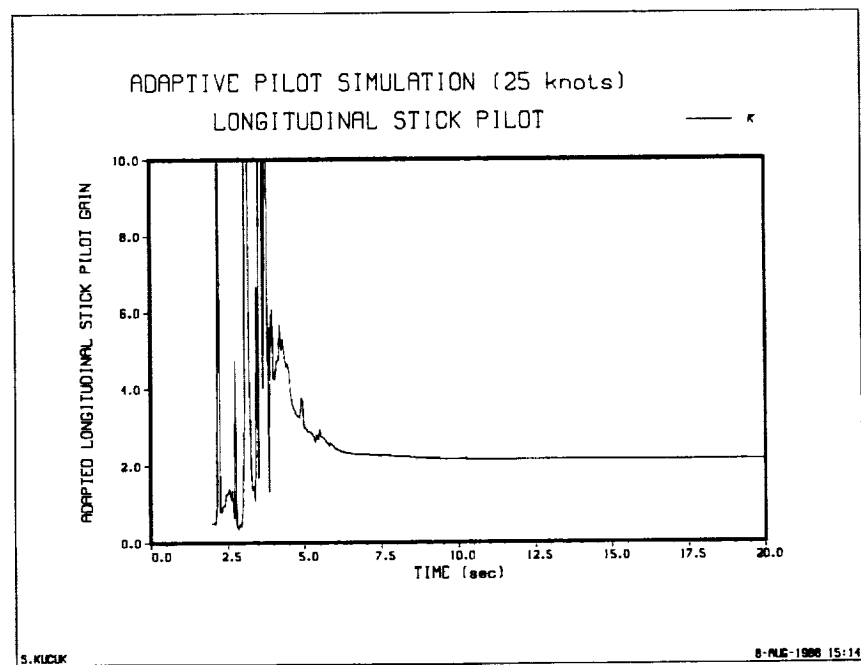
Figure 78. Longitudinal stick pilot, adapted pilot gain, two-pilot configuration, adaptive after *t*=2 sec
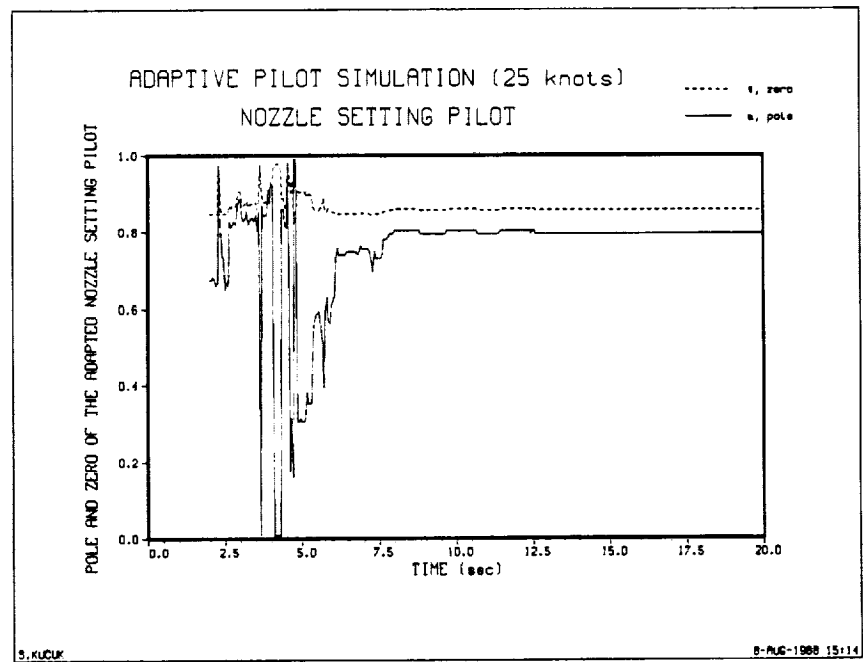
Figure 79. Nozzle setting pilot, adapted pilot pole/zero, two-pilot configuration, adaptive after $t=2$ sec
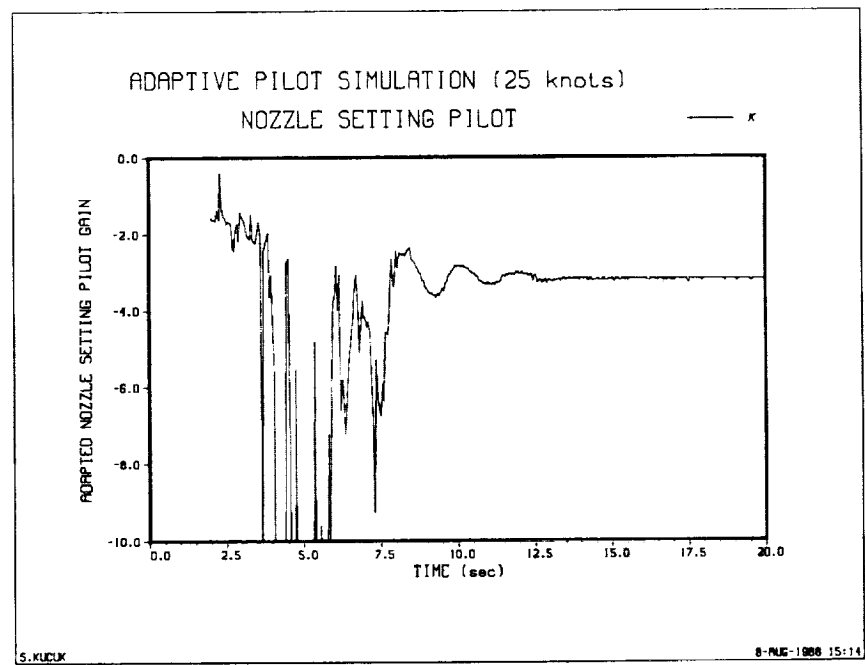
Figure 80. Nozzle setting pilot, adapted pilot gain, two-pilot configuration, adaptive after $t=2$ sec

ADAPTIVE PILOT SIMULATIONS
TRIMMED AT θ=6.5°, h=100 ft.
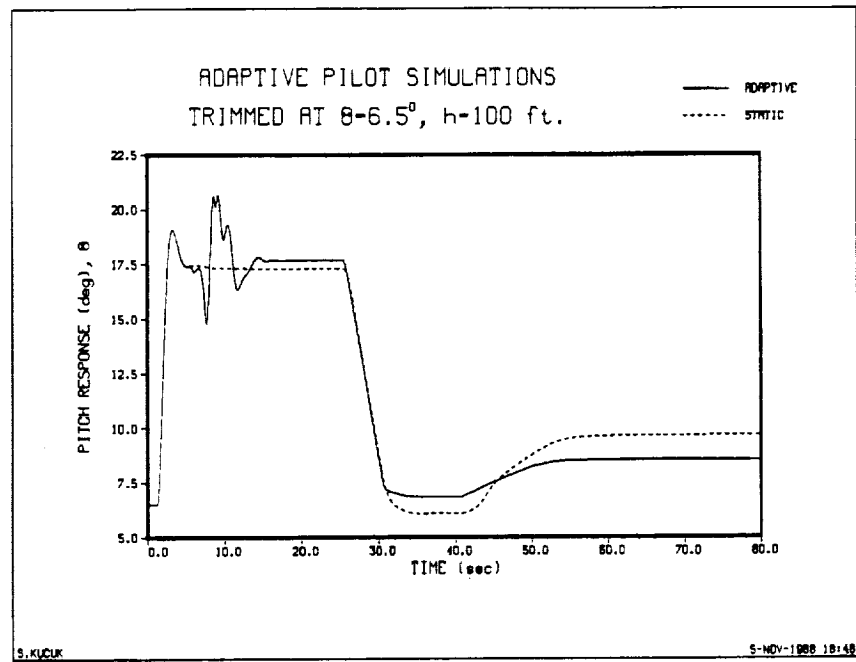
Figure 81. Pitch response, two-pilot configuration, adaptive after
$t=5$ sec

ADAPTIVE PILOT SIMULATIONS
TRIMMED AT θ=6.5°, h=100 ft.
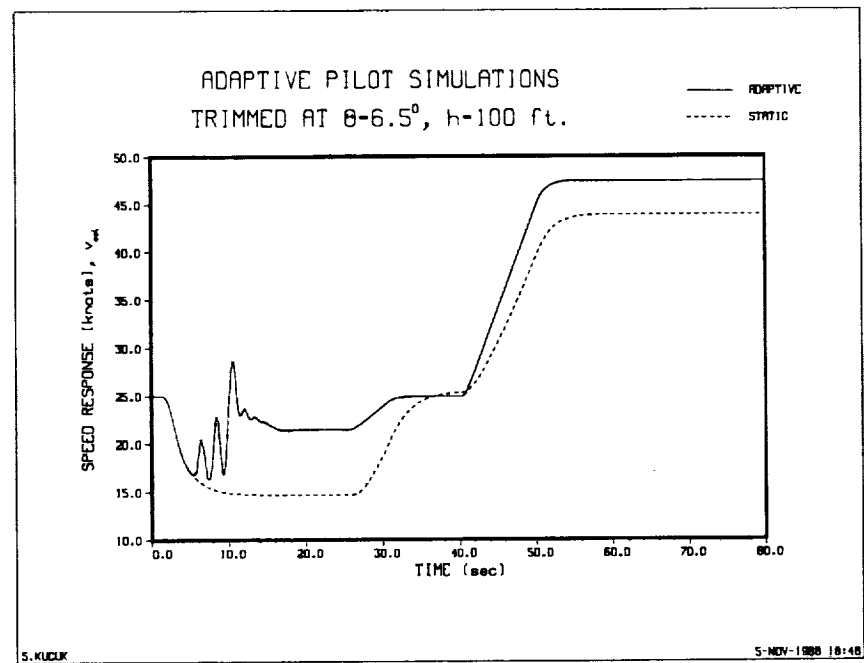
Figure 82. Airspeed response, two-pilot configuration, adaptive
after $t=5$ sec
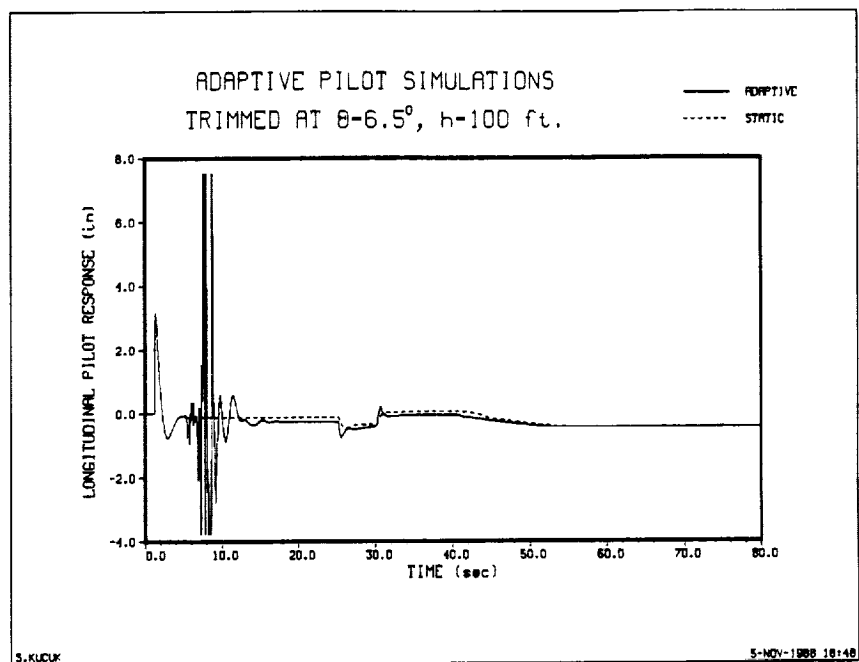
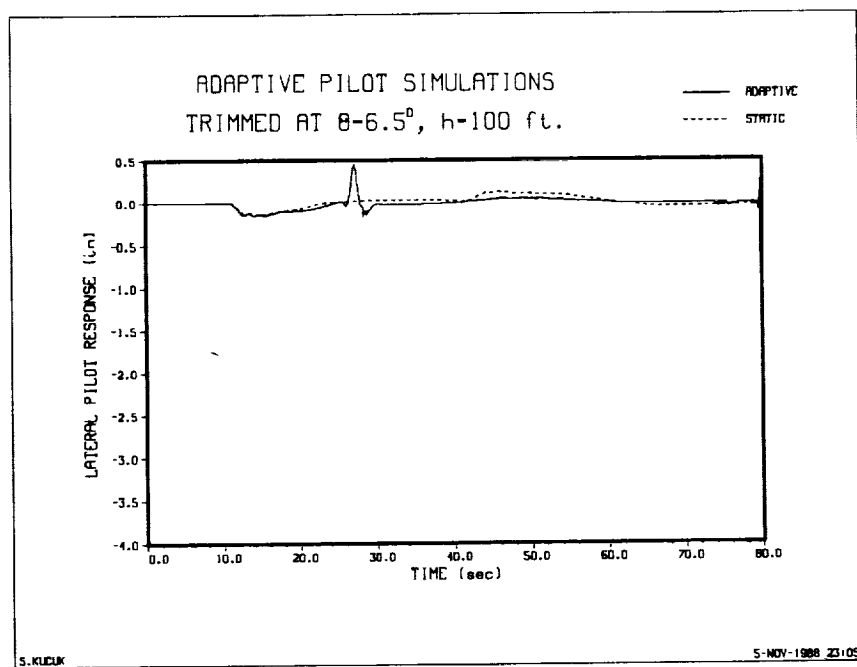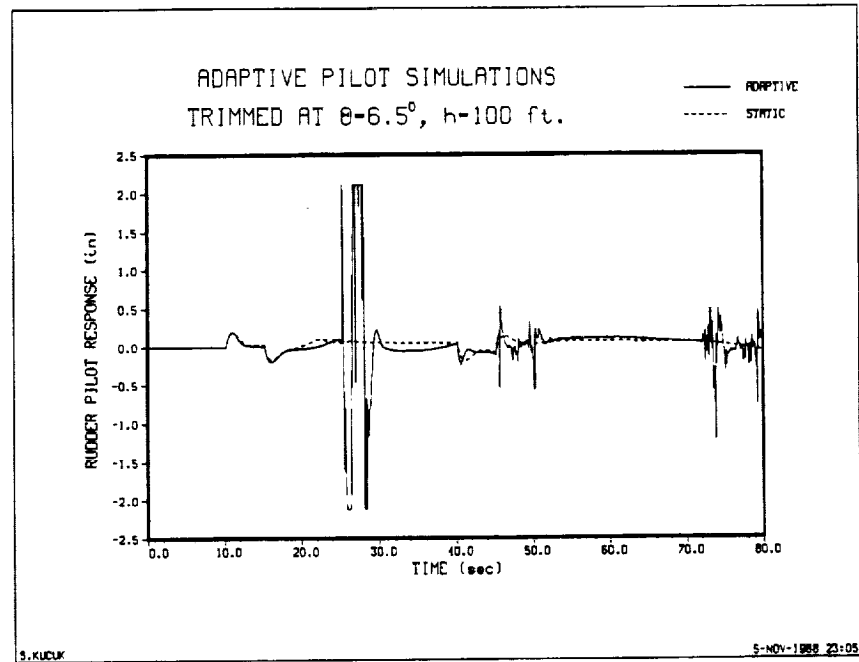**Figure 83.** Longitudinal stick pilot response, two-pilot configuration, adaptive after *t*=5 sec
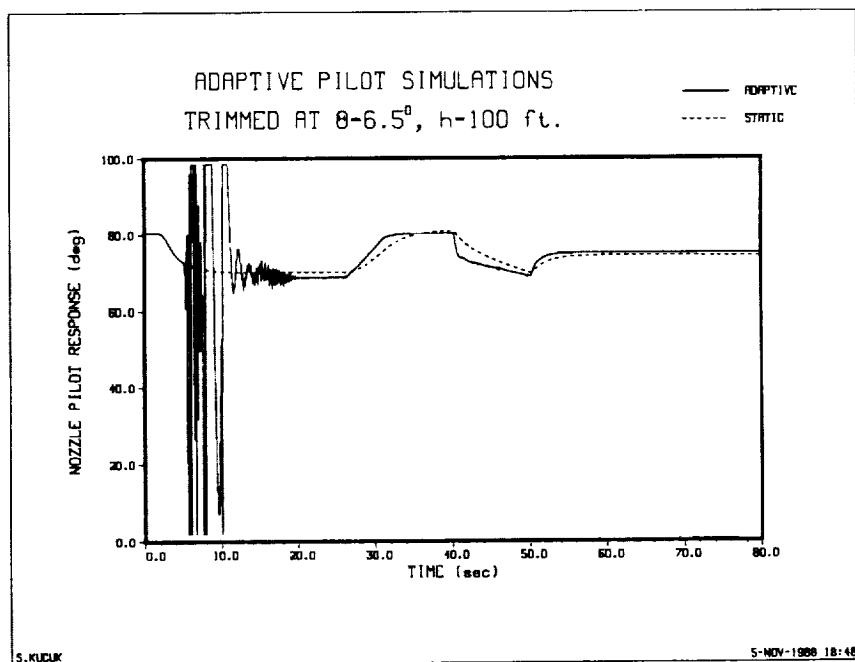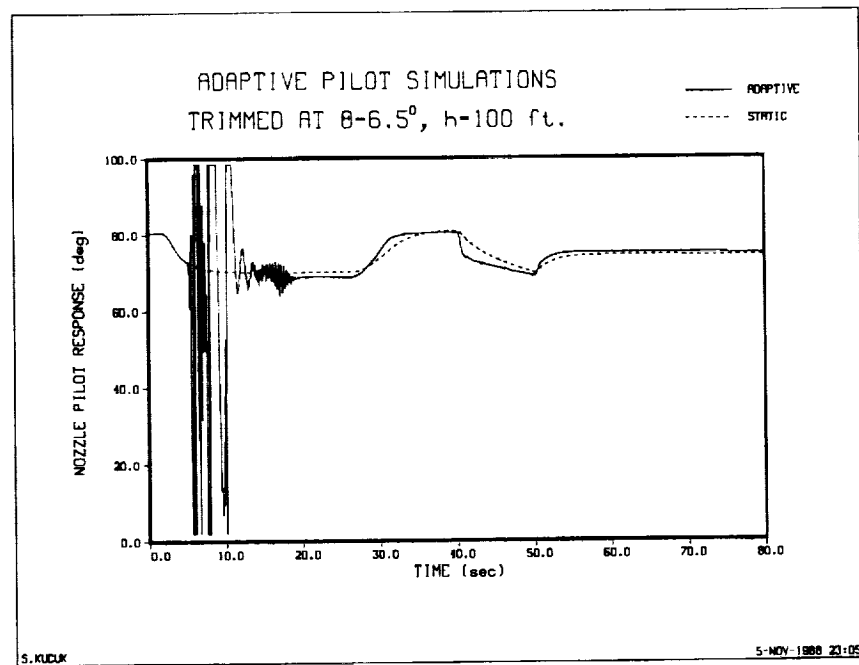

Figure 84. Nozzle setting pilot response, two-pilot configuration, adaptive after *t*=5 sec
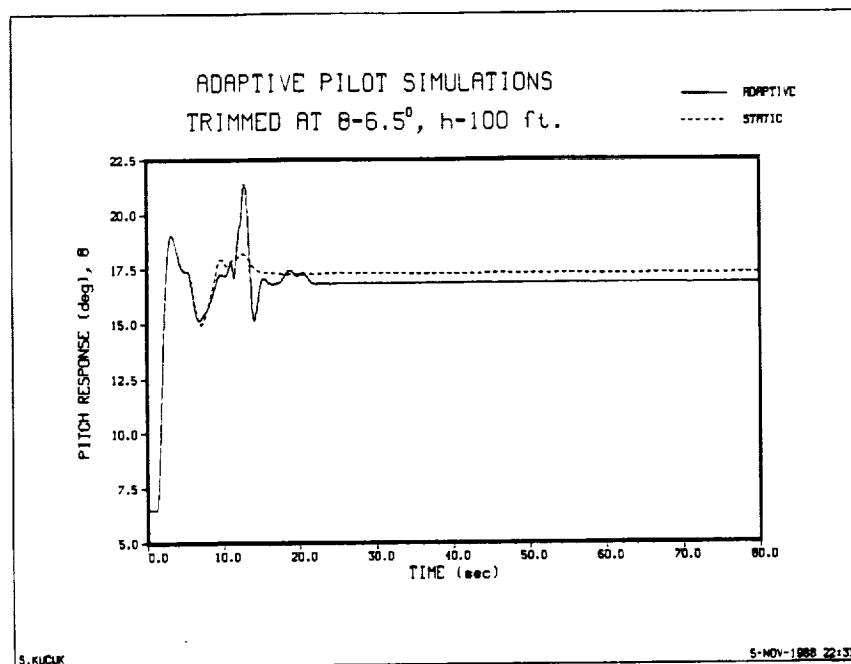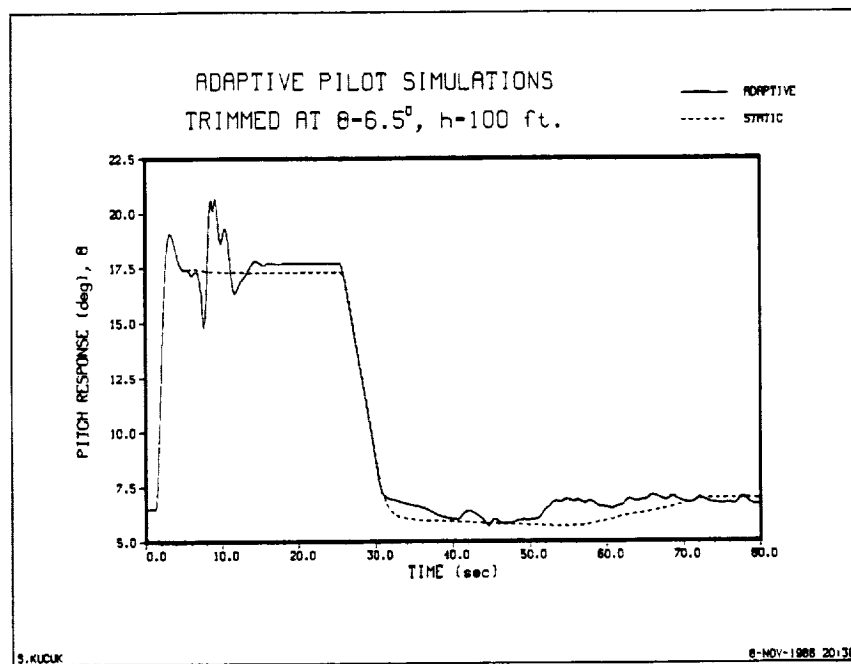
Figure 85. Pitch response, five-pilot configuration, adaptive after $t=5$ sec
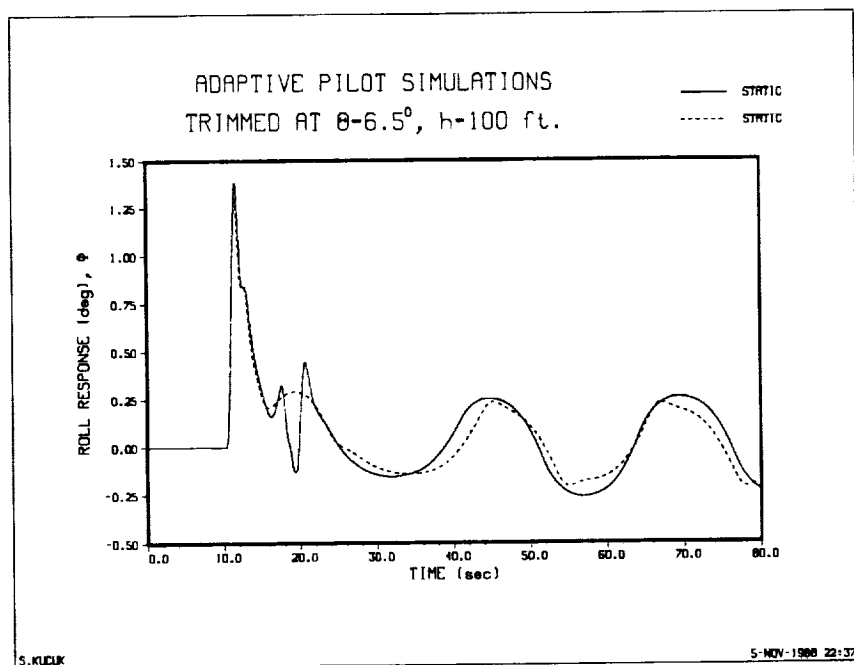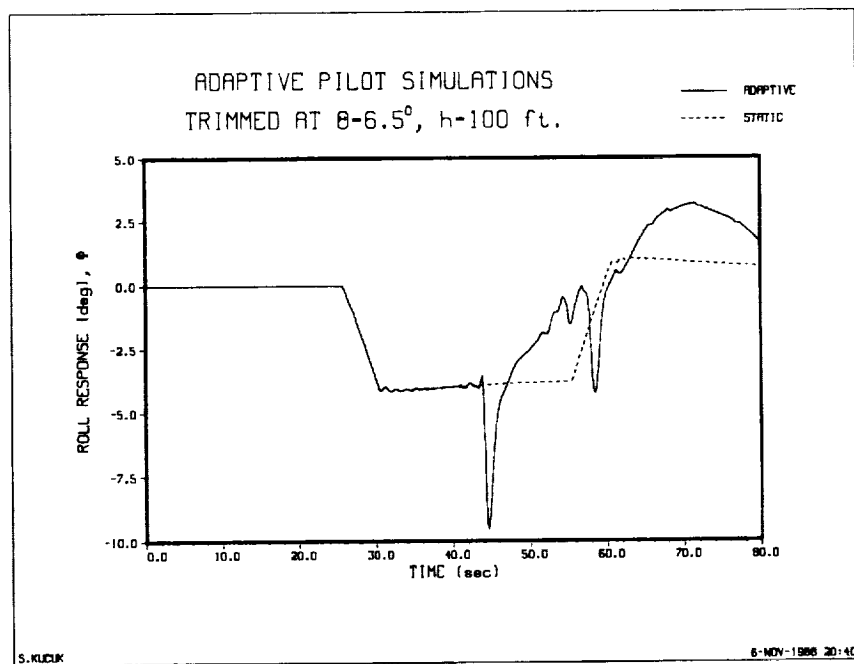

Figure 86. Roll respose, five-pilot configuration
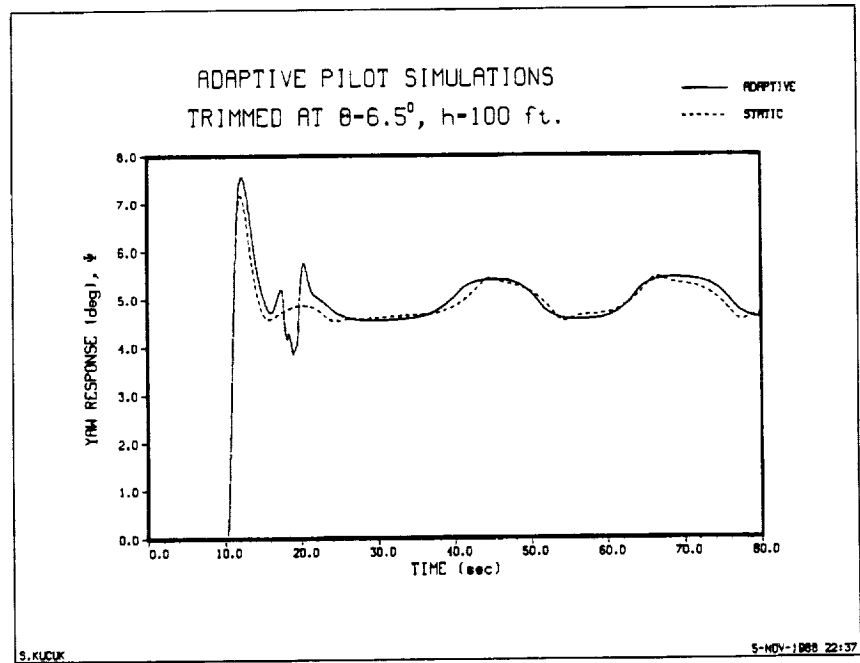
Figure 87. Yaw response, five-pilot configuration, adaptive after
t=15 sec
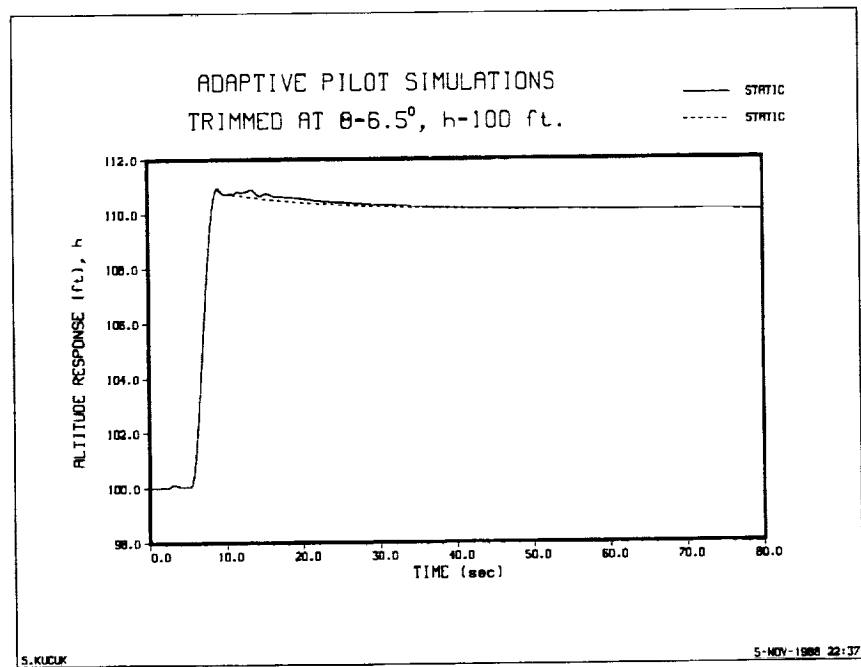
Figure 88. Altitude response, five-pilot configuration
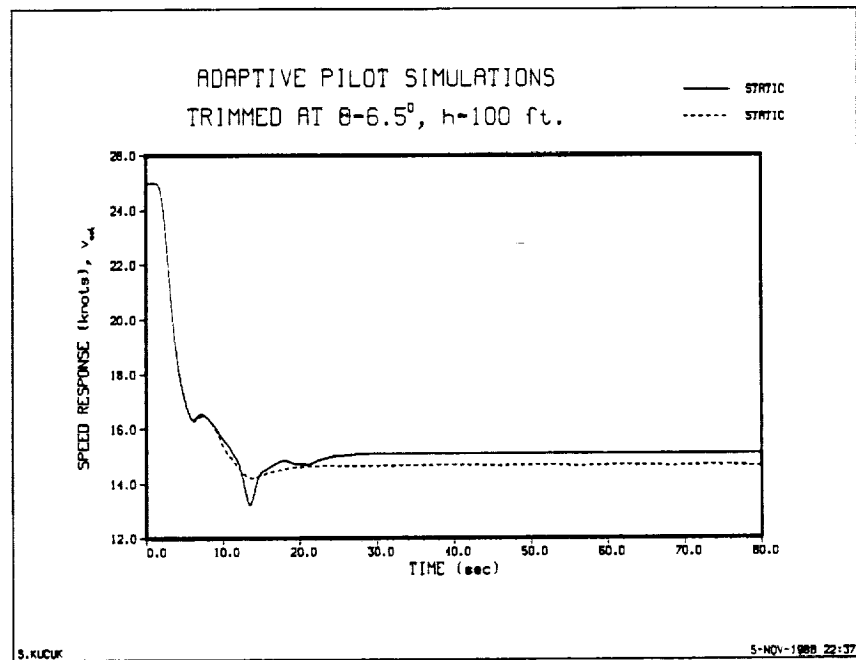
Figure 89. Airspeed response, five-pilot configuration
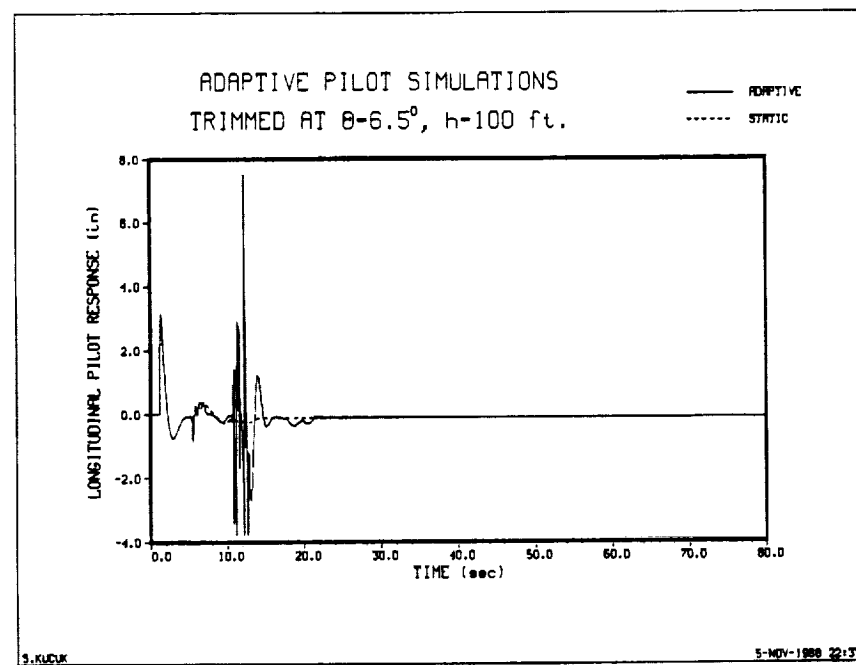
Figure 90. Longitudinal stick pilot response, five-pilot configuration, adaptive after $t=5$ sec
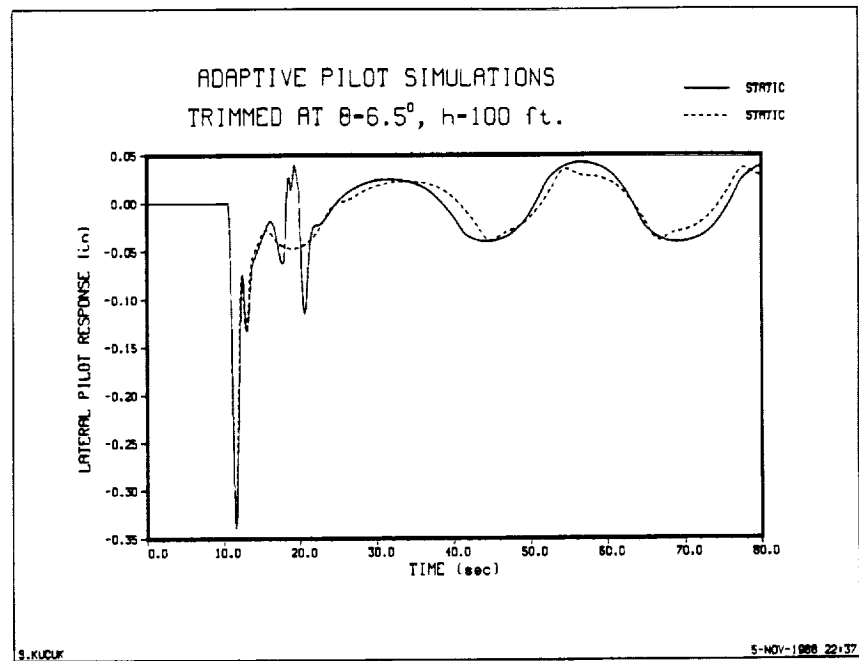
Figure 91. Lateral stick pilot response, five-pilot configuration

Figure 92. Rudder pedal pilot response, five-pilot configuration, adaptive after *t*=15 sec
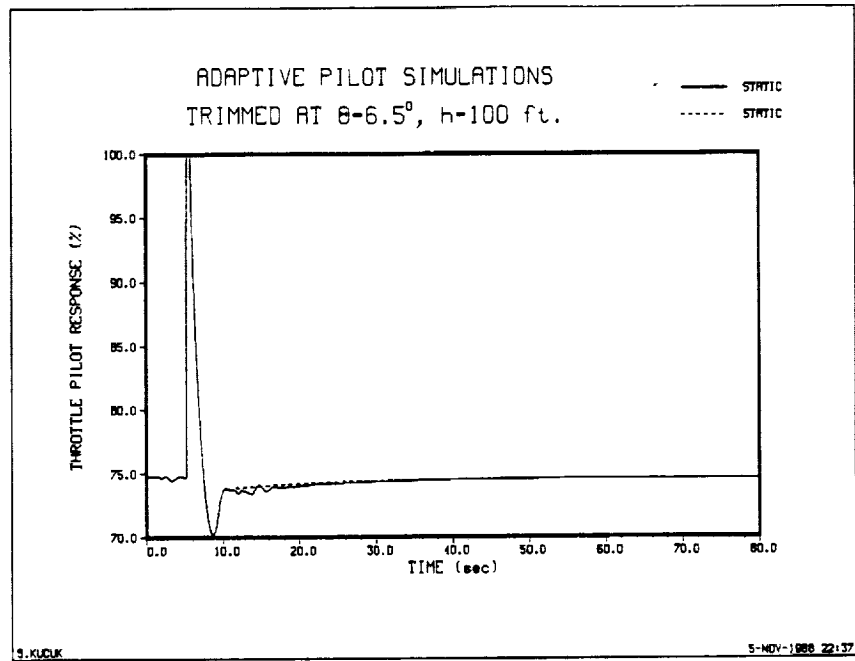
Figure 93. Throttle setting pilot response, five-pilot configuration
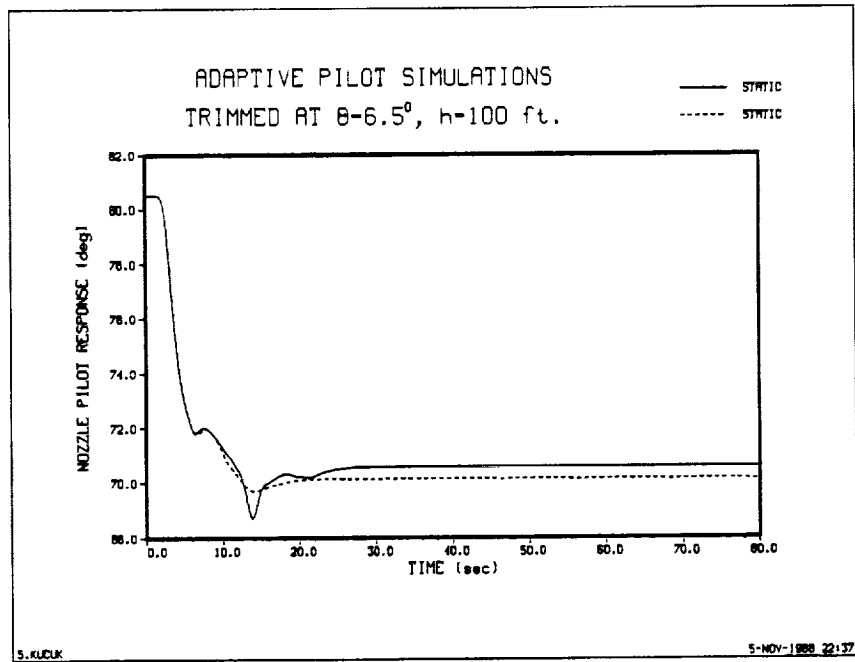
Figure 94. Nozzle setting pilot response, five-pilot configuration
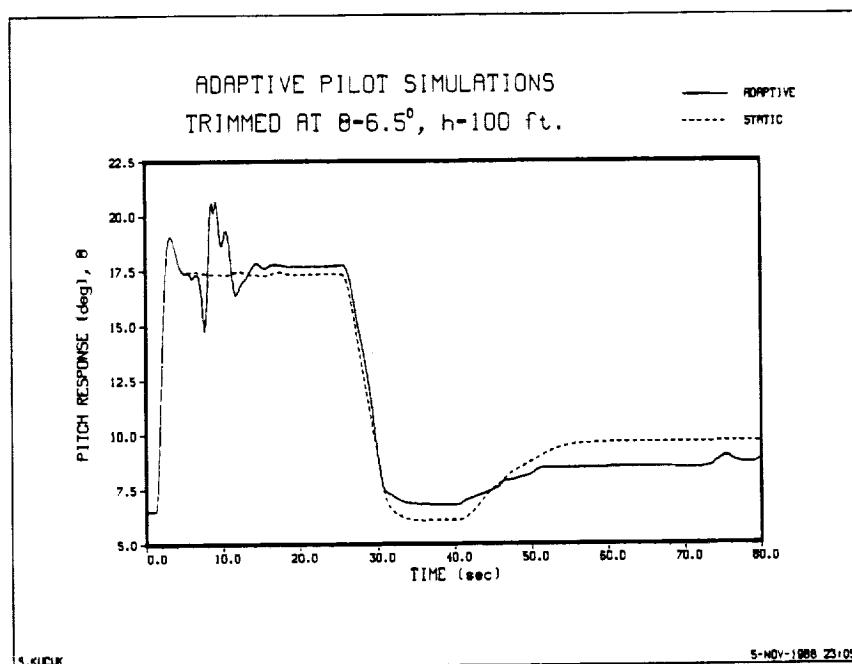
Figure 95. Pitch response, four-pilot configuration, adaptive after
t=5 sec
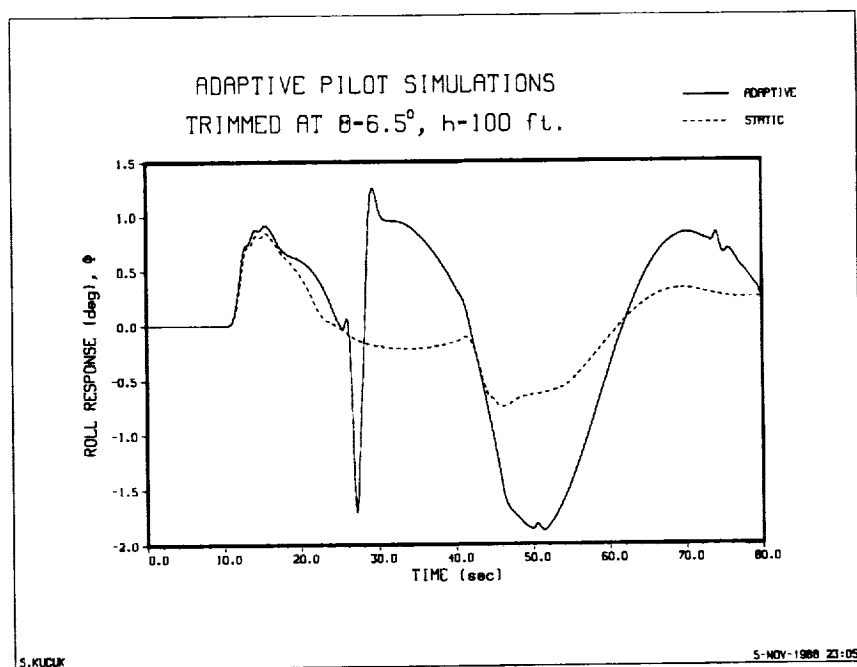
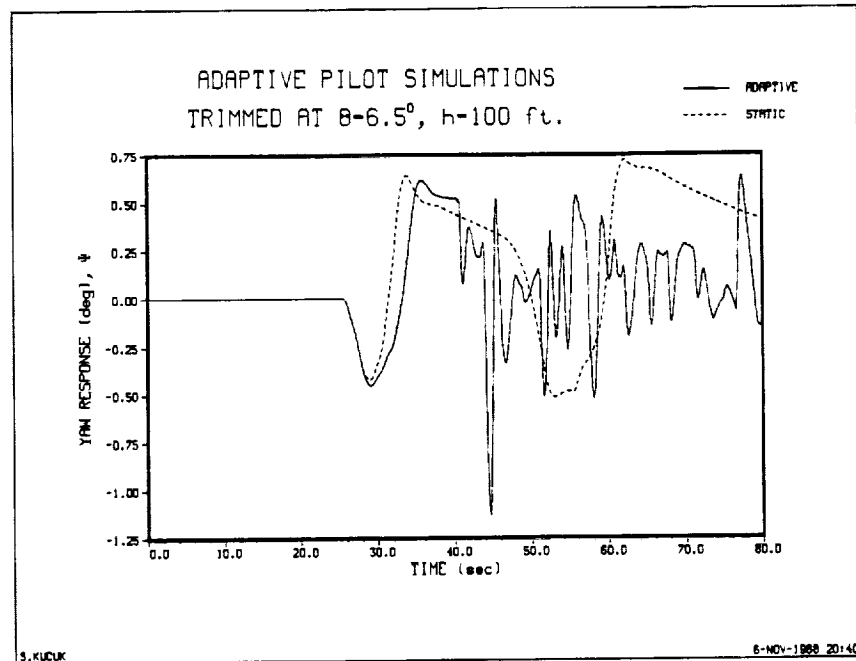**Figure 96.** Roll respose, four-pilot configuration, adaptive after
t=28 sec

Figure 97. Yaw response, four-pilot configuration, adaptive after
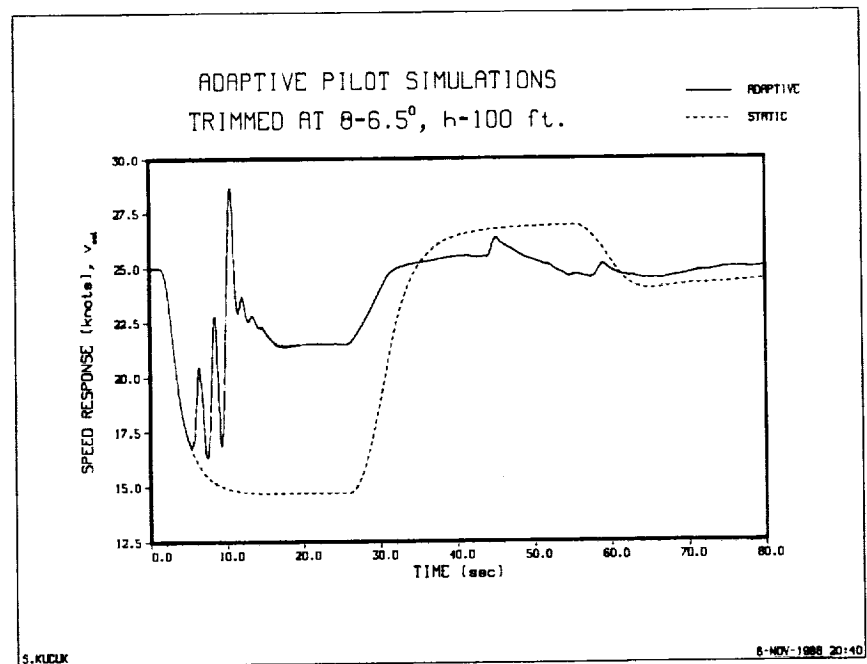t=25 sec

Figure 98. Airspeed response, four-pilot configuration, adaptive
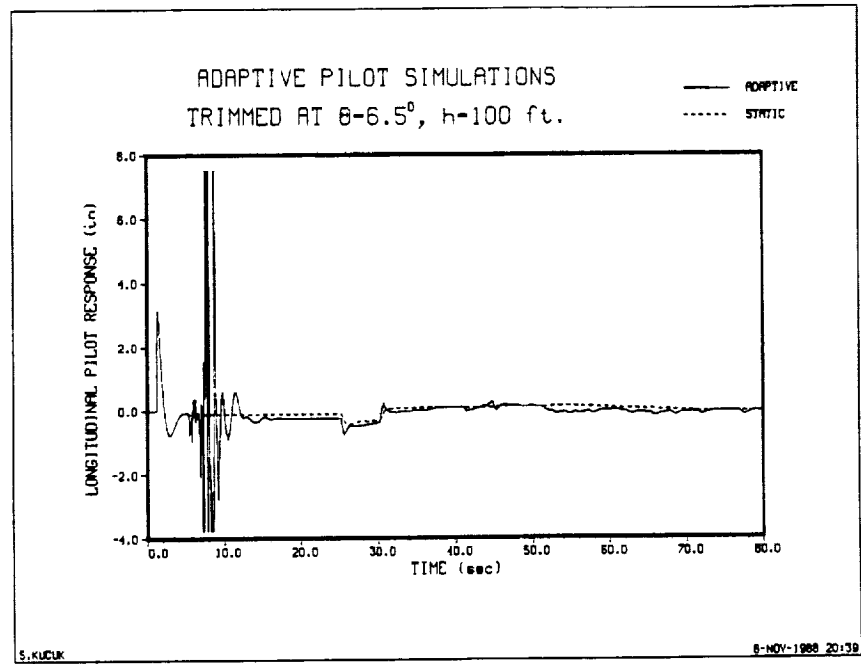after t=5 sec

Figure 99. Longitudinal stick pilot response, four-pilot configuration, adaptive after $t=5$ sec
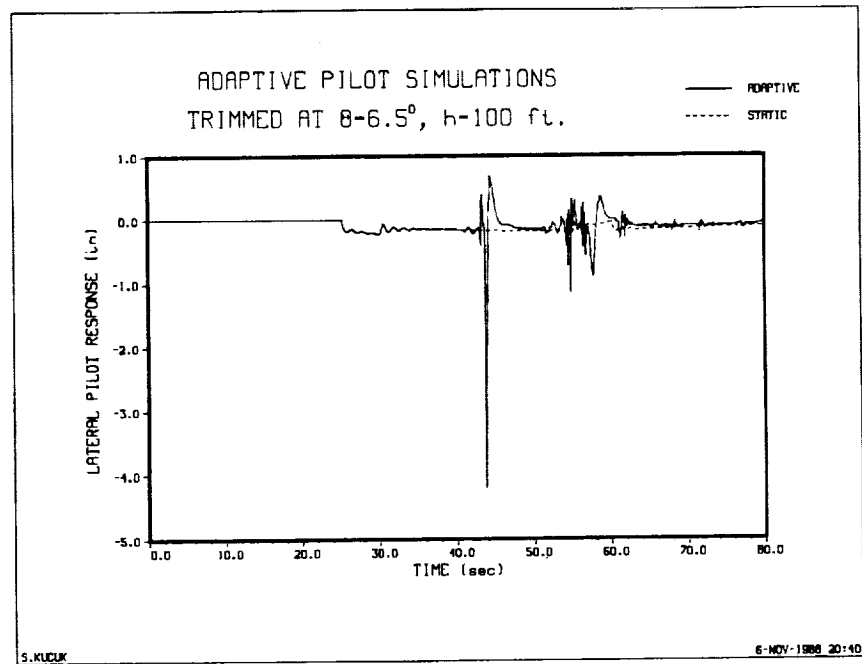

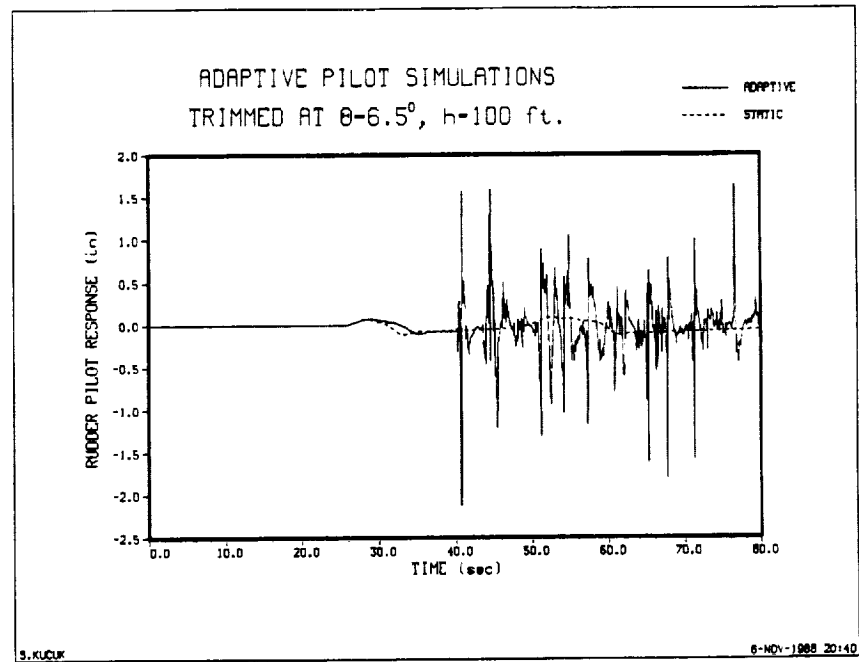**Figure 100.** Lateral stick pilot response, four-pilot configuration, adaptive after $t=28$ sec

Figure 101. Rudder pedal pilot response, four-pilot configuration, adaptive after *t*=25 sec
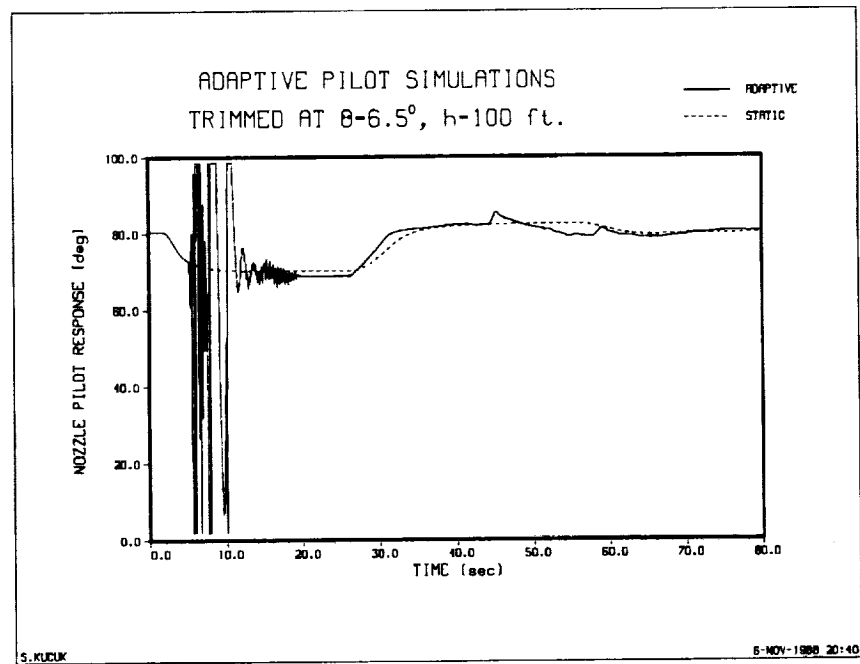

Figure 102. Nozzle setting pilot response, four-pilot configuration, adaptive after *t*=5 sec

Figure 103. Pitch response, four-pilot configuration, adaptive after
$t=5$ sec

Figure 104. Roll respose, four-pilot configuration, adaptive after
$t=40$ sec

Figure 105. Yaw response, four-pilot configuration, adaptive after
t=43 sec

Figure 106. Airspeed response, four-pilot configuration, adaptive
after *t*=5 sec

Figure 107. Longitudinal stick pilot response, four-pilot configuration, adaptive after t=5 sec

Figure 108. Lateral stick pilot response, four-pilot configuration, adaptive after t=40 sec

Figure 109. Rudder pedal pilot response, four-pilot configuration, adaptive after t=43 sec

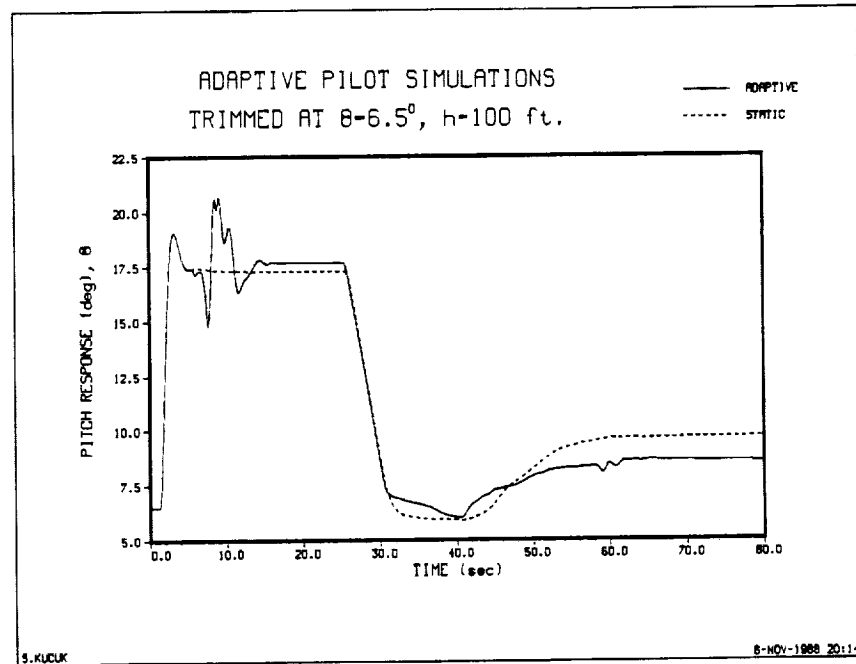**Figure 110.** Nozzle setting pilot response, four-pilot configuration, adaptive after t=5 sec

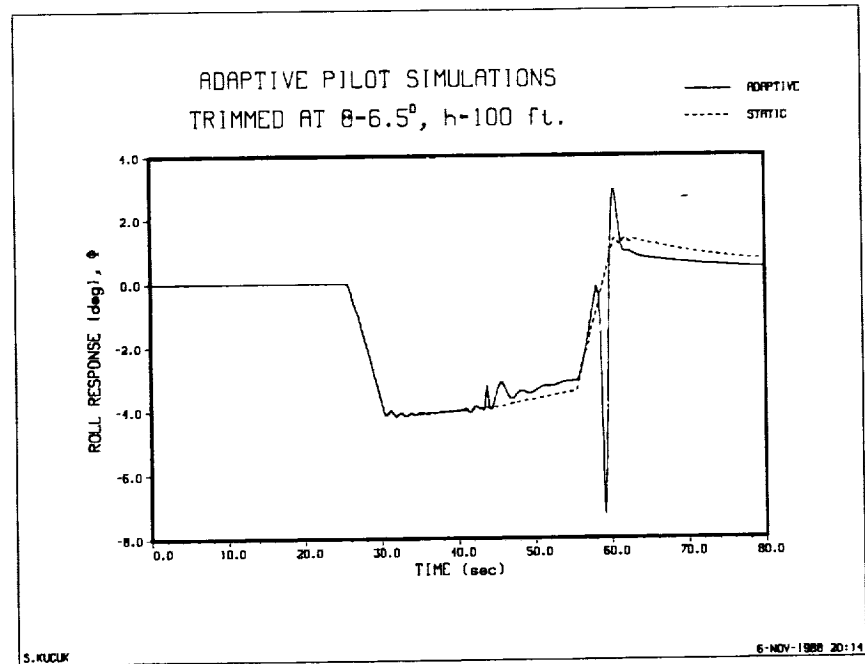**Figure 111.** Pitch response, four-pilot configuration, adaptive after
t=5 sec

Figure 112. Roll respose, four-pilot configuration, adaptive after
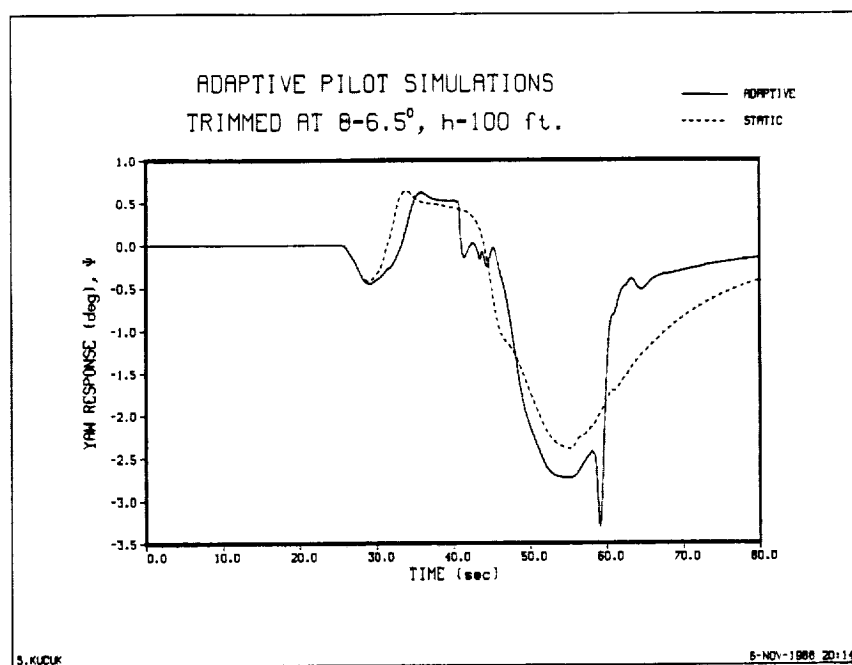*t*=40 sec

Figure 113. Yaw response, four-pilot configuration, adaptive after
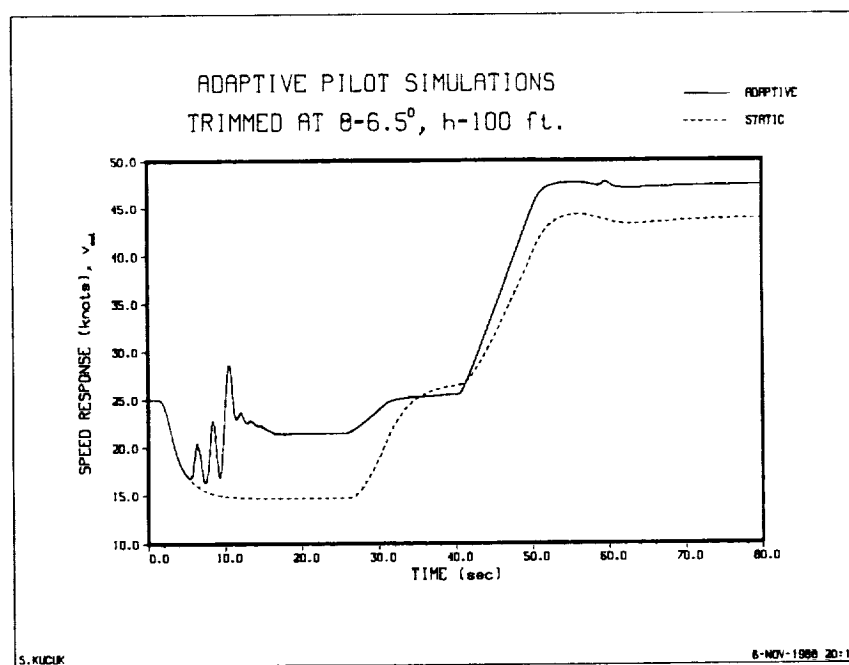*t*=43 sec

Figure 114. Airspeed response, four-pilot configuration, adaptive
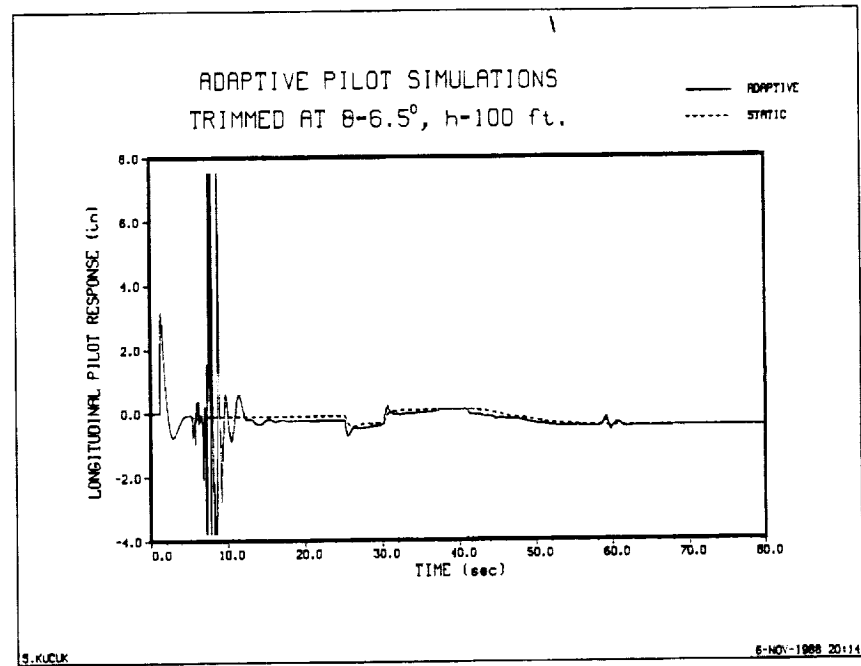after *t*=5 sec

Figure 115. Longitudinal stick pilot response, four-pilot configuration, adaptive after *t*=5 sec
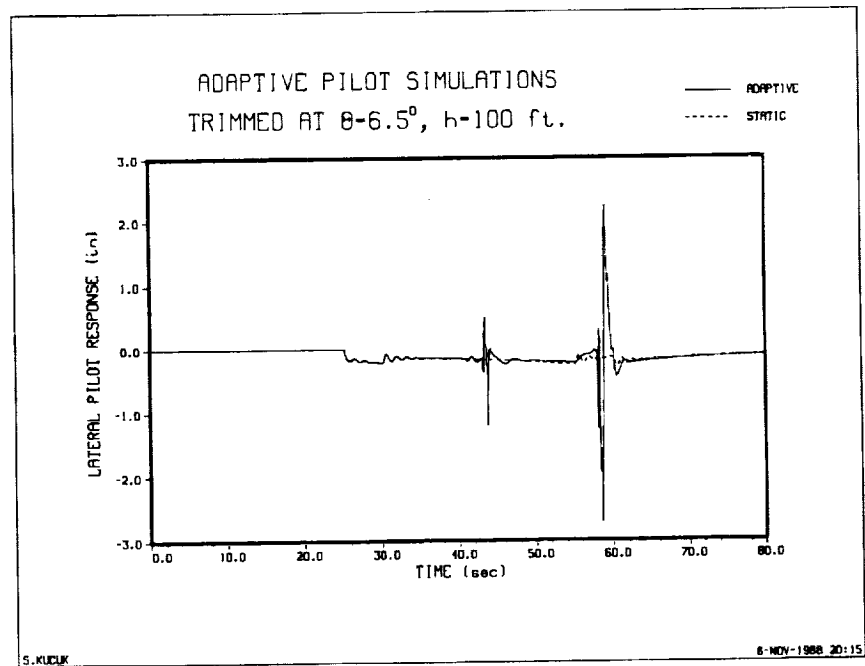

Figure 116. Lateral stick pilot response, four-pilot configuration, adaptive after *t*=40 sec
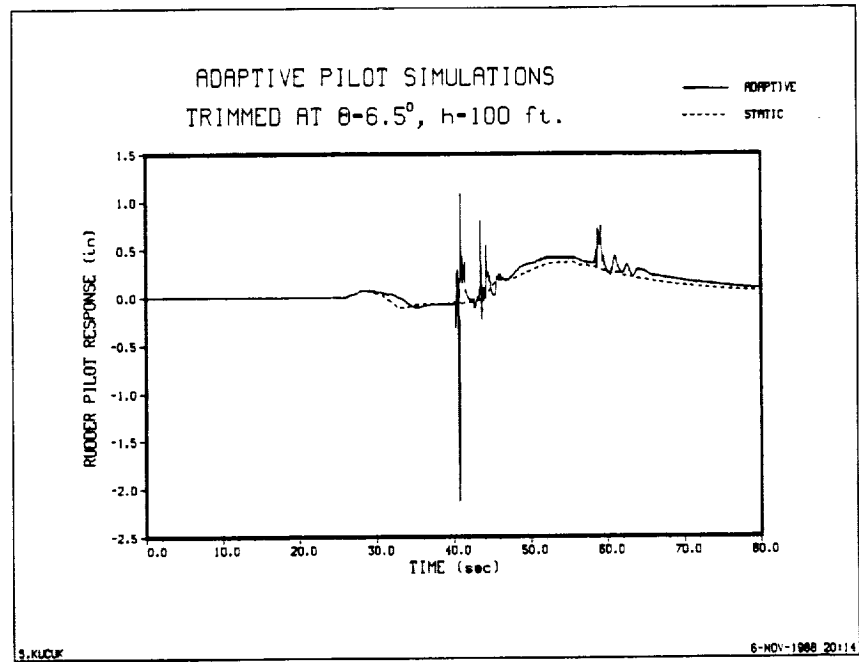
Figure 117. Rudder pedal pilot response, four-pilot configuration, adaptive after t=43 sec
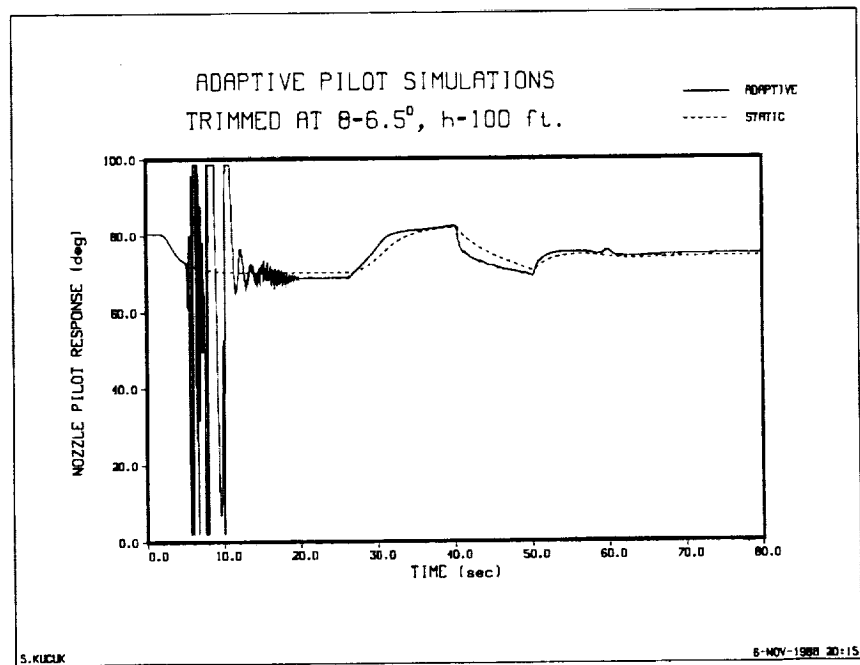

Figure 118. Nozzle setting pilot response, four-pilot configuration, adaptive after t=5 sec

6.4 Matching Actual Pilot Data

Some actual pilot data was provided by NASA-Lewis for the evaluation of the computer pilot simulations and comparisons. We chose the vertica tracking task where the actual trained pilots were subjected to vertical maneuvers over the aircraft. In order to simulate such a case, a careful reasoning of the actual pilot reaction must be undertaken. It is very important to be able to choose the primary responses of the aircraft to be consistent with the actual pilot commands. The concern becomes "why" and "when". After a careful analysis the altitude, and the heading (yaw) were found to be the primary response which the pilot is controlling. The others, like the pitch, roll, and speed were constrained to have magnitudes within an allowed region to be consistent with the actual data. The actual aircraft was sitting on the ground with no thrust. The pilot activated the throttle at t=15 sec. and continued to gain altitude until h=80 ft. He maintained his altitude until t=75 sec., when he started a descent to h=40 ft. and went back to h=80 ft. after t=105 sec. Meanwhile at t=25 sec. the rudder pedals were activated by the pilot to change the heading of the aircraft which started at 15°. The heading changed in a ramp-like behavior when the pilot finally decided to stop the heading of 70° at t=55 sec. All the time and relative aircraft parameter references are approximate. Due to some limitations of the simulation environment, our simulations had to be given approximate aircraft parameters like the initial speed, altitude and angular positions, but unlike the actual aircraft, without thrust the aircraft would have crashed if we did not trim the aircraft so that it will stay at approximately 5 ft. in the air. In the simulation, all aircraft parameters are calculated with respect to the center of gravity (CG), and 5 ft. corresponds to the altitude of the CG. Although the actual aircraft is on the ground with an CG altitude of 5 ft., the same situation applies to an aircraft at 5 ft. above the ground in the simulation. The actual pilot waited for 15 sec. before the he activated the throttle

but since the aircraft was on the ground, neither the altitude nor the speed of the aircraft did change. On the other hand, in a similar scenario, the same aircraft being simulated in the simulation environment crashed due to the lack of the thrust. For that reason, our pilot will have an initial thrust corresponding to a throttle setting that will trim the aircraft.

We used the static pilot transfer functions of equations (6-7a), (6-7b), (6-7c), (6-7d), and (6-7e) to close the loops with the decoded references of each loop corresponding to the above observations of the actual data. We did not use the adaptive pilot algorithms because of the fact that the adaptive pilots may cause undesirable responses within the "adaptation" process and may carry-off the aircraft to a configuration other than the one being simulated. The decoded reference here means the appropriate selection of the reference signals of the single-variable loops. For example, the heading loop was given a ramp signal at t=25 sec. and a step input at t=75 sec., so the rudder pilot will try to follow these references and minimize the error just like the actual pilot. However, the rudder pilot had some difficulties in controlling the heading angle in the simulations. In order to examine the actual pilot parameters, we subjected the rudder pilot data of the actual pilot response to the discrete time McRuer-Krendel model where the pilot pole, zero and gain were estimated. The analysis revealed a discrete pole at approximately, $z=-0.45$. This was a surprising result, and explained the failing behavior of our rudder pilot model in this particular case. Throughout the analysis, we assumed that such a pole can not exist in the model since all the poles are expected to be positive and stable, resulting in the fact that the poles and zeros of our pilot model should be located between $z=0$ and $z=1$, inside the unit circle. Another observation is that this pole has almost the same magnitude with the rudder pilot model of equation (6-7c) but has an opposite sign. Therefore, by using the approximated rudder pilot parameters given in equation (6-8),

$$H^{\delta}_{\Psi_f}(z^{-1}) = 0.288z^{-4}\frac{(z^{-1}-0.96z^{-2})}{(1-0.6065z^{-1})(1+0.448z^{-1})} \tag{6-8}$$

we obtained results which were very close to the actual pilot data. Figures* (119), (120), (121), (122), (123), (124), (125), (126), (127), and (128) compare the actual and simulated aircraft responses and the control movements of the actual pilot and simulated pilot models. As we mentioned earlier, the pitch and roll loops were not primary responses of the aircraft for this case. For that reason, these responses of the actual and simulated aircraft do not match exactly, but in the average sense the responses follow each other. Furthermore, in actual pilot control case, any longitudinal movement of the stick may have non-zero effects on the lateral stick due to human limitations, and vice versa. The human pilot may want to move the stick only in the longitudinal direction, but this may cause the activation of small lateral movements. However, the simulated pilot will not have this kind of behavior unless it is told so. That is why, as soon as the human pilot activates the longitudinal stick, the lateral stick also has small movements which result in small changes in the roll angle of the aircraft. Figure (124) compare the longitudinal stick input of the pilots. Notice the very close behavior of the pilots. Since both pilots are giving full thrust to gain altitude (refer to Figure (127)), the aircraft will pitch-up. The pilot must then use the stick to regulate the pitch. Figure (124) shows that both pilots push the stick in the same manner to compensate the latter. The roll responses of the actual and simulated cases have same boundaries but due to the reasons explained before they are not exactly the same. However, the altitude and heading responses follow each other closely, being the primary responses of the simulated case. The throttle settings are also very close to each other. Both pilots require full thrust from the aircraft for fast altitude changes. Notice that the throttle setting of the actual pilot starts from 0%,

---

*The actual pilot control inputs had initial offsets and were shifted to origin for comparison purposes

while our pilot starts from approximately 75%, due to the startup conditions. The rudder pedal inputs are approximately same for a period, but as the configuration of the aircraft changes, the responses differ, although they both fulfill the heading requirements. Also, the nozzle setting of our simulated pilot had to be adjusted slightly to stabilize the speed changes, but once again in the average sense the actual pilot nozzle setting and the simulated nozzle setting follow each other. Finally, we should mention that it is not surprising to expect some differences from the actual pilot data. While the actual pilot is using all his training experience and skills, our model has only five, second-order transfer functions to simulate the human pilot. However, the responses are remarkably close to each other, and the pilot models can in fact control the aircraft, similar to the human pilot.

Figures (129), (130), (131), (132), (133), (134), (135), (136), (137), and (138) compare the static pilots with the actual pilot data for a lateral tracking task, and Figures (139), (140), (141), (142), (143), (144), (145), (146), (147), and (148) show the adaptive pilot performances for the same maneuver. As we mentioned before, after the adaptive pilots converge, the responses are similar.
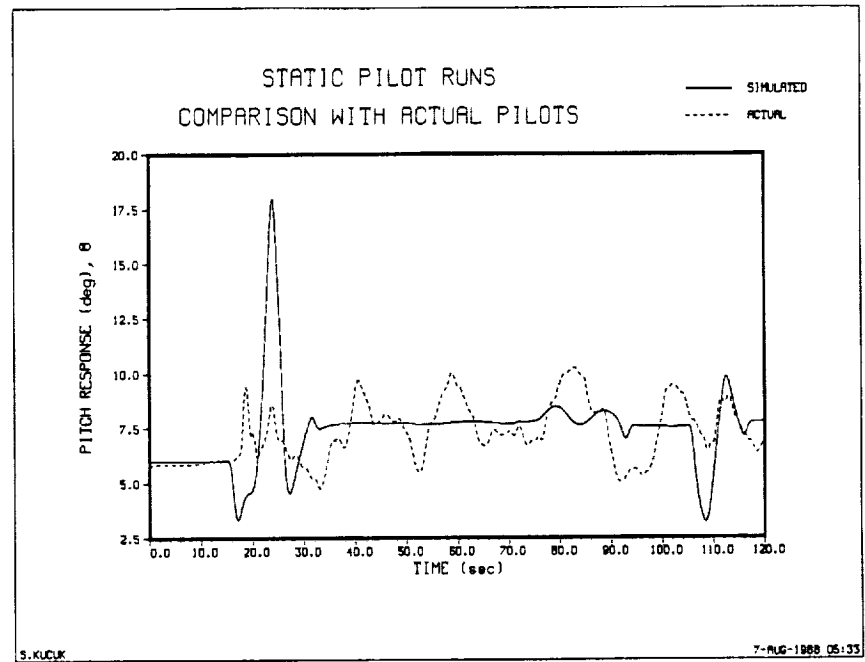
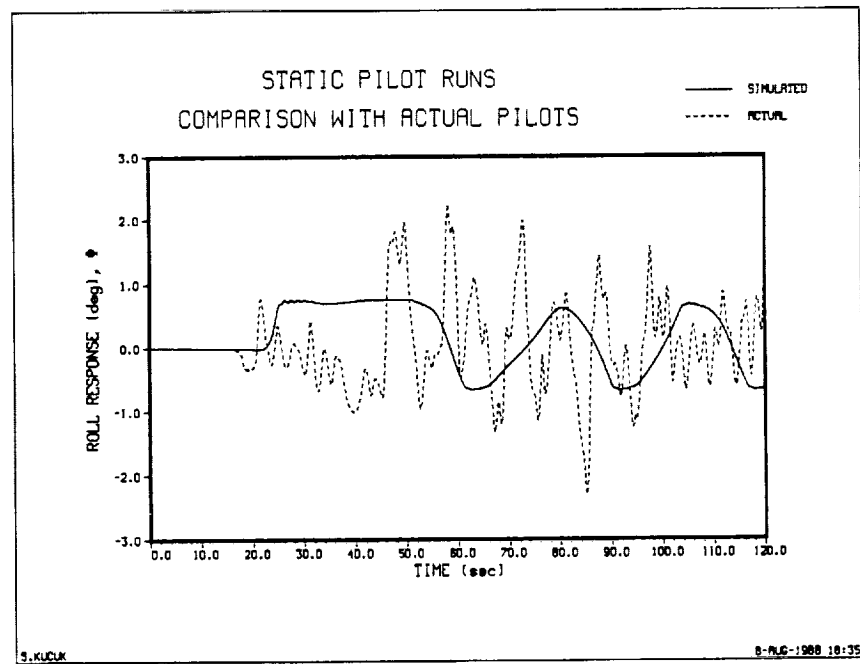**Figure 119.** Actual vs simulated pitch response (from NASA data)

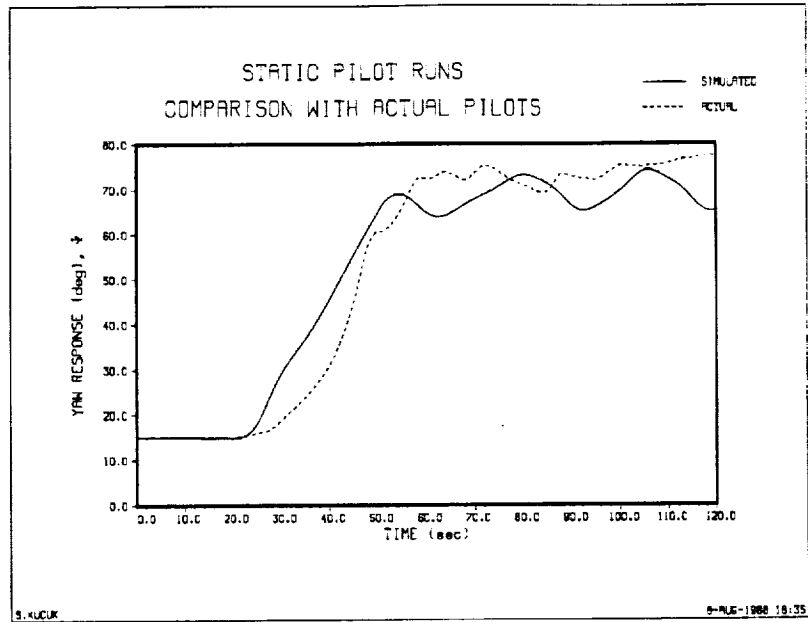**Figure 120.** Actual vs simulated roll response (from NASA data)

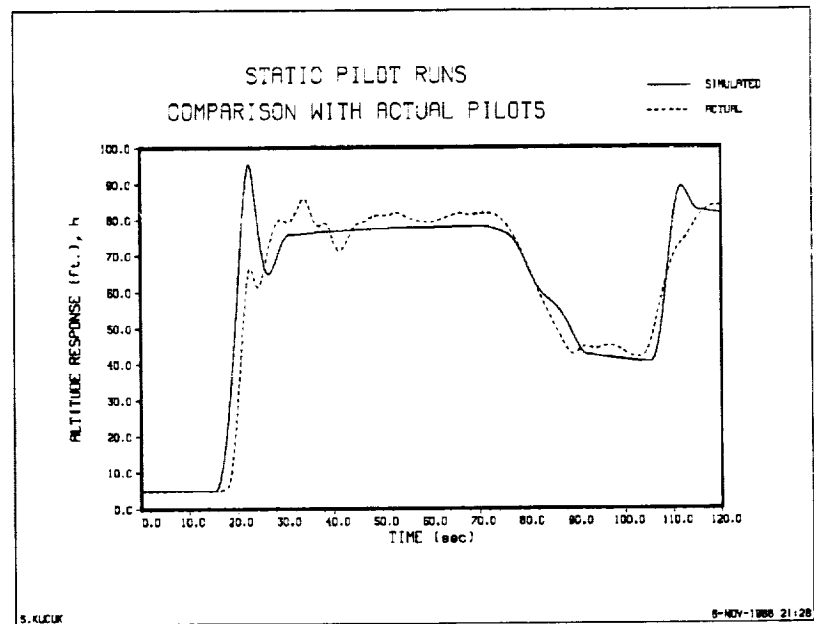**Figure 121.** Actual vs simulated yaw response (from NASA data)

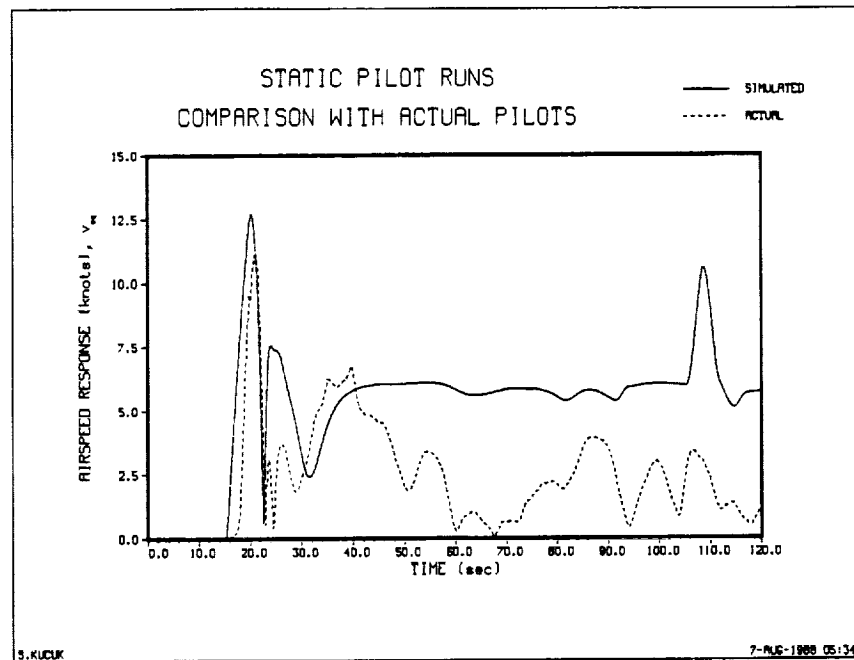**Figure 122.** Actual vs simulated altitude response (from NASA data)

Figure 123. Actual vs simulated speed response (from NASA data)

Figure 124. Actual vs simulated longitudinal stick input (from NASA data)

Figure 125. Actual vs simulated lateral stick input (from NASA data)

Figure 126. Actual vs simulated rudder pedal input (from NASA data)

Figure 127. Actual vs simulated throttle setting input (from NASA data)

Figure 128. Actual vs simulated nozzle setting input (from NASA data)
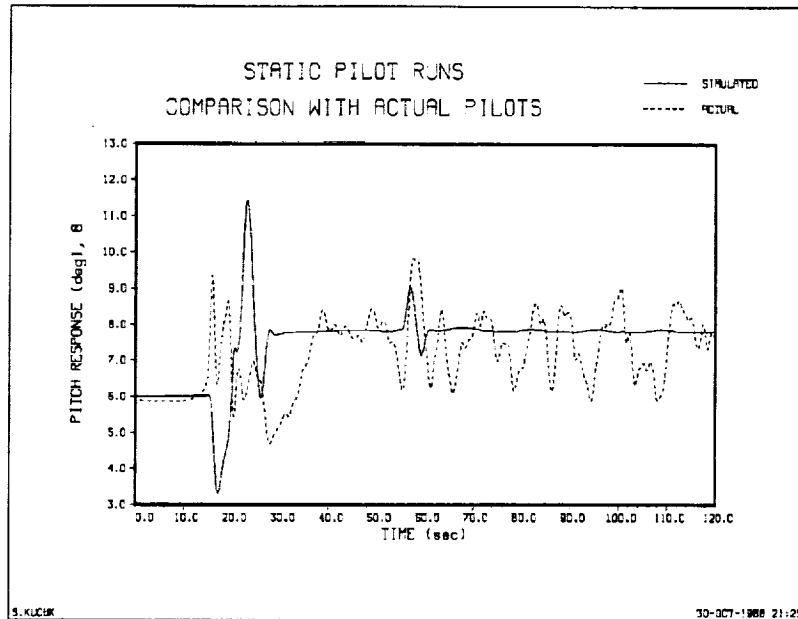
Figure 129. Actual vs simulated pitch response (from NASA data)
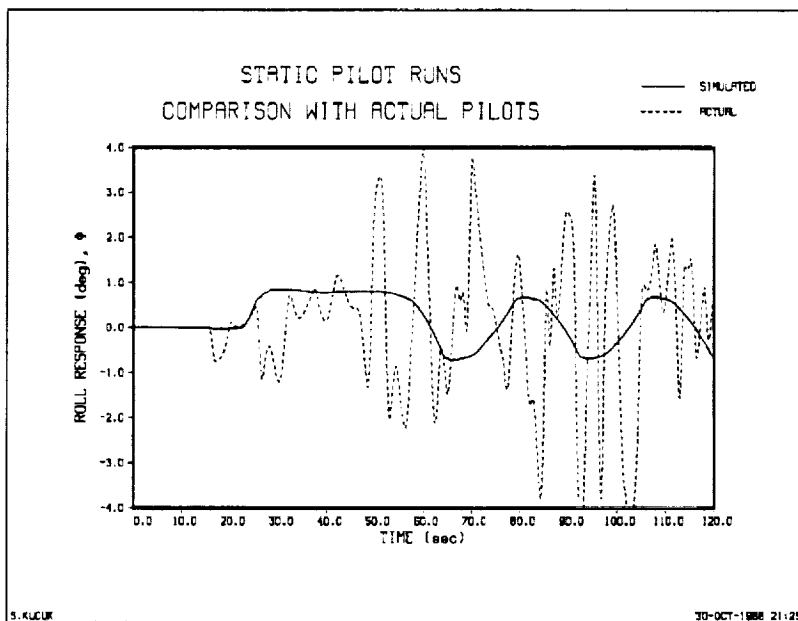
Figure 130. Actual vs simulated roll response (from NASA data)
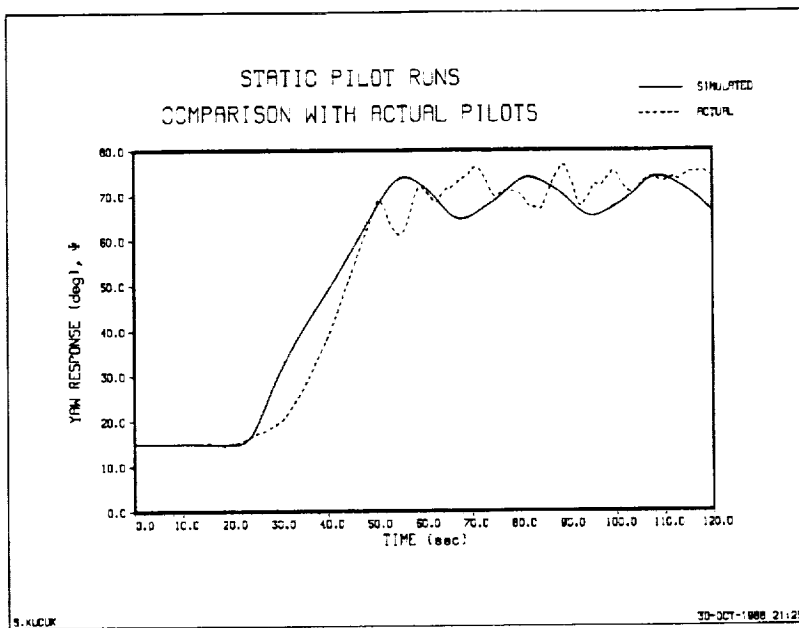
Figure 131. Actual vs simulated yaw response (from NASA data)
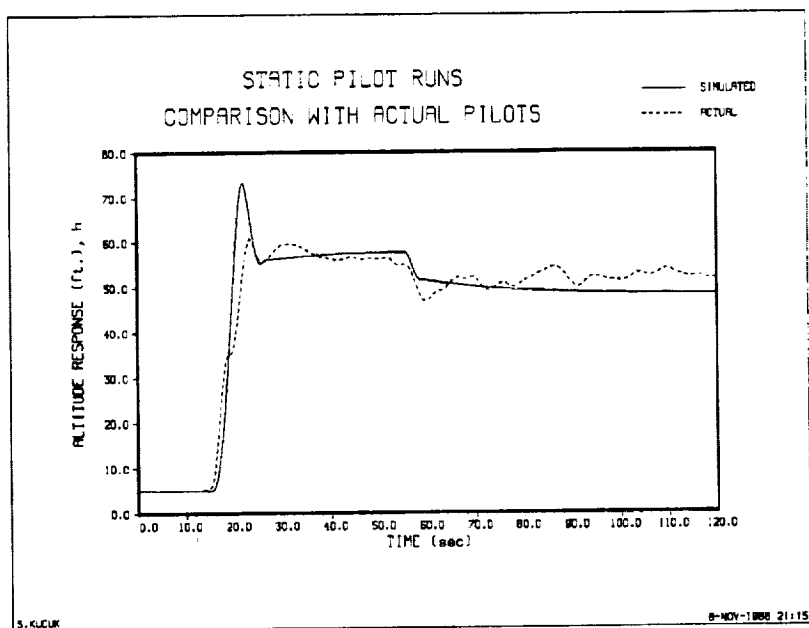
Figure 132. Actual vs simulated altitude response (from NASA data)
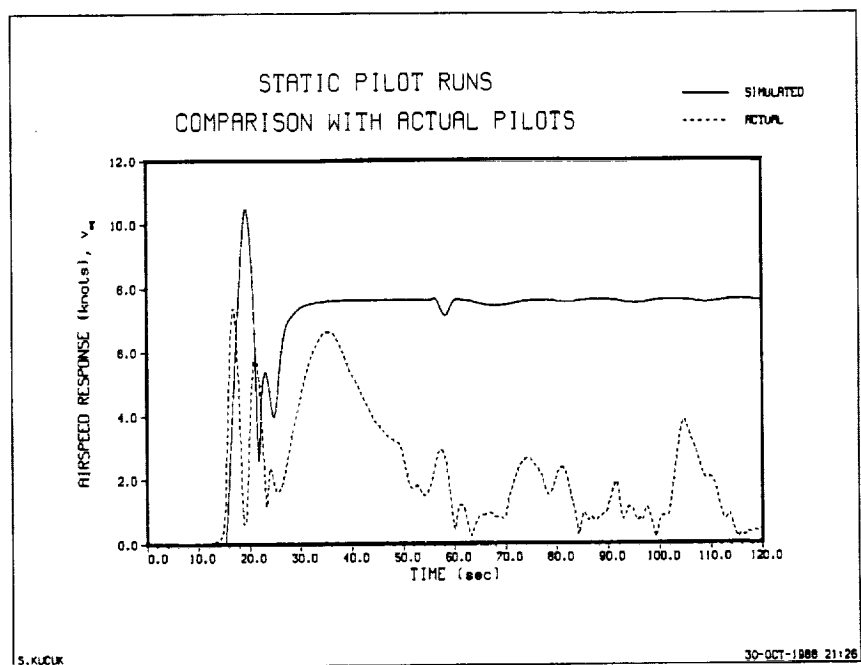
Figure 133. Actual vs simulated speed response (from NASA data)
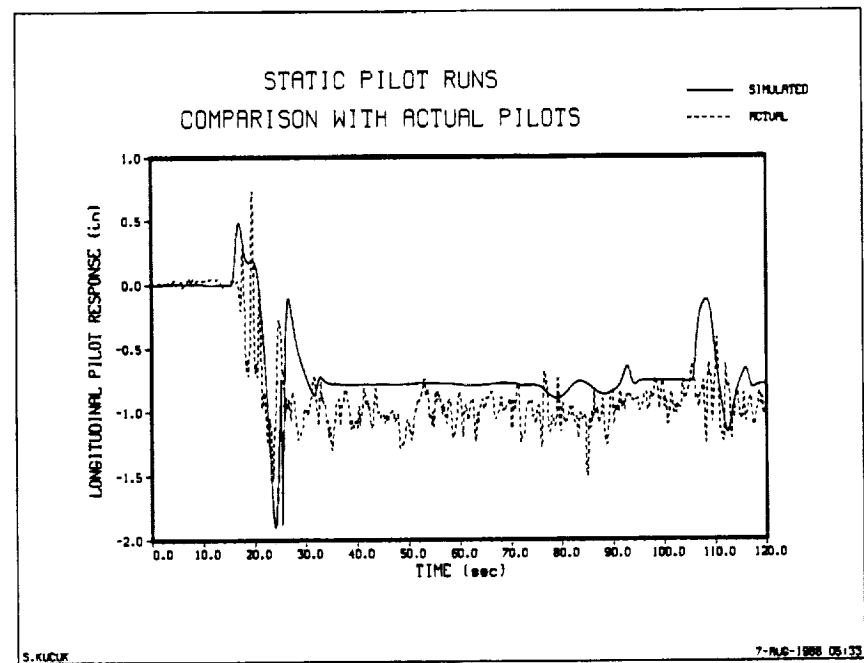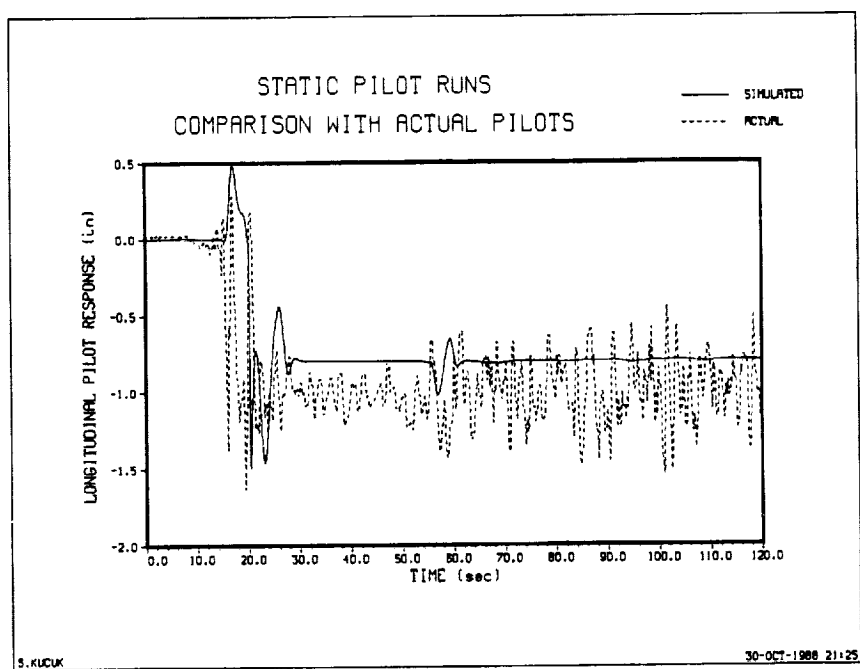

Figure 134. Actual vs simulated longitudinal stick input (from NASA data)
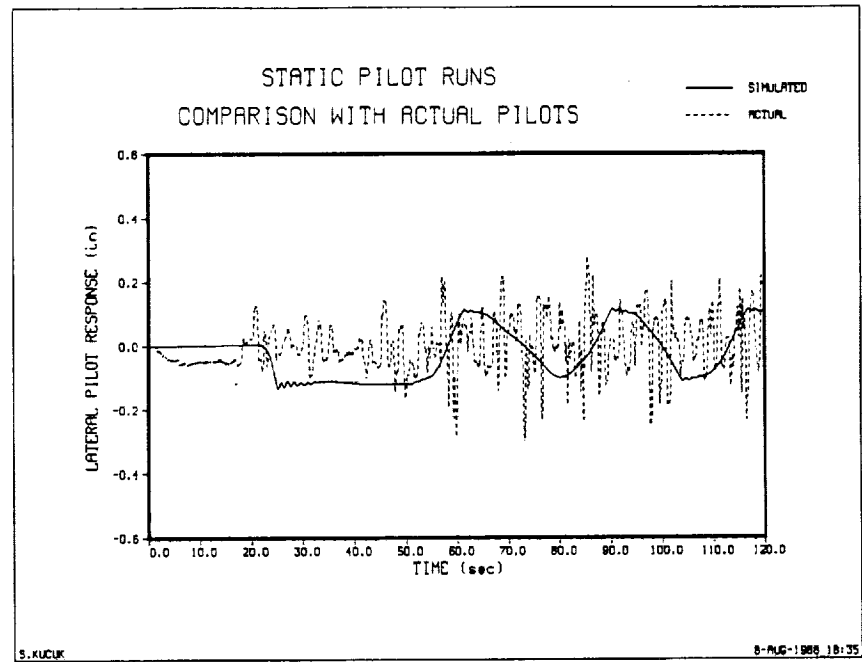
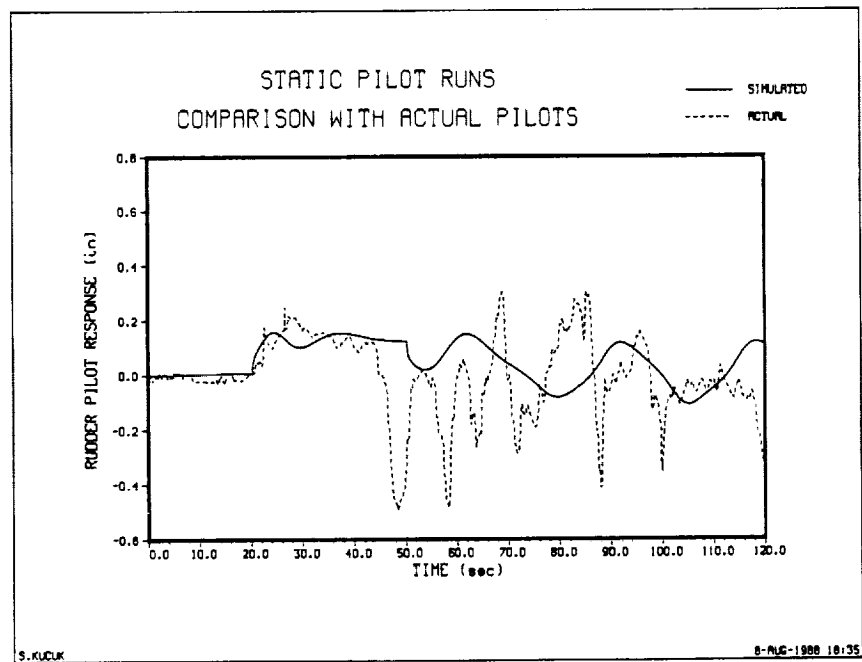**Figure 135.** Actual vs simulated lateral stick input (from NASA data)

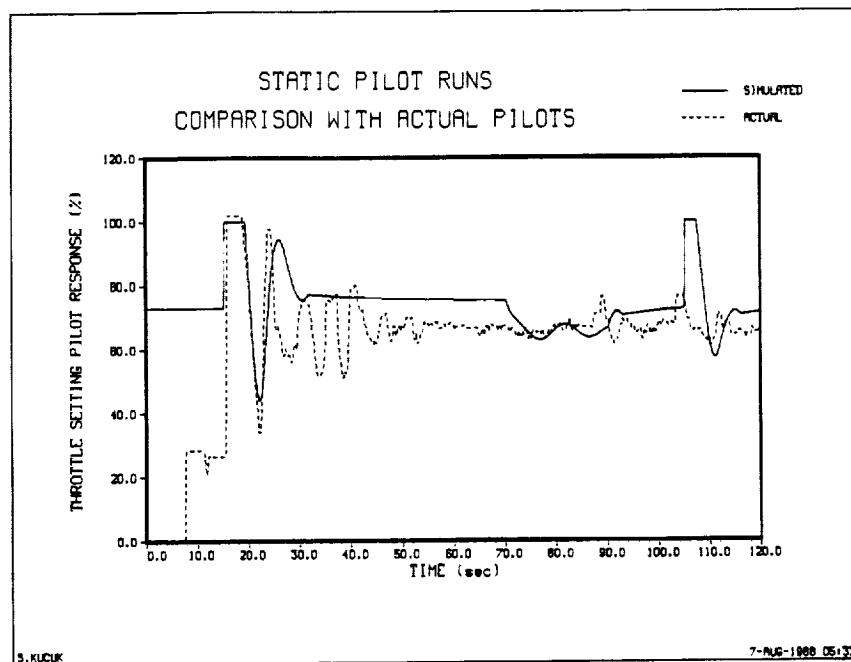**Figure 136.** Actual vs simulated rudder pedal input (from NASA data)

Figure 137. Actual vs simulated throttle setting input (from NASA data)
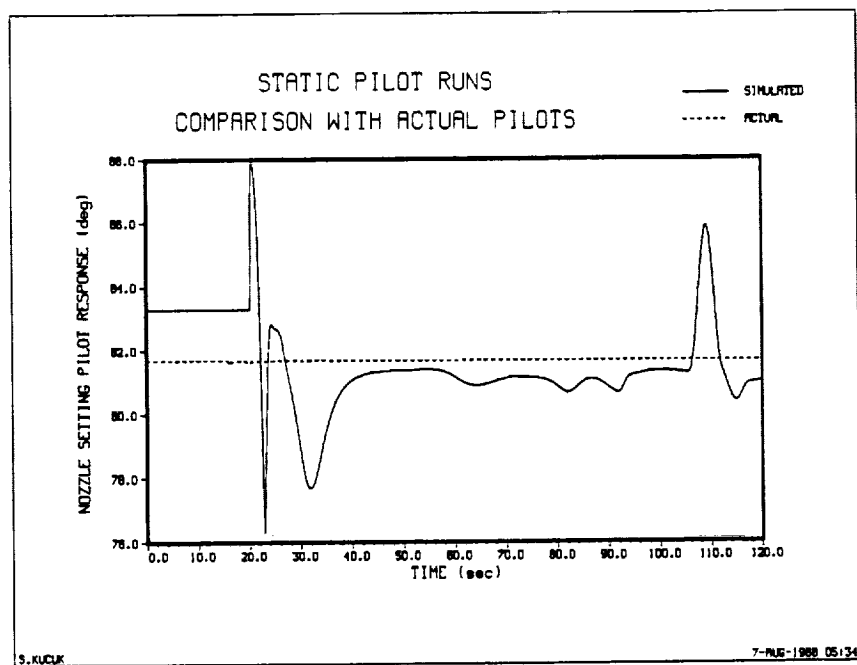

Figure 138. Actual vs simulated nozzle setting input (from NASA data)
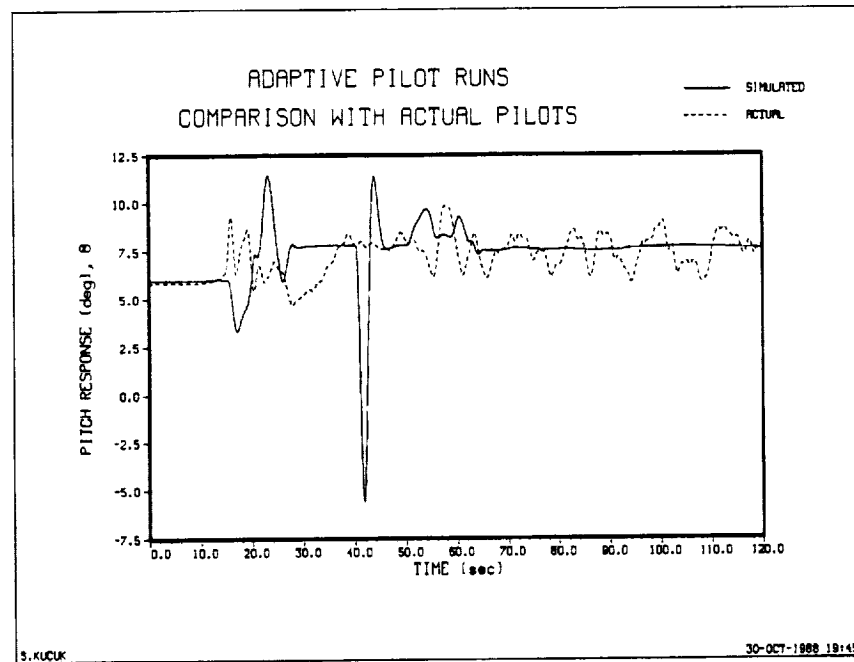
Figure 139. Actual vs simulated pitch response (from NASA data)
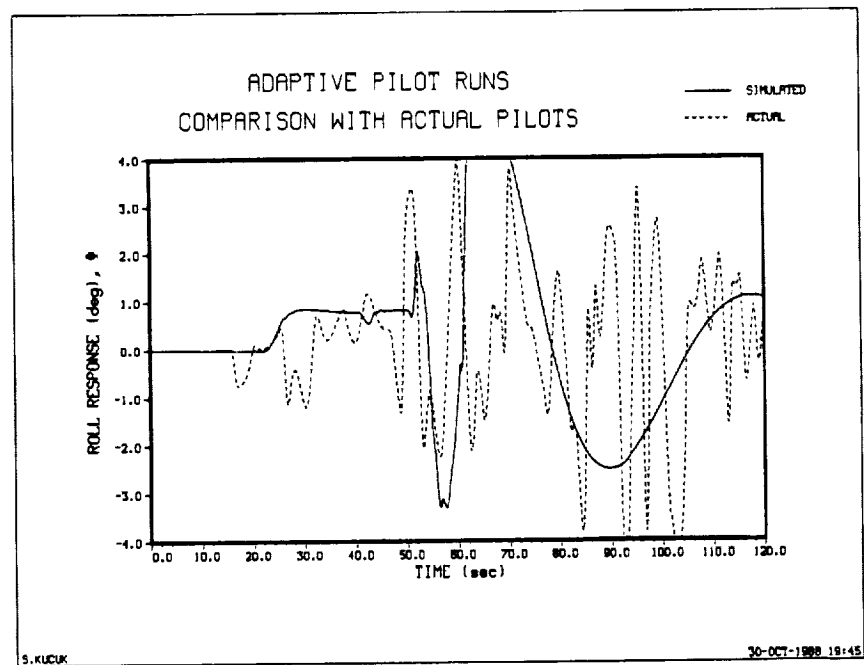
Figure 140. Actual vs simulated roll response (from NASA data)
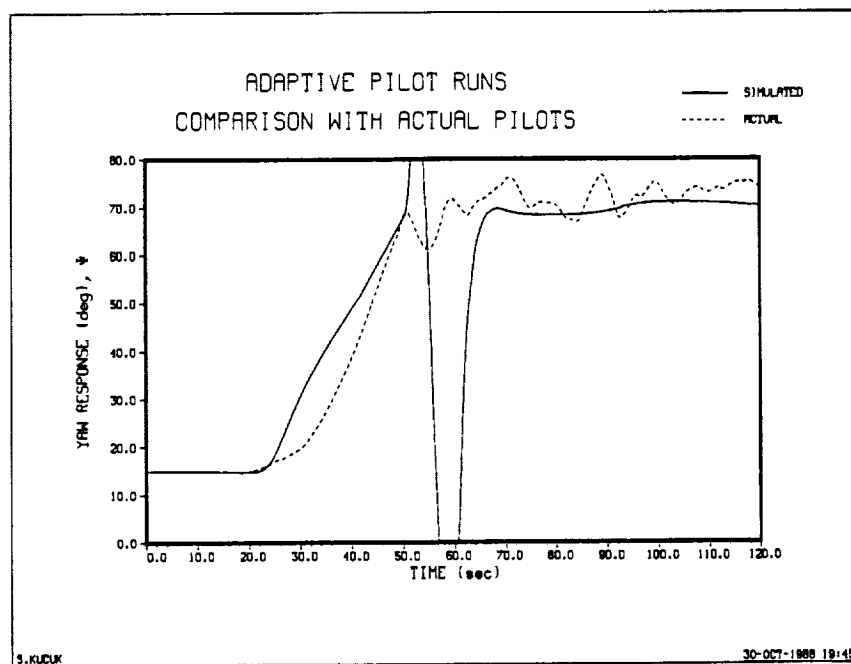
Figure 141. Actual vs simulated yaw response (from NASA data)
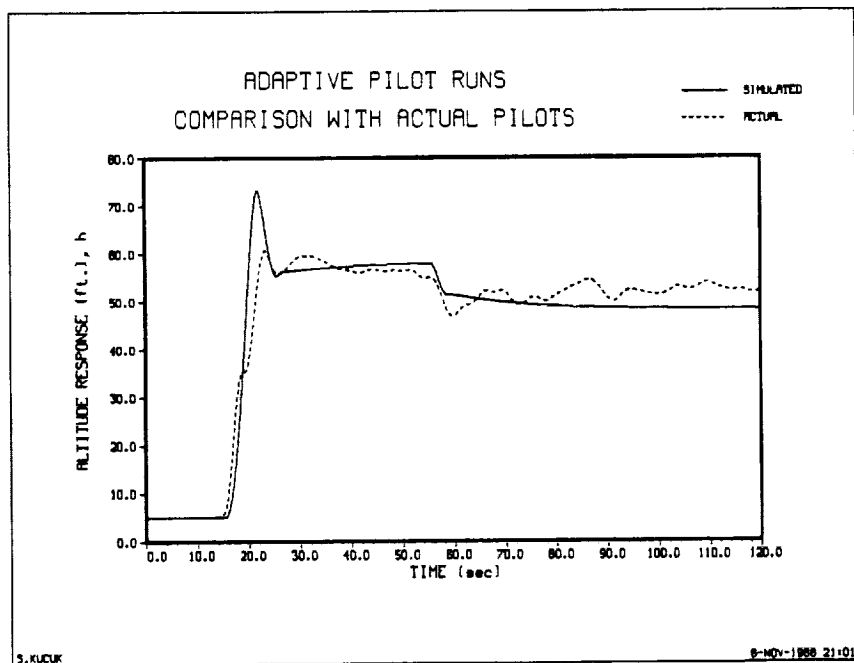
Figure 142. Actual vs simulated altitude response (from NASA data)
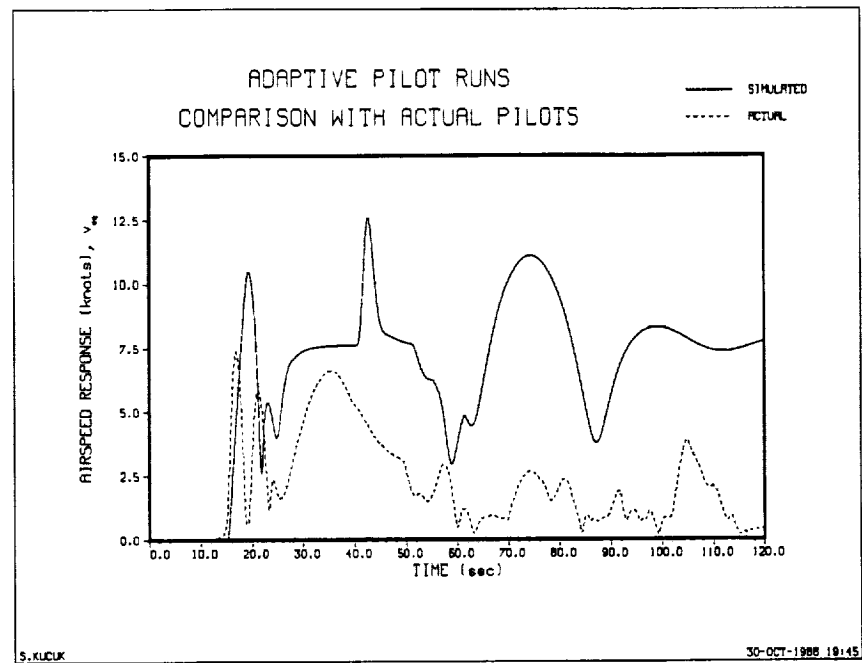
Figure 143. Actual vs simulated speed response (from NASA data)
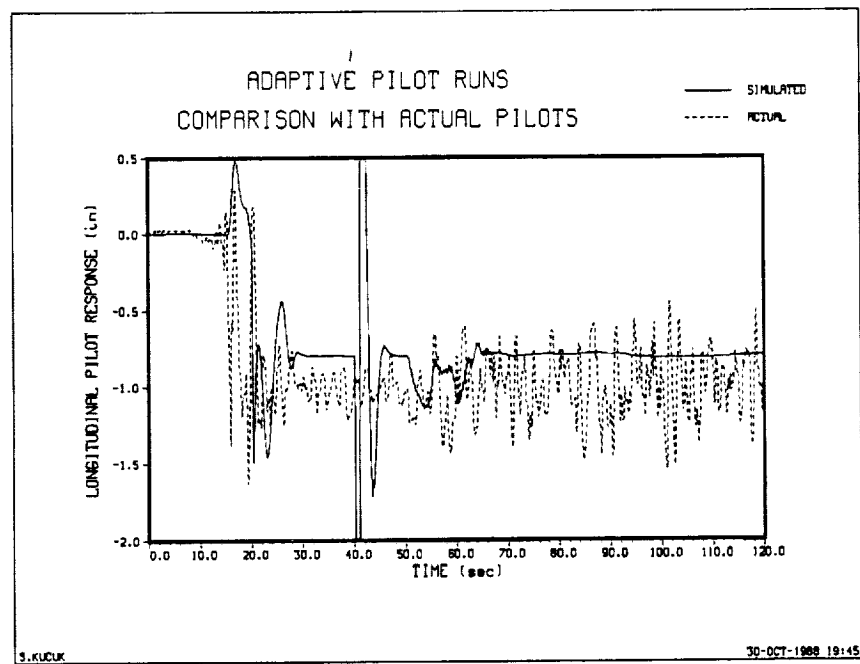
Figure 144. Actual vs simulated longitudinal stick input (from NASA data)
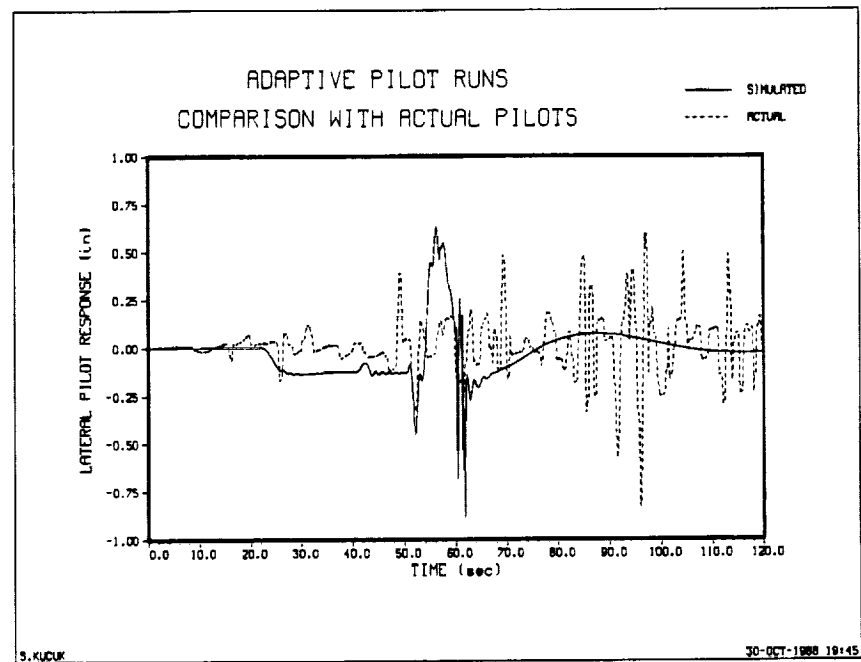
Figure 145. Actual vs simulated lateral stick input (from NASA data)
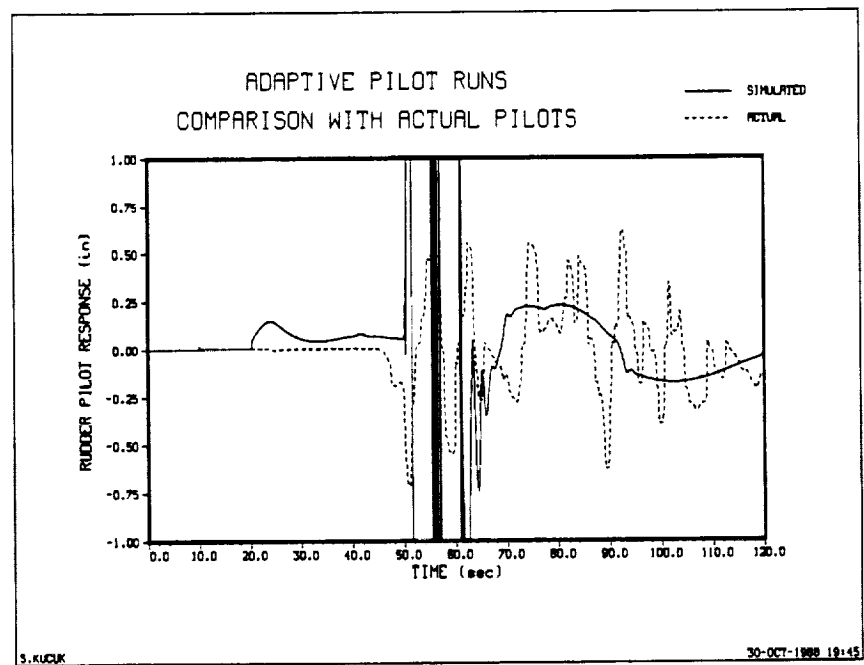
Figure 146. Actual vs simulated rudder pedal input (from NASA data)
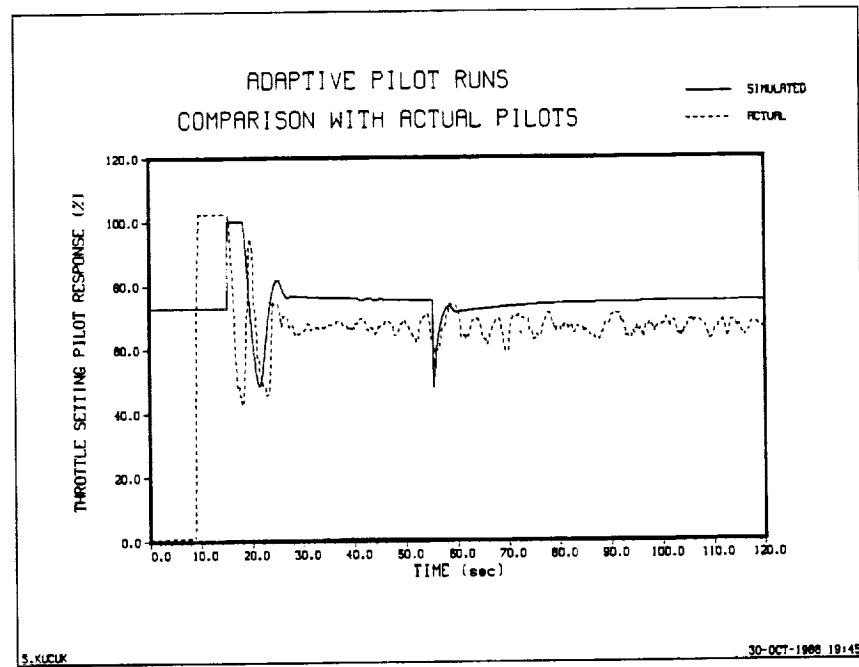
Figure 147. Actual vs simulated throttle setting input (from NASA data)

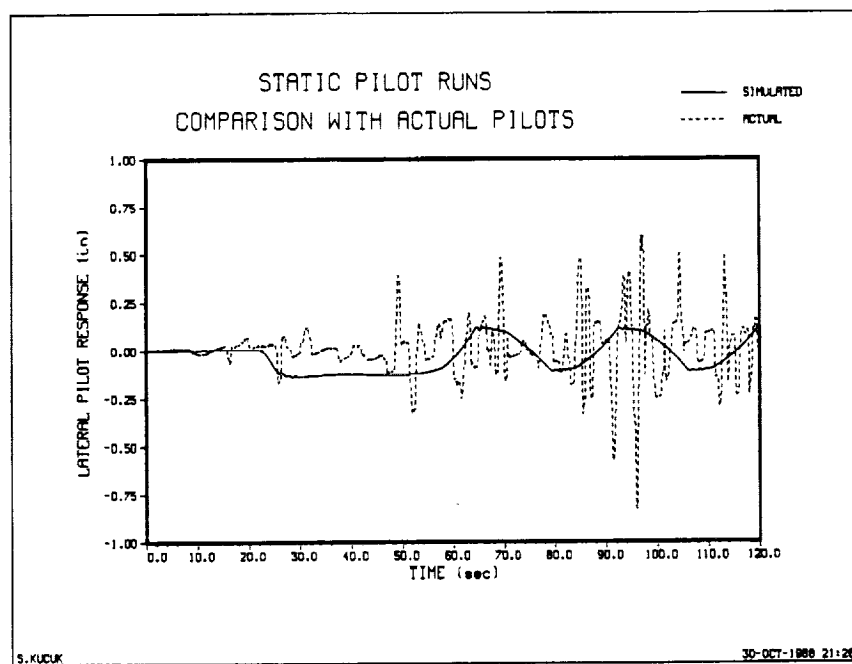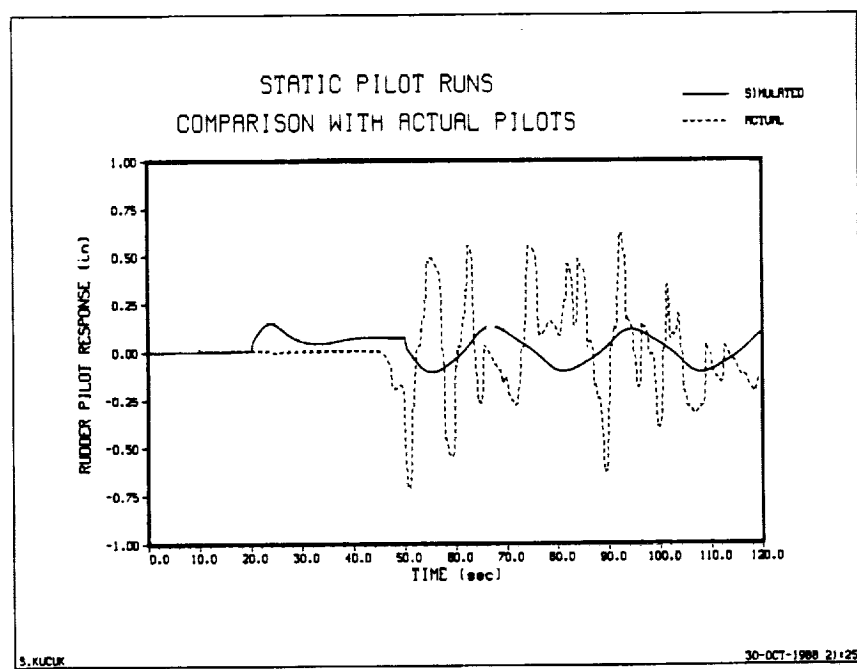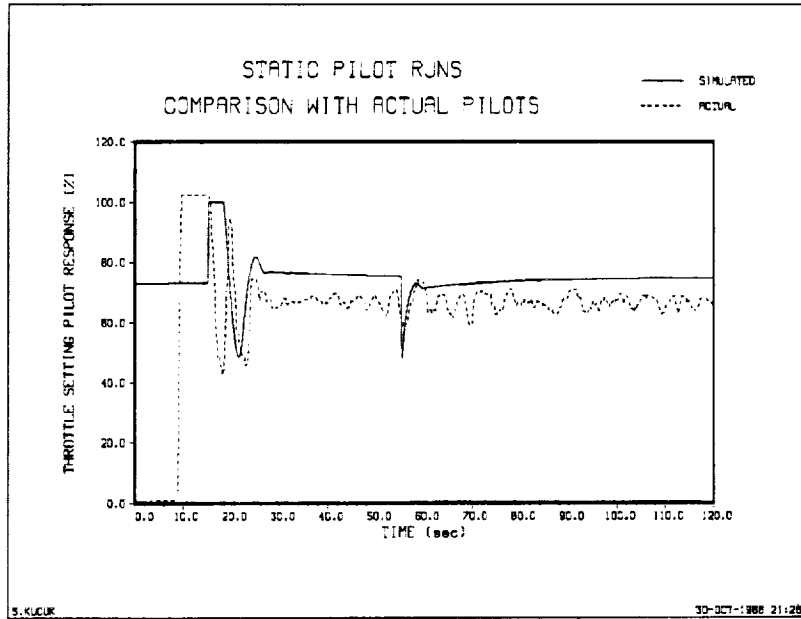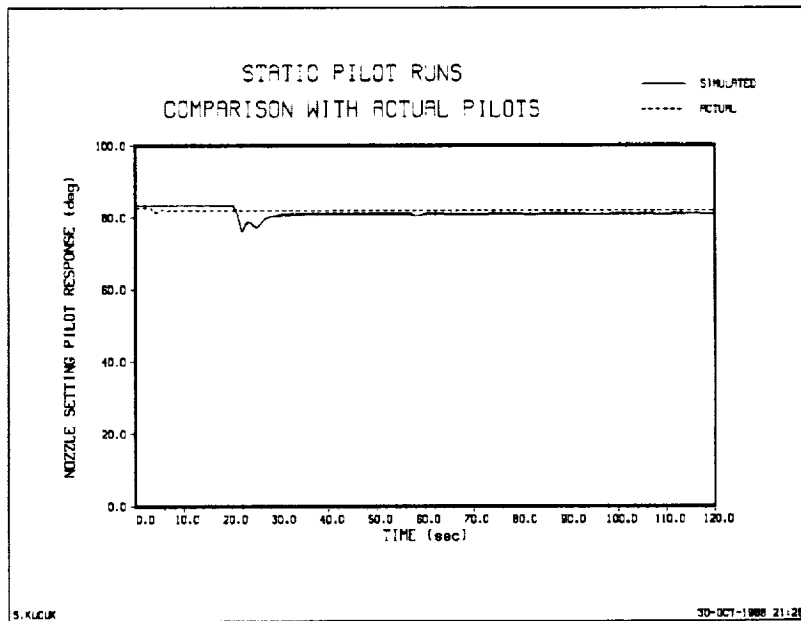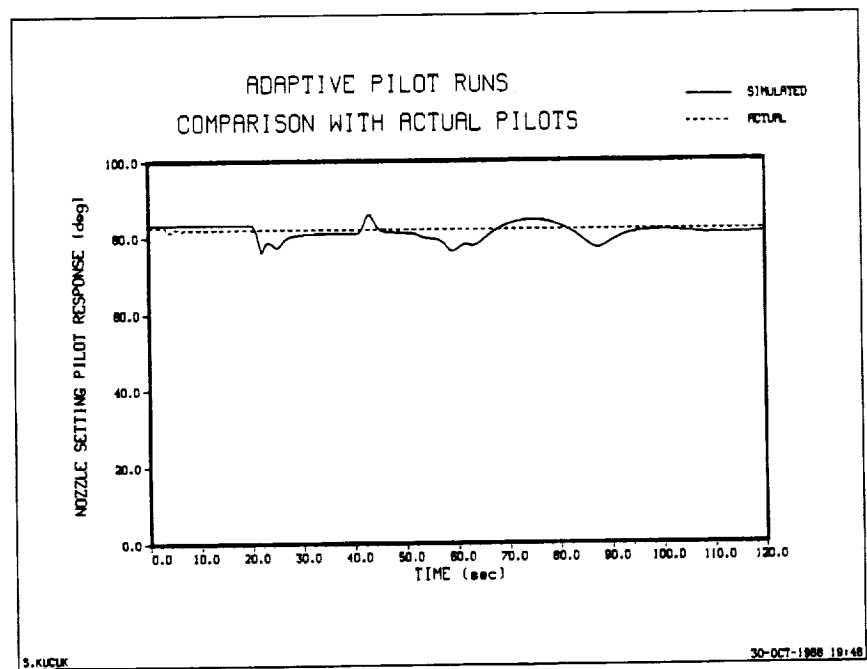**Figure 148.** Actual vs simulated nozzle setting input (from NASA data)

7.0 CONCLUSION

7.1 Results and Discussions

We have developed an adaptive human response model for compensatory type feedback systems. Although the adaptation of a human will not necessarily be the adaptation of our model, the model is based on physical evidence. The model is verified in a non-linear aircraft simulation environment closing all the control loops generally closed by the Harrier AV-8B pilot. Though simple in approach, the de-coupled, multi-variable control structure consisting of single variable control loops fulfills the requirements. This can be related to the basic idea in the design of the aircraft control mechanisms. Each control unit is coupled to the quasi-totality of the aircraft dynamic equations, but each control unit has a "primary" response perceived by the human pilot. For example, rolling moments are created by the lateral stick and equivalently by the lateral movements of the main stick. But as the roll-yaw coupling is excited by increasing the roll angle, the heading as well as the sideslip, the pitch angle, and the altitude of the aircraft are disturbed. Then the rudders are used to supress the roll-yaw coupling, the throttle setting is used to hold the altitude, and the longitudinal stick is activated for the pitch angle adjustments. It is clear that, the secondary controls are for the regulation of the disturbed modes of the aircraft. The other aspect is the "parallel processing" capability of the human structure. Each single variable control loop can be thought as one parallel processing unit related for one specific purpose but actively monitoring the other control loops.

The first step in the model development is the compilation of the physical data where the typical behavior of the human pilot is analyzed within the process of controlling the aircraft. The control mechanisms and their effects are carefully examined. The importance of this stage is inevitable because it is that particular behavior of the human pilot that we wish to be able to predict and to model the human pilot's appearance in the aircraft by means of mathematical equations.

The findings are that, the human pilot uses feedback, sensing and estimating all the information he could get through or without the instrumentation as well as deciding experiencing and remembering his performance. Not all the information is used for the control process. He also has constraints on the aircraft variables. His aim is to stabilize, re-position, and follow trajectories without risking the aircraft meaning that he should avoid dangerous maneuvers. The combat pilot may not be in this category.

These constraints lead to classical control concepts like the settling time, overshoot, rise time, closed loop bandwidth, and damping ratio. This is where we branch to the area of mathematics from physics. Fortunately, many successful studies have been done on the handling qualities of pilots throughout the years.

Then we assume the existence of a "human-describing function" in the sense that the model will generate outputs similar to that of the actual pilot in a similar environment. The response must be approximately the same in the frequency domain and preferably the same in the time domain.

The third step is the simulation where we place this model in a feedback type control loop. There, the open loop is described by the pilot model and the aircraft dynamics.

We chose a well-developed and documented, low order human response mechanism proposed in the late 1950's by D.T. McRuer and E.S. Krendel. This model was a result of a controls approach idea, to the human response, that began by Tustin. The human operator in the control loop of a feedback system is assumed to compensate the open loop transfer function, being capable of integrating and differentiating, while moving the closed loop to the desired operating regions.

The McRuer-Krendel model has variable parameters and ranges of the parameters to model the adaptivity of the human response. However, the selection of these parameters is rather complex and not trivial. In their studies, McRuer and Krendel showed that by appropriate selection of these parameters, within the frequency region assumed to be the bandwidth of the human mechanism, the model can fit a variety of experimental data.

As mentioned earlier, studies on the pilot handling qualities relate the closed loop bandwidth and damping to the pilot performances. This idea is used to apply the root locus technique to select the human response model parameters that will close the control loop of an aircraft control mechanism with the desired damping and bandwidth[9][10][11]. As a part of this research, simulation programs were provided by NASA-Lewis, where they were used to get information of the aircraft control mechanisms, and the open loop aircraft transfer functions by injecting control sequences to the specific control surfaces of the aircraft. The resulting data is analyzed to approximate low order transfer function models of the aircraft dynamics both in time and frequency domains. The low order approximations were used in conjunction with the human response model in the root locus method to select the pilot parameters. However, once the model parameters are chosen, the model becomes static and capable of only operating at that specific flight configuration which the approximate transfer function was taken.

We studied the adaptation process of the human pilot and concluded that the typical adaptation involved detection, identification, optimization and modification processes. By appropriate assumptions, these four concepts led to an adaptive human response model. We related the detection to the pilot senses. The identification was a parameter estimator where the open loop aircraft dynamics were approximated by low order discrete transfer functions. The proper selection of the model parameters was related to the optimization where constraints like closed loop bandwidth and damping, as well as stability and minimum steady state error criteria were applied. Finally, the optimal model parameters were used to modify the human response model.

In order not to go back to the s-domain from the z-domain by approximate transformations, we transformed the human response model into the z-domain. There, concepts like the sampling theorem and step invariant transformation were effectively applied. The sampling theorem was used to make sure that the bandwidth of the human response model was preserved in s to z transformation by putting constraints on the sampling time consistent with human limitations. The step invariant transformation used the fact that the pilot's error information and corresponding control displacement were approximately constant for a brief period of time during which the decision and action of the pilot took place. Also, the discrete model had some advantages over the s-domain model. Thus, we had the basic modules of the adaptive model.

As in every adaptive control system, we needed a rule for the adaptation. The human response model has an adjustable pole-zero pair which corresponds to the lead-lag network compensator of the s-domain McRuer-Krendel model, a neuro-muscular pole constant, a gain, a delay and a remnant. We assumed a zero remnant based on the observation that an experienced pilot will behave almost deterministicly. Moreover, the

time delay and the neuro-muscular pole were assumed to be constants based on the fact that pilots with similar experiences would have similar behaviors. Therefore, the adjustable pole-zero pair and most importantly the pilot's adjustable gain were to be subjected to the adaptation law.

The solution in selecting an effective adaptation law was to use the root locus criterion on-line for the modification of the model parameters. As in an off-line root locus design procedure, first the desired closed loop pole is selected. Then, the phase contribution of each open loop pole and zero are calculated leading to the amount of phase to be compensated to force the closed loop system's characteristic equation to have the desired closed loop poles, and that they are the dominant poles. Furthermore, the stability and phase margin requirements must be assured.

The pilot gain does not have a significant effect in the phase calculation, except that a positive or a negative pilot gain changes the phase constraint of the root locus criterion. The most important contributor is the pole-zero pair since neither the open loop dynamics nor the neuro-muscular bandwidth of the pilot model can be changed. They need to be re-located to give the necessary phase compensation.

Not all the values of the open loop transfer function are required in the calculation involving the effect of the aircraft dynamics. Once the pilot gain is characterized in terms of the open loop transfer function this becomes more clear. The only information required to continue with the adaptation is the value of the open loop aircraft transfer function evaluated at the desired closed loop pole. The magnitude and phase of this complex number will be used in the root locus criterion to adapt the model. Therefore, although we use a parameter estimator to approximate the aircraft dynamics in terms of

transfer functions, only a specific frequency information of the transfer function is used in calculating the phase to be compensated by the pilot model. Also, it is used to define the pilot boundaries where the resonances of the aircraft dynamics at the operating region are monitored.

We used a pre-calculated table look-up for the appropriate selection of the pole-zero pairs. Throughout the simulation, rather than calculating the necessary pole and zero that will fit the current requirements at each sample, the table is searched and the entries of that specific row are used for the adaptation.

Once the adaptive pole-zero pair is available, the pilot gain is calculated and checked to prevent any excess gain to be provided by the pilot to the control mechanisms. This process is repeated at each sampling time, thus providing an on-line adaptive human response mechanism. Adaptive, since the aircraft dynamics are continuously monitored to sense any model changes due to the non-linearities, and human response, since the adaptation is constrained on the values of the human describing function model which has a similar bandwidth and frequency response as the human pilot.

We needed initial pilot parameters to start the algorithm. For that reason, we assumed that these initial parameters will reflect pilot's experience and his knowledge of the aircraft. In general, the control process of the human pilot has two stages. First, the available information is used to activate the control. Any differences of the controlled element behavior than the predicted one are corrected in the next stage. That is more likely where the adaptation process occurs. However, it is essential that the initial knowledge is accurate since the adaptation will not be of much help if the aircraft becomes unstable as a result of the initial reaction of the pilot. In the case of the human

pilot, this is guaranteed by extensive training of the pilots where the pilot has enough initial knowledge of the aircraft dynamics. The predicted and commanded behavior of the aircraft will very likely be the same. Therefore, we supplied the static pilot parameters that were calculated off-line from the aircraft data as our initial model parameters. By inserting the static pilots to the aircraft control loops and testing their performances, we modelled the training process of the human pilots. As mentioned earlier, this is a primitive attempt to describe pilot training. Even though we supply the initial pilot parameters, we can not apply the proper starting control sequence. The static pilot activated the control and the adaptive pilot took the control after sufficient amount of time that will leave enough time for the transfer function estimators to converge.

Thus, we have analyzed and simulated an adaptive human response mechanism where the root locus method is used as the adaptation law. This approach is also applicable for other type of feedback systems where the controller is not necessarily a human pilot model.

For most of the simulated cases, the adaptive model performed better than the static models trying to minimize a possible non-zero steady-state error caused by the static pilot's performance. However, we concluded that the adaptation with the current constraints is more suitable to the longitudinal control set of the aircraft mechanism although it performed well for the lateral control sets. An analysis of some actual pilot data in a lateral tracking task, provided by NASA-Lewis, suggested that, for this particular scenario, the McRuer-Krendel model does not seem to be adequate.

Furthermore, the adaptive model should operate at a variety of flight configurations since any changes in the aircraft dynamics are sensed and compensated on-line as the human pilot will try to compensate.

We also showed for a specific case that the model is capable of performing the tasks that were carried by human pilots. Although a careful investigation of the actual scenario is necessary, the results were satisfactory.

We also concluded that, for the simulated cases, the single variable approach to a complete multi-variable control mechanism is very efficient as well as simple. However, the effects of the remnant and the time delay, the neuro-muscular approximation, and the performance of the adaptive model in other aircraft environments, remain to be studied. A variety of actual pilot data should be analyzed for better understanding of the actual pilot behavior towards the development of efficient describing functions of the human response with an expert system-like adaptive mechanism. The adaptive model will remain the same but it should have a database of extra rules to follow just like the human pilot. Fortunately, this will compensate for the absence of a "remembering" process of the pilot which our model does not have at this time. Only the current information is processed by the adaptive pilot model. For that reason, the models should be constrained with rules defined by the actual pilot behavior. Throughout the years, different models were investigated for those human behavior that would fit in one model but not another. Nevertheless, without any human reasoning, no such model will ever find any use.

7.2 Suggestions for Further Research

The key factor in modelling of the human mechanism is decisinmaking. Of all the possible choices the best reaction will be "selected" by the human operator. It is certain that there is no unique adaptation procedure performed by the human. Instead a set of rules define his reactions and boundaries. The more the rules, the more complicated the decision making process becomes. However, it is that decisionmaking that makes the

human operator's appearance safe and reliable. These aspects like decisionmaking, adapting, defining and updating the rules together with many others define his intelligence.

In that sense, the model proposed in this thesis is not "decisionmaking". Although adaptive, there is only a few rules satisfied by the model compared with the human pilot. The closed loop bandwidth of the pilot-aircraft combination resembles actual human pilot operating regions. Also the simulated control movements of the model are consistent with the human muscular limitations. As an adaptation law the root-locus performs well but within the process of adaptation the model generates somewhat undesirable outputs which may be dangerous.

This can partly be solved by supplying the model a set of transfer function estimates corresponding to different flight configurations. The detail of these transfer functions will directly depend on the pilot's knowledge of the aircraft. In this way, the model will not only have initial human describing function parameters but an initial information of specific flight configurations which the human pilot gets through training. Unfortunately, the training can not be efficiently modelled by this approach. Instead the assumption of a well-trained pilot simplifies the situation.

A well-trained, experienced human pilot will be almost deterministic in his reactions. Furthermore, his reactions will be optimal for that configuration. In that respect, selecting the pilot poles and zeros for specific configurations resembles the human pilot's deterministic reactions since the model will select the same poles and zeros every time it is subjected to that same flight configuration; hence, it will react the same. However, a human pilot in a type-1 loop will not add an integrator to the system[24]. On

the other hand, when subjected to a type-0 system, the human operator will use his integrating ability to act as an integrator so that the "steady-state" error is minimized. For that reason, different sets of pole-zero selections for different aircraft control sets is more appropriate rather than having only one table look-up as in our adaptive simulations. For example, the longitudinal stick pilot and the nozzle setting pilot adaptations will be different because the former is a type-1 loop while the latter is almost type-0.

The "sampled human response" idea resulting from a "sampled external world" point of view fits the nature of the human mechanism. However, by starting from a continuous domain model and transferring into the discrete domain, as in our case, does not take the full advantage of the discrete domain. Left half plane poles and zeros are estimated by discrete models[16]. For that reason, better discrete human response models should be investigated by analyzing actual pilot data. In fact, we can record the typical responses of the human pilots and use them as a part of the adaptation procedure. It would be practically impossible to record all the time histories but the estimated pilot model poles and zeros can be used.

Considering the comparison of the actual and simulated pilot response of Section (6.4), the only problem in commanding the model is the selection of the primary reference variables and the application of the desired reference sequences. For example, if it is desired to gain altitude, then the command is an increment in the altitude loop reference. If a descent is required, then the altitude loop will be given a negative ramp as an input.

Starting the pilot model with no adaptation and then activating the adaptation process seems to be a good approach to model a human's reaction where he first uses the

best knowledge about that situation. However, as is shown in the adaptive pilot simulations, the problem is how to start the adaptation "smoothly". The estimated pilot gains oscillates for a brief period of time during which the adaptation procedure converges. This should be solvable by adding artificial intelligence or decisionmaking to the model by adding extra rules to be followed. This is a very rich area for future research.

APPENDIX A.

APPENDIX A.

DEFINITION OF THE AIRCRAFT PARAMETERS

Center of gravity

θ-rotation

ψ-rotation

ϕ-rotation
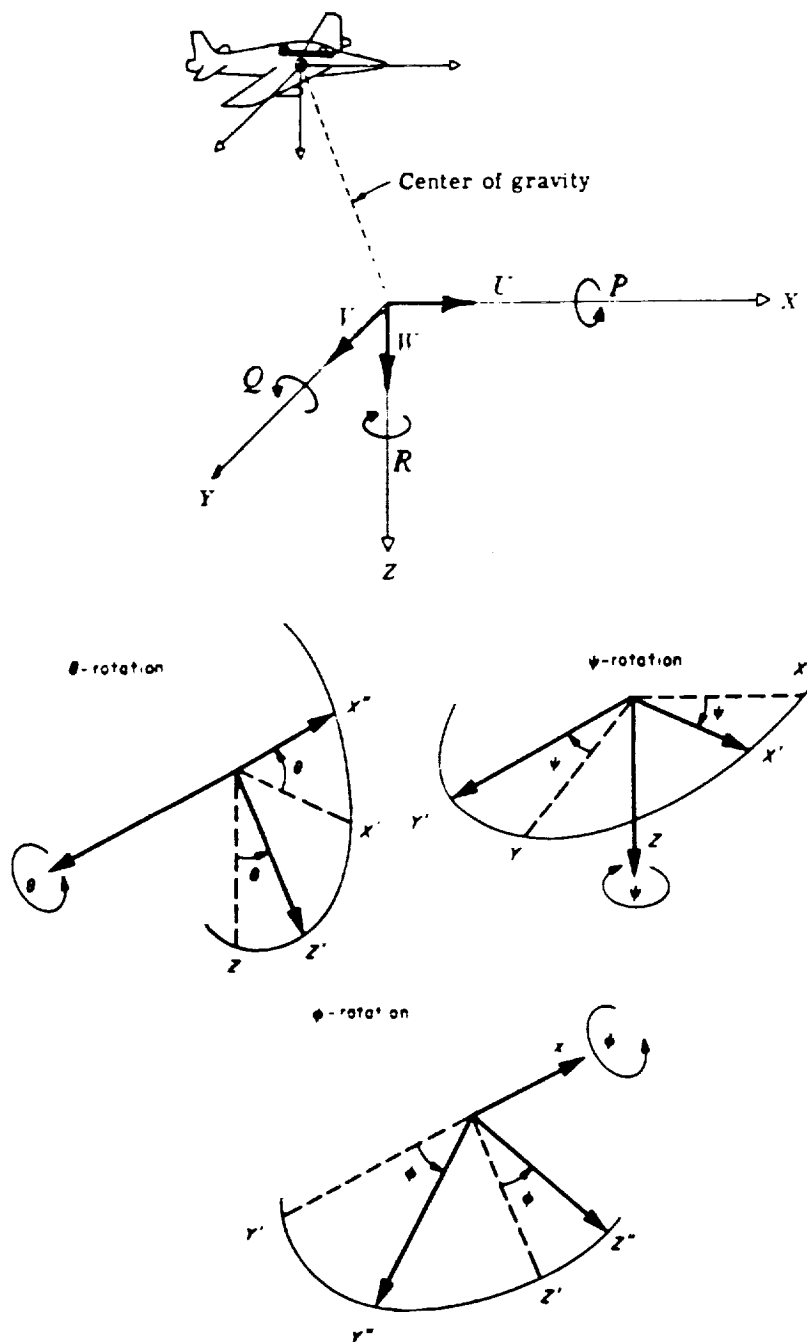
APPENDIX B.

STEP-INVARIANT TRANSFORMATION OF THE HUMAN RESPONSE

MODEL
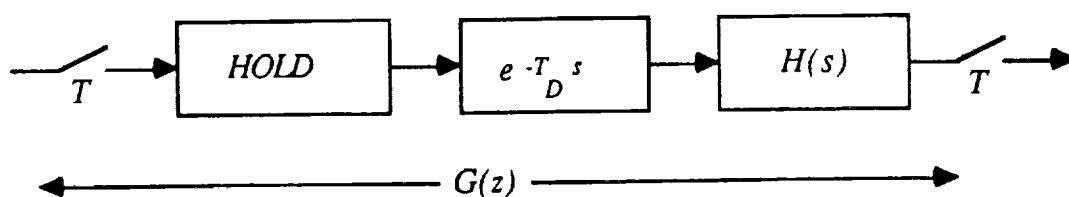
The step-invarient transformation is defined by:

$$G(z) = \frac{z-1}{z} Z \left\{ \mathcal{L}^{-1} \left\{ \frac{e^{-T_D s} H(s)}{s} \right\} \bigg|_{t=kT} \right\}$$

let

$$F(s) = \frac{H(s)}{s}$$

then, if

$$f(t) \leftrightarrow F(s)$$
$$\therefore \quad f(t-T_D) \leftrightarrow e^{-T_D s} F(s)$$

it follows that

$$\mathcal{L}^{-1} \left\{ e^{-T_D s} H(s) \right\} = f(t-T_D)$$

then, let

$$f(kT) \leftrightarrow F(z)$$
$$\therefore \quad f[(k-d)T] \leftrightarrow z^{-d} F(z)$$

by choosing, $T_D = dT$

$$Z\left\{ f(t-T_D) \Big|_{t=kT} \right\} \leftrightarrow z^{-d} F(z)$$

$$\therefore \quad G(z) = \frac{z-1}{z} z^{-d} F(z)$$

where

$$F(z) = Z\left\{ \pounds^{-1}\left\{ \frac{H(s)}{s} \right\} \Big|_{t=kT} \right\}$$

for the McRuer-Krendel human reponse model

$$H(s) = K_P \frac{(T_L s + 1)}{(T_N s + 1)(T_I s + 1)}$$

<u>Case. I</u> $(T_N \neq T_I)$

$$\frac{H(s)}{s} = K_P\left\{ \frac{1}{s} + \frac{T_L - T_N}{T_N - T_I} \frac{1}{T_N s + 1} + \frac{T_L - T_I}{T_I - T_N} \frac{1}{T_I s + 1} \right\}$$

then

$$F(z) = K_P \frac{z(b_1 z + b_2)}{(z-1)(z - e^{-T/T_I})(z - e^{-T/T_N})}$$

where

$$b_1 = 1 - \beta \frac{T_L - T_N}{T_I - T_N} + \alpha \frac{T_L - T_I}{T_I - T_N}$$

$$b_2 = \beta\alpha - \alpha \frac{T_L - T_N}{T_I - T_N} + \beta \frac{T_L - T_I}{T_I - T_N}$$

then

$$G(z) = K z^{-d} \frac{(z^{-1} - \gamma z^{-2})}{(1 - \alpha z^{-1})(1 - \beta z^{-1})}$$

with

$$\alpha = e^{-T/T_I}$$
$$\beta = e^{-T/T_N}$$

$$K = K_p b_1$$

$$\gamma = -\frac{b_2}{b_1} = 1 - \frac{(1-\beta)}{1 + \frac{(T_L - T_N)}{(T_I - T_N)} \frac{(\alpha-\beta)}{(1-\alpha)}}$$

Case. II $(T_N = T_I)$

In the same way

$$G(z) = Kz^{-d} \frac{(z^{-1} - \gamma z^{-2})}{(1 - \beta z^{-1})^2}$$

with

$$\beta = e^{-T/T_N}$$
$$K = K_p[\beta T(T_L - T_N) + 1 - \beta]$$
$$\gamma = 1 - \frac{(1-\beta)^2}{1 - \beta[T(T_L - T_N) - 1]}$$

APPENDIX C.

APPENDIX C.

KALMAN FILTER PARAMETER ESTIMATION ALGORITHM (PSEUDO CODE)

```
/* SISO case, input is u_{k-d}, output is y_k */
/* Given n,m and d */
/* Gain update */
   sum_1 := 0;
   for i := 1 to N do begin
      sum_2 := 0;
      for j := 1 to N do begin
         sum_2 := sum_2 + P[i,j] * H[j];
      end;
      T[i] := sum_2;
      sum_1 := sum_1 + H[i] * T[i];
   end;
   sum_1 := sum_1 + R_k;
   for i := 1 to N do begin
      K[i] := T[i] / sum_1;
   end;
/* Parameter update */
   sum_3 := 0;
   for i := 1 to N do begin
      sum_3 := sum_3 + H[i] * θ̂[i];
   end;
   ε_k := z_k - sum_3;
   for i := 1 to N do begin
      θ̂[i] := θ̂[i] + K[i] * ε_k;
   end;
/* Covariance update */
   for i := 1 to N do begin
      for j := 1 to i do begin
         P[j,i] := P[j,i] - K[i] * T[j];
         P[i,j] := P[j,i];
      end;
      P[i,i] := P[i,i] + ρ_k;
   end;
/* Regressor update */
   for i := 0 to n - 2 do begin
      H[n - i] := H[n - i - 1];
```

```
            end;
            H[1]  := z_k;
            for i := 0 to m - 2 do begin
                H[n + m - i]  := H[n + m - i - 1];
            end;
            H[n + 1]  := u_{k-d+1};
    /* End of one update */
```

APPENDIX D.

APPENDIX D.

SIMPLIFIED KALMAN FILTER PARAMETER ESTIMATION ALGORITHM

(PSEUDO CODE)

```
/* SISO case, input is u_{k-d}, output is y_k */
/* Given n,m and d */
/* Gain update */
   sum_1 := 0;
   pointer_1 := 1;
   for i := 1 to N do begin
       sum_2 := 0;
       pointer_2 := pointer_1 + i - 2;
       for j := 1 to N do begin
           if (j≤i) then (pointer_2 := pointer_2 + 1);
                    else (pointer_2 := pointer_2 + j - 1);
           sum_2 := sum_2 + P_{LINEAR}[pointer_2] * H[j];
       end;
       T[i] := sum_2;
       sum_1 := sum_1 + H[i] * T[i];
       pointer_1 := pointer_1 + i - 1;
   end;
   sum_1 := sum_1 + R_k;
   for i := 1 to N do begin
       K[i] := T[i] / sum_1;
   end;
/* Parameter update */
   sum_3 := 0;
   for i := 1 to N do begin
       sum_3 := sum_3 + H[i] * θ̂[i];
   end;
   ε_k := z_k - sum_3;
   for i := 1 to  N do begin
       θ̂[i] := θ̂[i] + K[i] * ε_k;
   end;
/* Covariance update */
   pointer_1 := 1;
   for i := 1 to N do begin
       pointer_2 := pointer_1 + i - 2;
       for j := 1 to i do begin
           pointer_2 := pointer_2 + 1;
```

```
                    P_LINEAR[pointer_2] := P_LINEAR[pointer_2]- K[i] * T[j];
                end;
                P_LINEAR[pointer_2] := P_LINEAR[pointer_2] + ρ_k;
                pointer_1 := pointer_1 + i - 1;
            end;
    /* Regressor update */
            for i := 0 to n - 2 do begin
                H[n - i] := H[n - i - 1];
            end;
            H[1] := z_k;
            for i := 0 to m - 2 do begin
                H[n + m - i] := H[n + m - i - 1];
            end;
            H[n + 1] := u_{k-d+1};
    /* End of one update */
```

APPENDIX E.

APPENDIX E.

KALMAN FILTER ESTIMATES OF THE "BALL-IN-THE-HOOP" PROBLEM

$$\hat{\Phi}_{T=0.10} = \begin{bmatrix} 0.00000000 & 0.00000000 & -0.07729860 & 0.00000000 \\ 0.00000000 & 0.00000000 & -1.48918450 & 0.00000000 \\ 0.00000000 & 0.00000000 & 0.30050501 & 0.00000000 \\ 0.00000000 & 0.00000000 & -3.71993697 & 0.00000000 \end{bmatrix}$$

$$\hat{\Phi}_{T=0.20} = \begin{bmatrix} 0.00107484 & 0.02070723 & -0.07591160 & 0.05172603 \\ 0.00682456 & 0.13147752 & -1.48037796 & 0.32842678 \\ 0.00188267 & 0.03627024 & 0.30293443 & 0.09060195 \\ 0.00839500 & 0.16173255 & -3.70910391 & 0.40400292 \end{bmatrix}$$

$$\hat{\Phi}_{T=0.30} = \begin{bmatrix} 0.08688898 & 0.31142050 & 0.01461274 & -0.07129169 \\ 0.32585235 & 1.21225070 & -1.14383923 & -0.12891131 \\ 0.03723846 & 0.15604535 & 0.34023085 & 0.03991812 \\ -0.42391242 & -1.30279900 & -4.16514002 & 1.02373153 \end{bmatrix}$$

$$
\hat{\Phi}_{t=0.40} = \begin{bmatrix} 0.14098586 & 0.21043570 & 0.17209159 & -0.04043441 \\ 0.56745262 & 0.76124586 & -0.44052820 & 0.00889937 \\ 0.13203274 & -0.02091092 & 0.61618198 & 0.09398952 \\ -1.18354381 & 0.11523515 & -6.37646677 & 0.59043187 \end{bmatrix}
$$

$$
\hat{\Phi}_{t=0.50} = \begin{bmatrix} 1.00000000 & 0.09173982 & -0.01741165 & -0.00060458 \\ 0.00000000 & 0.83965469 & -0.31534503 & -0.01741165 \\ 0.00000000 & -0.00266704 & 0.64530913 & 0.08786757 \\ 0.00000000 & -0.04830323 & -6.63756304 & 0.64530913 \end{bmatrix}
$$

$$
\hat{\Gamma}_{t=0.10} = \begin{bmatrix} 0.07729860 \\ 1.48918450 \\ -0.30050501 \\ 3.71993697 \end{bmatrix}
$$

$$
\hat{\Gamma}_{t=0.20} = \begin{bmatrix} 0.07868559 \\ 1.49799103 \\ -0.29807558 \\ 3.73077002 \end{bmatrix}
$$

$$\hat{\Gamma}_{t=0.30} = \begin{bmatrix} 0.16920993 \\ 1.83452976 \\ -0.26077916 \\ 3.27473392 \end{bmatrix}$$

$$\hat{\Gamma}_{t=0.40} = \begin{bmatrix} 0.32668878 \\ 2.53784079 \\ 0.01517197 \\ 1.06340716 \end{bmatrix}$$

$$\hat{\Gamma}_{t=0.50} = \begin{bmatrix} 0.13718554 \\ 2.66302396 \\ 0.04429912 \\ 0.80231090 \end{bmatrix}$$

BIBLIOGRAPHY

BIBLIOGRAPHY

1. Anderson, L. C. and J. W. Bunnell, <u>AV-8B Simulation Model</u> (Palo Alto, California: Systems Control Technology, Inc., November 1985).

2. MacFarland, Richard E., <u>A Standard Linematic Model for Flight Simulation at NASA-Ames</u>, NASA CR-2497, (Mountain View, California: Computer Sciences Corporation, January, 1975).

3. Anderson, L. C., <u>AV-8B System Identification Results: Low and High Speed Longitudinal Model</u> (Palo Alto, California: Systems Control Technology, Inc., April 1984).

4. Anderson, L. C. and J. C. Bunnell, <u>AV-8B Simulation Software User's Guide</u> (Palo Alto, California: Systems Control Technology, Inc., May 1985).

5. Anderson, L. C., and J. C. Bunnell, <u>AV-8B Simulation Model, Engineering Specification</u> (Palo Alto, California: Systems Control Technology, Inc., January 1985).

6. McRuer, D. T., D. Graham, E. Krendel, and W. Reisner, Jr., "Human Dynamics in Compensatory Systems", Air Force Flight Dynamics Laboratory", AFFDL-TR-65-15, 1965.

7. McRuer, D. T. and E. S. Krendel, <u>Dynamic Response of Human Operators</u>, (Wright Air Development Center, TR-56-524, October, 1957).

8. Kuo, B. C., <u>Automatic Control Systems</u> (4th edition; Englewood Cliffs, New Jersey: Prentice Hall, 1982), pp. 454-455.

9. <u>Proceedings of the Eighteenth Modeling and Simulation Conference</u>, University of Pittsburgh, <u>April 23-24, 1987</u>, "Computer Simulation of Multiple Pilots Flying a Modern High Performance Helicopter, by Mark E. Zipf, William G. Vogt, Marlin H. Mickle, Ronald G. Hoelzeman, Fei Kai, James R. Mihaleow", pp. 1295-1314.

10. <u>Proceedings of the Eighteenth Modeling and Simulation Conference</u>, University of Pittsburgh, <u>April 23-24, 1987</u>, "Computer Simulation of a Single Pilot Flying a Modern High Performance Helicopter, by Mark E. Zipf, William G. Vogt, Marlin H. Mickle, Ronald G. Hoelzeman, Fei Kai, James R. Mihaleow", pp. 1279-1294.

11. Proceedings of the Nineteenth Modeling and Simulation Conference, University of Pittsburgh, May 5-6, 1988, "A Computer Simulation of Low Order Pilot Models Flying a Thrust Vectored V/STOL Research Aircraft, by Mark E. Zipf, William G. Vogt, Marlin H. Mickle, Senol Kucuk, James R. Mihaleow", (Preprint), 44p.

12. Second Annual NASA-University Conference on Manual Control, February 28-March 2, 1966, pp.39-43.

13. McRuer, D. T. and E. S. Krendel, "Human Operator as a Servo System Element", Journal of the Franklin Institute, Vol. 267, (May, 1959), pp. 381-403.

14. Kleinman D. L., S. Baron, and W. H. Levison, "An Optimal Control Model of Human Response, Part I: Theory and Validation", Automatica, Vol. 6, (1970), pp.357-369.

15. Kleinman D. L., S. Baron, and W. H. Levison, "An Optimal Control Model of Human Response, Part II: Prediction of Human Performance in a Complex Task", Automatica, Vol. 6, (1970), pp.371-383.

16. Gloeckner, M., "Identification of a Parametric Model of the Human Operator in Closed Loop Control Tasks", Identification and System Parameter Estimation, Vol.2, IFAC, pp. 809-816.

17. Landyshev, Alexander, N. "Human Poles and Zeros", ISA Transactions, Vol.8, No.4, (1969), pp. 322-328.

18. Bekey, G., "Mathematical Models of the Human Operator", Instruments and Control Systems, Vol.33, (July, 1960), pp. 1121-1125.

19. Salvendy, Gavriel, (ed.), "Handbook of Human Factors", (New York: Johm Wiley & Sons, 1987), pp. 1216.

20. Anderson, Brian D. O. and John B. Moore, Optimal Filtering, (Englewood Cliffs: New Jersey, Prentice Hall, 1979), pp. 223-254.

21. Anderson, Brian D. O. and John B. Moore, Optimal Filtering, (Englewood Cliffs: New Jersey, Prentice Hall, 1979), pp. 50-52.

22. Goodwin, Graham C. and Kwai Sang Sin, Adaptive Filtering Prediction and Control, (Englewood Cliffs: New Jersey, Prentice Hall, 1984), pp. 67.

23. Johnson, Richard, C. Jr., "Lectures on Adaptive Parameter Estimation", (Englewood Cliffs: New Jersey, Prentice Hall, 1988), Thomas, Kailath, (ed.), pp. 42-45.

24. McRuer, D. T., "Human Dynamics in Man-Machine Systems", Automatica, Vol. 16(3), (1980), pp. 237-253

REFERENCES NOT CITED

REFERENCES NOT CITED

Ashley, Holt, Engineering Analysis of Flight Vehicles (Reading, Massachusetts: Addison-Wesley, 1974)

Babister, A. W., Aircraft Stability and Control (New York: MacMillan Company, 1961)

Etkin, Bernard, Dynamics of Flight (New York: John Wiley & Sons, 1959)

Etkin, Bernard, Dynamics of Atmospheric Flight (New York: John Wiley & Sons, 1972)

Goodwin, Graham C. and Kwai Sang Sin, Adaptive Filtering Prediction and Control (Englewood Cliffs, New Jersey: Prentice-Hall, 1984)

Hacker, T., Flight Stability and Control (New York: American Elsevier, 1970), Bellmann, Richard (ed.)

Kelley, C. R., Manual and Automatic Control (New York: John Willey & Sons, 1968)

Kolk, W. R., Modern Flight Dynamics (Englewood Cliffs, New Jersey: Prentice-Hall, 1961)

Miele, Angelo, Flight Mechanics (Reading Mass.: Addison-Wesley, 1962)

Mises, Richard Von, Theory of Flight (New York: Dover, 1959)

Seckel, Edward, Stability and Control of Airplanes and Helicopters (New York: Academic Press, 1964)